UNIVERSITAT POLITÈCNICA DE VALÈNCIA

ESCUELA TÉCNICA SUPERIOR INGENIEROS INDUSTRIALES VALENCIA

TRABAJO FIN DE MASTER EN INGENIERÍA QUÍMICA

CHARACTERIZATION OF MORPHOLOGY AND WATER INTERACTION IN INJECTABLE HYDROGELS OF GELATIN AND HYALURONIC ACID FOR TISSUE ENGINEERING

AUTHOR: MARÍA CULEBRAS MARTÍNEZ

SUPERVISOR: GLORIA GALLEGO FERRER

SUPERVISOR: APOSTOLOS KYRITSIS

Academic year: 2016-17

ACKNOWLEDGEMENTS

First, I would like to thank the financial support of the Spanish Ministry of Economy and Competitiveness (MINECO) through the project MAT2016-76039-C4-1-R and the support of the Erasmus+ program.

I would like to thank my tutor and co-tutor, Dr. Gloria Gallego Ferrer and Dr. Apostolos Kyritsis for making me a participant in this project. Thank you for their professionalism and dedication, their explanations and clarifications, which have made this project a continuous learning process, making me grow both personally and professionally.

On the other hand, to thank all the people of the CBIT who helped me during my stay in the laboratory to solve any problem raised. Especially thanks to Rosa Morales and Carmen Antolinos who were at all times to explain and clarify any doubts that might arise.

Thanks also to the entire DRG at the National Technical University of Athens who, during my stay, made me feel like one more. Thanks in particular to Konstantinos, a colleague with whom I shared very good moments helping each other with any problems raised.

Thanks to all my friends from Cuenca, Valencia and Athens, who have been interested in my work and have helped me disconnect whenever I needed it. Torri. Felix. Thank you Kostas for all that was experienced during this trip.

Last but not least, thanks to my parents and my sister for their unconditional support, always believe in me and make me see things from another point of view when I have needed it.

GENERAL INDEX

ABSTRACT

Recent advances in tissue engineering have led to the development of polymer scaffolds with suitable characteristics and properties capable of mimicking natural tissue and fulfilling the different functions that the extracellular matrix (ECM) performs during the stages of tissue regeneration. In the natural tissue, ECM serves as a structural support, allows cell adhesion, migration and proliferation as well as transport of nutrients and metabolic wastes. Specifically, in the extracellular matrix of soft tissues, components such as collagen, hyaluronic acid or fibronectin perform these functions in a highly hydrated environment.

In the present Master thesis, the synthesis and characterization of a family of injectable gelatin hyaluronic acid hydrogel mixtures modified with tyramine for the regeneration of soft tissues was carried out. Both components have good biocompatibility and biodegradability, avoiding any rejection reaction of the organism after their implantation. The combination of the two hydrogels is intended to improve the properties of the pure components since, while gelatin provides cellular adhesion sequences (RGD), hyaluronic acid provides better mechanical properties and greater hydration. The cross-linking of the hydrogels was carried out enzymatically by the combined action of the enzyme peroxidase and the hydrogen peroxide at non-cytotoxic amounts. As the hydrogels are injectable, the gel precursors with bioactive agents can be administered to the patient by a syringe in the liquid state, and gelification takes place in the body. In this way, the total and homogeneous occupation of the defect is assured regardless of the shape of the defect, besides not requiring invasive surgeries for implantation of the hydrogels in the patient.

One series of hydrogels with different percentages of gelatin and hyaluronic acid were performed and the physico-chemical characterization of them was carried out in order to select the best composition for a future application in tissue engineering. For that, on the one hand, the molecular weight and degree of tyramine grafting of the raw materials, gelatin and hyaluronic acid, were studied. On the other hand, macroscopic and microscopic morphology of synthesized hydrogels was analysed by field emission scanning electron microscopy. Their water retention capacity, the miscibility of the different mixtures and the interactions of the polymer with water were studied by differential scanning calorimetry test at different relative humidities in order to simulate the different moist environments in which the cells can be found in the tissue. Although the mechanical properties and cell response of these matrices had been previously characterized in the research group, it is for the first time that a deep study of their miscibility at different water activity conditions. Another novelty of this study is the evaluation of the different states of water in the hydrogels. The conclusions here extracted explain the microscopic environment the cells find when they are encapsulated in the hydrogels at different hydration levels and can serve us explain the results on cell differentiation found in the other works of the research group.

RESUMEN

Los recientes avances en ingeniería tisular han dado lugar al desarrollo de andamiajes polímeros con características y propiedades adecuadas capaces de imitar el tejido natural y cumplir las diferentes funciones que la matriz extracelular lleva a cabo durante las etapas de regeneración del tejido. En el tejido natural, la matriz extracelular (ECM) sirve como soporte estructural, permite la adhesión, migración y proliferación celular, así como el transporte de nutrientes y deshechos metabólicos. Concretamente, en la ECM de los tejidos blandos, componentes tales como el colágeno, el ácido hialurónico o la fibronectina realizan estas funciones en un ambiente altamente hidratado.

En el presente Trabajo Final de Master se ha realizado la síntesis y la caracterización de una familia de mezclas de hidrogeles inyectables de gelatina y ácido hialurónico modificados con tiramina de cara la regeneración de tejidos blandos. Ambos componentes presentan una buena biocompatibilidad y biodegradabilidad, evitando cualquier reacción de rechazo del organismo tras su implantación. Mediante la combinación de los dos hidrogeles se pretende mejorar las propiedades de los dos componentes puros ya que, mientras la gelatina proporciona secuencias de adhesión celular (RGD), el ácido hialurónico proporciona mejores propiedades mecánicas y una mayor hidratación. El entrecruzamiento de los hidrogeles se ha llevado a cabo enzimáticamente mediante la acción combinada de la enzima peroxidasa y el peróxido de hidrógeno en cantidades no citotóxicas. Como los hidrogeles son inyectables, soluciones acuosas de sus precursores pueden ser administradas al paciente por medio de una jeringa en estado líquido, y la gelificación tiene lugar en el cuerpo. De este modo, se asegura la ocupación total y homogénea del defecto independientemente de la forma de éste además de no requerirse cirugías invasivas para la implantación de los hidrogeles en el paciente.

Se han realizado una serie de hidrogeles con distintas proporciones de gelatina y ácido hialurónico y se ha llevado a cabo la caracterización físico-química de éstos de cara a seleccionar la mejor composición para una futura aplicación en ingeniería tisular. Para ello, por un lado, se ha analizado el peso molecular y el grado de injerto de tiramina de los materiales de partida, gelatina y ácido hialurónico y, por el otro, los hidrogeles sintetizados fueron analizados morfológicamente a nivel macroscópico y microscópico mediante microscopía electrónica de barrido de emisión de campo. La capacidad de absorción de agua y la miscibilidad de las diferentes mezclas, así como las interacciones del polímero con el agua han sido estudiadas mediante calorimetría diferencial de barrido a distintas humedades relativas con el objetivo de simular los diferentes entornos húmedos en los que se pueden encontrar las células en el tejido. Aunque las propiedades mecánicas y la respuesta celular de estas matrices ya han sido caracterizadas en el grupo de investigación, es la primera vez que se ha realizado un estudio exhaustivo de la miscibilidad de las matrices en entornos de distinta actividad del agua. Otra de las novedades del estudio es la evaluación de los diferentes estados del agua en los hidrogeles. Las conclusiones aquí extraídas explican el entorno microscópico que las células encuentran cuando están encapsuladas en los hidrogeles a diferentes niveles de hidratación que pueden servirnos para explicar los resultados de diferenciación celular encontrados en otros trabajos del grupo de investigación.

DOCUMENT I: PROJECT REPORT

PROJECT REPORT INDEX

1. OBJECTIVE

The loss of functionality, the degeneration and the appearance of defects in some organs and tissues are frequent problems that the field of science and medicine are trying to solve. Among the most advanced techniques for the repair of these defects is tissue engineering, whose objective is the regeneration of damaged tissue from biomaterials capable of temporarily mimicking the functions and properties of these tissues, stimulating the generation of new healthy tissue and functional.

Hydrogels based on natural polymers have become especially attractive in the field of tissue engineering because they have unique properties such as good biodegradability and biocompatibility, high water retention capacity, allowing transport of nutrients and metabolic wastes and providing a three dimensional environment of cells in them encapsulated for their proper differentiation. They offer a natural-like cellular environment capable of stimulating the secretion of new extracellular matrix to replace the hydrogel if the adequate composition is selected.

The main objective of this Final Master's Project is the synthesis and characterization of injectable mixtures of hyaluronic acid-gelatin hydrogels in terms of their morphology, water sorption ability, miscibility and water interaction for the selection of the best composition for a successful tissue engineering therapy. To achieve this objective, the following tasks have been fulfilled:

- Study of the properties and characteristics of soft tissues.
- Synthesis and modification of the raw materials, hyaluronic acid and gelatin, to transform them into injectable hydrogels by the grafting of tyramine molecules.
- Characterization of the tyramine conjugates.
- Synthesis of a series of gelatin hyaluronic acid mixtures.
- Placement of samples in different humidity environments.
- Physical-chemical characterization of synthesized hydrogels mixtures.
- Selection of the best mixtures for a successful tissue engineering therapy.
- Synthesis of two different series of gelatin hyaluronic acid mixtures.

2. MOTIVATION

The project carried out, which is included in the Final Master Project (TFM), is motivated by my personal interest in biopolymer research and development in the field of tissue engineering, as well as the techniques used for the characterization of these materials.

This project has been partially performed in the Centre for Biomaterials and Tissue Engineering of the Polytechnic University of Valencia and partially in the Department of Physics of the National Technical University of Athens by an Erasmus stay of the candidate for four months. There, I have been able to apply my knowledge in the field of polymers and laboratory techniques acquired during my university education. In addition, I have learnt and reinforced skills and knowledge such as:

- Knowledge in tissue engineering, chemical synthesis and material properties.
- Skills in polymer chemistry: grafting, purification and crosslinking.
- Knowledge of the structure and behaviour of hydrogels.
- Teamwork skills, decision-making skills and foreign language skills.
- Competences on swollen, diffusion, dielectric and calorimetry measures.
- Skills in the scientific discussion of results, graphic representation and selection of materials.
- Bibliographic search and writing of reports.

Furthermore, I have been able to contribute in the field of tissue engineering through the development and analysis of new biomaterials with applications in the world of biomedicine. Finally, all the acquired skills and abilities can be of great importance and interest for my future professional career.

3. INTRODUCTION

3.1. Introduction to Tissue Engineering

The loss of tissue or terminal organ failure is one of the most devastating and costly problems in the field of medicine. Every year, more than ten million people in Europe undergo surgical procedures to treat these types of disorders. [1], [2]

All procedures in which restoration of damaged tissue is carried out involve the use of some structure to replace the damaged area. In previous years, the replacement devices used have been fully artificial, such as prostheses for joints; processed inert tissues, like the case of the creation of heart valves; or tissues from another patient, such as organ transplants. [3], [4]

However, all these techniques present a number of limitations due to different factors. Artificial prostheses are not perfect and can be fractured with the time or implantation. In the particular case of bone, osteolysis or progressive loss of bone tissue adjacent to the implant has been described. This process is due to the difference of mechanical properties of the material used in the prosthesis and the bone, being the bone Young's modulus much lower than the implanted material modulus. [5] In addition, the appearance of wear particles cause an inflammatory process called foreign body reaction that provoke tissue resorption which only ends with the removal of the prosthesis. [6], [7]

Regarding organ and tissue transplants, the limitations are given by the shortage of donors with respect to the number of patients needing transplants and organs, as it is shown in **Figure 1**. [8] Another limitation is that transplant recipients must follow a lifetime immunosuppression, taking into account the risks of infection, tumour development and unwanted side effects. [3]

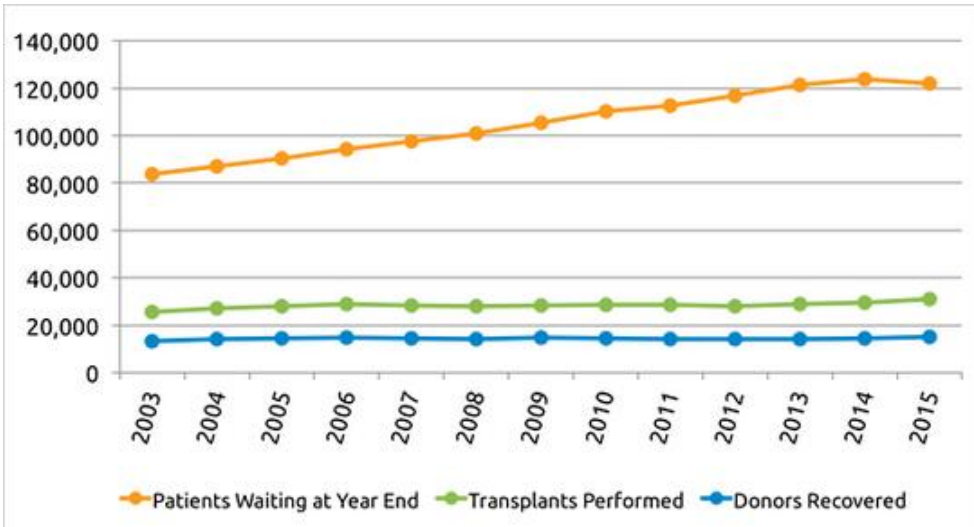

Figure 1. Annual report from 2003 to 2015 of the Unites States scientific registry of transplant recipients and organ procurement and transplantation. Orange line shows the number of patients waiting for a transplant, green line the number of transplants performed and blue line numbers of donors recovered. [9]

All these drawbacks have generated the need to search for new solutions to restore tissue or organ functions, being the most recent tissue engineering of great impact in the field of biomaterials companies.

Tissue engineering can be defined as the interdisciplinary field that applies the principles of engineering and life sciences to the development of biological substitutes that restore, maintain or improve the function of tissues. Specifically, tissue engineering replaces damaged patient tissue with living tissue designed and constructed to meet the needs of each individual patient. [10], [11]

Tissue engineering is based on three fundamental pillars: cells, bioactive growth factors and scaffolds. [12]

i. Cells

From which the new tissue will be secreted. For clinical applications these are obtained from the patient himself, from close relatives or from other individuals.

ii. Scaffolds

These are porous polymeric materials that mimic the extracellular matrix (ECM) during the stages of tissue regeneration. They serve as a three dimensional support to which cells adhere, allows transport, storage and release of active molecules, stimulates specific cellular responses and contributes to the structural and mechanical integrity of the treated area. The materials used for the synthesis of scaffolds as well as the properties of these will depend on the type of tissue to be regenerated and the specific application to be carried out. [13], [14]

iii. Bioactive growth factors

They are polypeptides that contribute to cell multiplication and differentiation. Cell growth begins by binding of a growth factor to a specific receptor of the cells inserted into the polymer scaffold, which accelerate tissue growth.

In this process, the harmful tissue is removed and the cells needed for repair are introduced into a configuration that optimizes the survival of the cells in an environment that will allow the body to heal itself. [12]

Therefore, tissue engineering offers a number of advantages over the other types of procedures performed for tissue regeneration: [12], [15]

- It does not depend on a donor.
- It reproduces the functions of tissues and organs through the design and development of an organized three-dimensional tissue.
- Temporary presence of the implant due to the biodegradability of these, which means:

- A second surgery is not required for its extraction.
- It does not appear foreign body reaction or residual traces.
- Progressive transfer of loads to the regenerated tissue.

As already mentioned, in many cases the tissues have no capacity for self-repair or can only repair minor damages. Such behaviour is characteristic of tissues such as articular cartilage, because it is an avascular tissue where cells receive nutrients by diffusion [16], [17], dermis [18], or myocardium. [19]

All cases mentioned refer to soft tissues of the organism. Generally, the extracellular matrix (ECM) of the soft tissues consists of a highly hydrated three-dimensional network composed mainly of glycosaminoglycans (GAGs) such as hyaluronic acid, and proteins like collagen or fibronectin. ECM serves as a structural support for cell adhesion, migration and proliferation as well as allowing transport of nutrients and metabolic wastes. [20], [21], [22] Hydrogels are typically the scaffolds used in the regeneration of soft tissues because they can properly imitate the hydrated three dimensional environment that cells need in those tissues for a proper differentiation or maintenance of phenotype.

3.2. Hydrogels

Hydrogels are materials formed by hydrophilic polymer networks joined by cross-linking points (**Figure 2**). Due to the hydrophilicity of their chains, they are capable of absorbing large amounts of water, while the crosslinking points prevent the dissolution of these in water and give the material a three-dimensional structure. [23], [24]

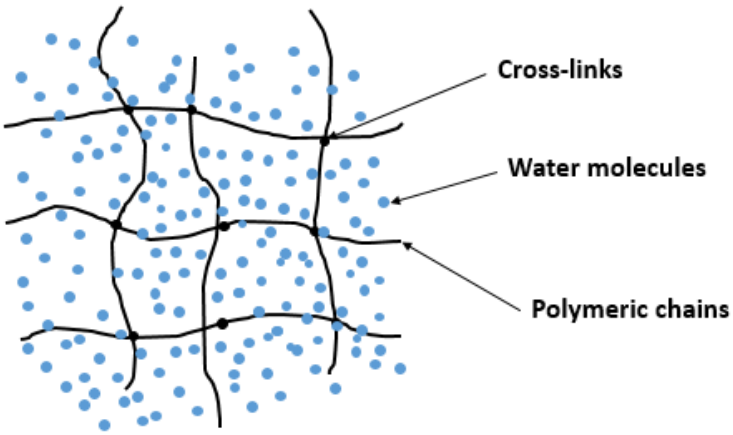

Figure 2. Hydrogel microstructure.

Depending on the type of crosslinking they present, hydrogels can be chemical, when crosslinking occurs by covalent bonding, or physical, when crosslinking is given by weaker forces such as hydrogen bonds, hydrophobic interactions or electrostatic forces. Chemical hydrogels can absorb water to an equilibrium state and exhibit high stability in aggressive environments. In contrast, physical hydrogels are weaker so they are reversible and respond to physical changes such as temperature or pH. [25], [26]

Hydrogels are materials of great interest for mimicking the extracellular matrix of soft tissues in tissue engineering because of their unique properties. Due to their high water content, hydrogels provide a very swollen three-dimensional environment, similar to the native tissue environment, which helps to promote cell differentiation, in addition to allowing transport of nutrients and metabolic wastes. Furthermore, these materials generally are biocompatible and can be biodegradable, can be easily modified with cell adhesion ligands and injected in vivo as a liquid which gelates at body temperature. [22], [23]

Apart from good hydration and good cell adhesion, the hydrogel must have adequate mechanical properties, since it must be able to withstand the normal loads and tensions of the native tissue, especially in the initial stages, before the cells begin to produce their own functional extracellular matrix. [27]

Depending on the polymers used, hydrogels can be classified as synthetic or natural. [23] Synthetic hydrogels generally have greater ease in controlling and regulating their characteristics and better mechanical properties. However, its use in the field of regenerative medicine is limited by the lack of cell adhesion and the possibility of obtaining cytotoxic degradation products. [28]

On the other hand, natural hydrogels have characteristics that have allowed the successful use of these in cell proliferation and tissue regeneration. Hydrogels composed of natural polymers resemble ECM structures, are non-toxic, do not stimulate inflammatory or immunological reactions and favor cell adhesion, growth, proliferation, differentiation and secretion. In addition, these materials may ultimately degrade and be absorbed by the metabolism. However, these hydrogels are limited by the insufficiency of their mechanical properties in some cases. It is for this reason, that they have been modified with structural reinforcements to adapt their mechanical properties until reaching the required conditions. [29]

3.3. Gelatin/Hyaluronic Acid Hydrogels

In this project, gelatin and hyaluronic acid hydrogels have been synthesized. Using these compounds, it has been obtained protein (gelatin) – polysaccharide (hyaluronic acid) hydrogels that mimic the extracellular matrix. Both materials are natural polymers that are present in the ECM of the tissues ensuring a good biocompatibility and avoiding any reaction of rejection of the organism after their implantation.

3.3.1. Gelatin

Gelatin is a natural protein obtained from denaturing and partial hydrolysis of collagen, a substance that constitutes a large part of the connective tissue in living beings. [30], [31], [32] It is formed by the union of different amino acids by peptide bond, mainly proline, hydroxyproline, glycine and glutamic acid. Due to these bonds, polymer chains are formed with a molecular weight between 15000 g/mol and 400000 g/mol. [33] [34] Gelatin contains in its structure free amino and carboxyl groups that allow it to react with other compounds and modify their properties. [35] **Figure 3** shows gelatin structure.

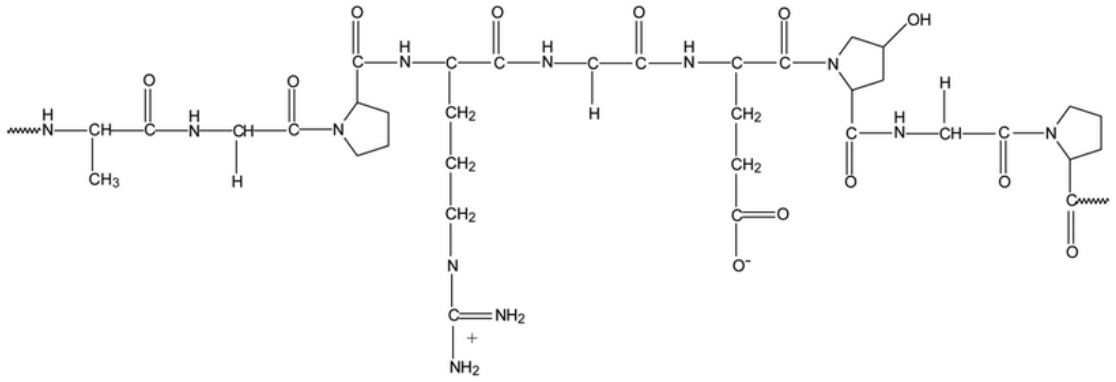

Figure 3. Typical structure of gelatin (-Ala-Gly-Pro-Arg-Gly-Glu-4Hyp-Gly-Pro-).

A unique property of gelatin is that it exhibits a thermally induced sol-gel transition. Below its melting temperature, about 23 ° C, gelatin acquires a helical structure joined by intramolecular hydrogen bonds similar to collagen, forming a water insoluble macroscopic gel. The rigidity of this gel will depend on the structure and molecular weight of the gelatin chains as well as on the pH, temperature and the presence of any additive. In contrast, above the melting temperature the intramolecular bonding points are weakened and the three-dimensional structure is not stable, therefore the dissolution of the gelatin in water occurs. [36], [33]

Gelatin is a biocompatible, biodegradable, non-toxic substance that promotes cell adhesion and has much lower antigenicity than collagen. [37], [38] All these properties make gelatine an excellent candidate for biomedical applications such as the creation of wound dressings or the formation of scaffolds for tissue repair in tissue engineering. [39], [40]

However, pure gelatin is rarely used for the formation of scaffolds in tissue engineering because of their low mechanical properties. [29] Hence the interest to explore the use of blends due to the possibility of combining and improving such properties. [36]

It should be noted that the good adhesion and cell proliferation of gelatin is given by the presence of some collagen adhesion sequences in its chains, such as argin-glycine-aspartic acid (RGD) sequence. [41], [29] Cells can recognize these sequences by the integrins present in the extracellular matrix which are connected via transmembrane and give rise to the formation of

the actin cytoskeleton inside the cells and proliferation and cell differentiation. [42], [43] That is why these signals are crucial for the regeneration and development of new tissues in the field of regenerative medicine.

3.3.2. Hyaluronic acid

Hyaluronic acid (HA) is a linear polysaccharide composed of about 250-25,000 repeating disaccharide units of N-acetyl-D-glucosamine and D-glucuronic acid linked by glycosidic bond (**Figure 4**). [44], [45] This polysaccharide is negatively charged, has a molecular weight between 10^5 and 10^8 Da [46]and the carboxyl and alcohol groups present in its structure allow it to be chemically modified, providing numerous possibilities for the creation of crosslinkable hyaluronic acid derivatives which will result in the formation of hydrogels after crosslinking. [47]

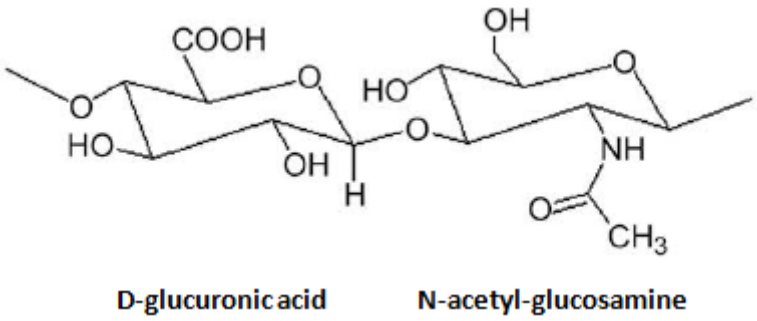

Figure 4. Structure of hyaluronic acid.

It is one of the most important components of the extracellular matrix (ECM). In the body, the highest concentrations of HA are found in soft connective tissues such as the umbilical cord, synovial fluid, skin and vitreous body, although it is also found in remarkable amounts in the lung, kidney, brain, cartilage and muscles. [37], [48]

Due to the abundance of hydrophilic groups in the chains, HA has a high water retention capacity, which gives it a high degree of viscoelasticity. [39] HA is responsible for tissue homeostasis, playing a very important role in tissue healing and remodelling, morphogenesis and angiogenesis, as it favors the infiltration of migratory cells in the injured tissue and promotes cell mobility and proliferation. [18], [34] In addition, it plays an important role in cell signaling events interacting with cells through cell surface receptors such as CD44, or RHAMM. These interactions mediate important physiological processes like signal transduction, pericellular layer formation and receptor-mediated internalization. [49], [50]

These features combined with its good biocompatibility and biodegradability make hyaluronic acid an attractive material for biomedical applications, among which stand out its use for tissue regeneration, including cartilage engineering and skin regeneration. However, HA-based biomaterials are also widely used to prevent protein absorption, inhibit cell attachment and prevent postsurgical adhesions. [28], [51]

Nevertheless, the development of HA-derived materials has been hampered by the fact that their hydrophilic and polyanionic surfaces do not thermodynamically favor the binding of the cells to the anionic surfaces. [21]In general, cells adhere better to neutral, hydrophobic or polycationic surfaces. This characteristic, coupled with the rapid degradation and inadequate mechanical properties of HA for certain applications, leads to the combination of HA with other materials with the aim of compensating and improving these properties. [39]

The combination of hyaluronic acid and gelatin is intended to provide fully biocompatible protein-polysaccharide hydrogels because both of them are natural polymers present in the extracellular matrix of tissues. In addition, it is also intended to rectify the limitations of both pure compounds. On the one hand, hyaluronic acid provides good hydration and diffusion of nutrients and cellular waste substances. Also, due to the stiffness of its chains in the hydrated state, it provides greater mechanical properties to the hydrogel. On the other hand, gelatin adhesion sequences can be recognized by the integrins of the cells giving the hydrogel good adhesion and cell proliferation.

3.4. Injectable hydrogels. Crosslinking mechanisms

Hydrogels may be used by implantation, which corresponds to preformed hydrogels prior to being introduced into the patient, or by injection, which are based on aqueous mixtures of gel precursors with bioactive agents that can be administered to the patient by a syringe. [52]

Injectable or *in situ* hydrogels have gained attention in recent years in the field of biomedicine in applications such as tissue engineering or drug administration because they have a number of advantages over conventional preformed hydrogels: [53], [54]

- Minimally invasive surgeries are required for implantation.
- Occupation of the defect regardless of the defect shape.
- Allow the homogeneous incorporation of molecules and / or therapeutic cells.

In situ hydrogels may be formed by chemical or physical crosslinking reaction mechanisms. Physically crosslinked hydrogels have the advantage of showing reversibility and good biocompatibility because the use of crosslinking agents in their preparation is avoided. These agents cannot only affect the integrity of the substances to be trapped, such as cells and proteins, but are also usually cytotoxic compounds which have to be extracted from the hydrogels before they can be used. However, physically crosslinked hydrogels have weak mechanical properties and their stability in vivo could be severely affected by changes in the environment like pH, temperature or ionic strength. These changes could lead to the elimination of the crosslinked network. Among the methods of formation of these hydrogels highlight the cross-linking by ionic forces, by crystallization and by hydrogen bridges. [55], [56]

In contrast, chemically crosslinked hydrogels have better chemical stability and mechanical properties. In addition, covalent crosslinking allows more precise control of crosslink

density of the hydrogels and, therefore, more control of their properties such as mechanical strength, degradation time or absorption capacity. [56], [57]

Different strategies have been adopted for the preparation of chemically cross-linked hydrogels, such as radical polymerization using redox-type initiators or photoinitiators, Michael-type addiction reactions, disulfide bond formation and aldehyde-mediated cross-linking. However, different studies have found that these methods give rise to the formation of cytotoxic cross-linking reactions, making unviable the use of them in the formation of in vivo hydrogels. [21], [58], [59], [60]

This is why in recent years enzymatically crosslinked hydrogels have emerged as an alternative way to overcome the difficulties associated with chemical crosslinking methods. Enzymatic cross-linking is a type of enzyme-mediated chemical cross-linking. Most enzymes involved in this type of cross-linking are enzymes that catalyze reactions that occur naturally in our body, which develop in an aqueous medium, at moderate temperatures and neutral pH. It is for this reason that they can also be used for the cross-linking of hydrogels in situ. [61], [62] Enzymatic cross-linking has the following advantages: [63]

- Smoothness of enzymatic reactions under normal physiological conditions, which is a solution for the crosslinking of natural polymers that cannot withstand extreme chemical conditions.
- Enzyme-substrate specificity, so it avoids undesired or toxic side reactions.
- Mechanical properties and absorption capacity similar to native tissue.
- Polymerization reaction can be controlled directly by controlling the activity of the enzyme.
- Possible loss of bioactivity is avoided.
- Gelation rate can be controlled, which is an essential characteristic for obtaining an appropriate cellular distribution and adequate integration of the hydrogel with the surrounding tissues.

Among the enzymes used for the enzymatic crosslinking of hydrogels highlight HRP horseradish peroxidise (HRP), tyrosinase and transglutaminase (**Figure 5**).

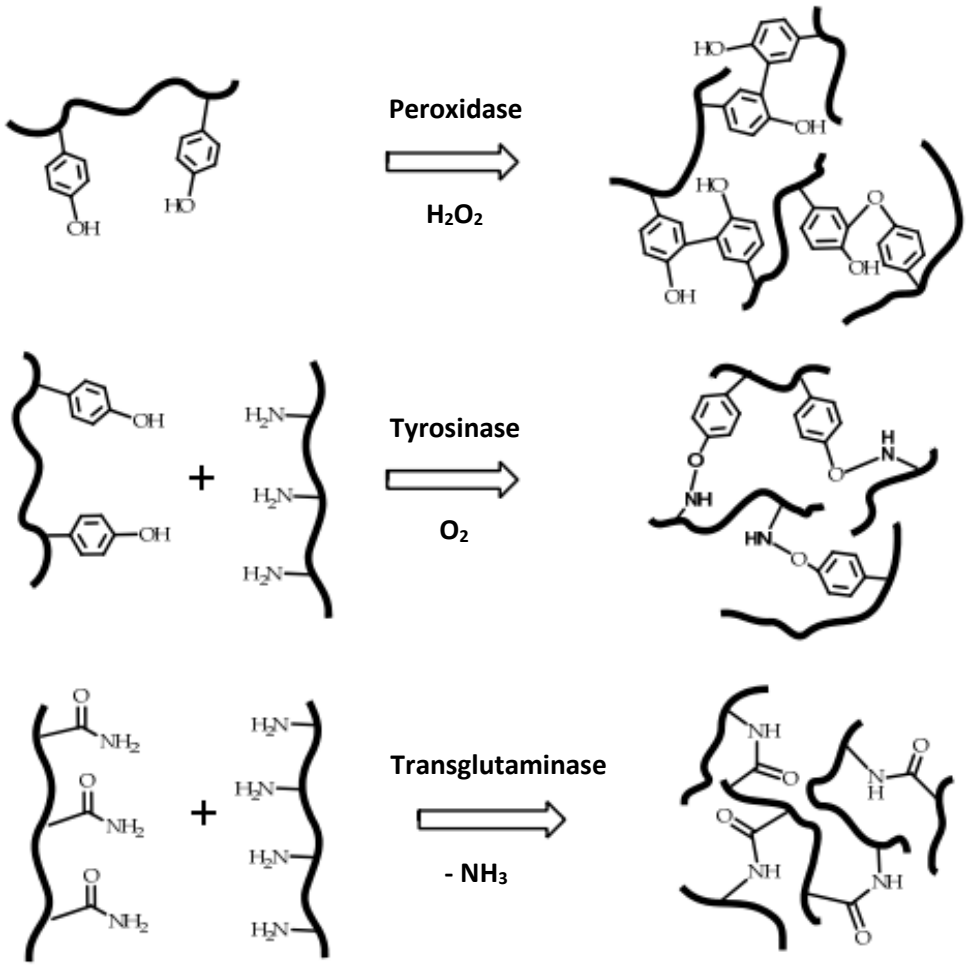

Figure 5. Scheme of the enzymatic reactions carried out by peroxidase, tyrosinase and transglutaminase. [56]

Tyrosinase is an enzyme present in animals and plants responsible for the production of various types of melanin in animal skin and blackening of the fruits. [64] The reaction mechanism of tyrosinase is based on the conversion of phenol to catechol by adding an additional hydroxyl group on the aromatic ring in the presence of oxygen. Oxidation of the catechol produces a reactive quinone capable of forming a covalent bond with other quinones. [65] The hydrogels formed using this enzyme do not require the use of cofactors and have a high adhesiveness. However, they are mechanically weak or unstable. [66]

As for transglutaminase, it catalyzes the cross-linking reaction between amine groups and the ϒ-carboxyamide groups of glutamine present in peptides and peptides. The use of transglutaminase also does not require the use of cofactors, it is highly cytocompatible and presents good transport properties. However, its possible involvement in the onset inflammatory response limits its use in the formation of hydrogels. [63]

Due to the disadvantages of the enzymes above, the use of peroxidase has been extended in the cross-linking of hydrogels in situ, since they have good stability, suitable mechanical properties and good control of the gelation rate. Specifically, HRP peroxidase is being used. It is a single-chain B-type hemoprotein that in the presence of hydrogen peroxide catalyzes the coupling of phenols or aniline derivatives. The crosslinking reaction takes place via

carbon-oxygen bond between the carbon atom in the ortho position and the phenoxy oxygen in the phenol moieties or by a carbon-carbon bond at the ortho positions. [56], [67], [68]

3.4.1. Gelatin/Hyaluronic acid injectable hydrogels with tyramine graft cross-linked with HRPand H_2O_2

For the synthesis of hydrogels of hyaluronic acid and gelatin it was first necessary to graft tyramine into the chains of these two compounds in order to obtain phenol groups capable of reacting for the subsequent formation of the hydrogel.

Tyramine grafting was performed using NHS (N-Hydroxysuccinimide) and EDC (N- (3-Dimethylaminopropyl) -N'-ethylcarbodiimide hydrochloride) as stabilizer and catalyst of the reaction respectively. **Figure 6** and **Figure 7** show the scheme of the reaction performed for the tyramine graft in the hyaluronic acid and gelatin chains.

First, it takes place the reaction of EDC with gelatin and hyaluronic acid chains producing O-acylisourea (**Figure 6**).

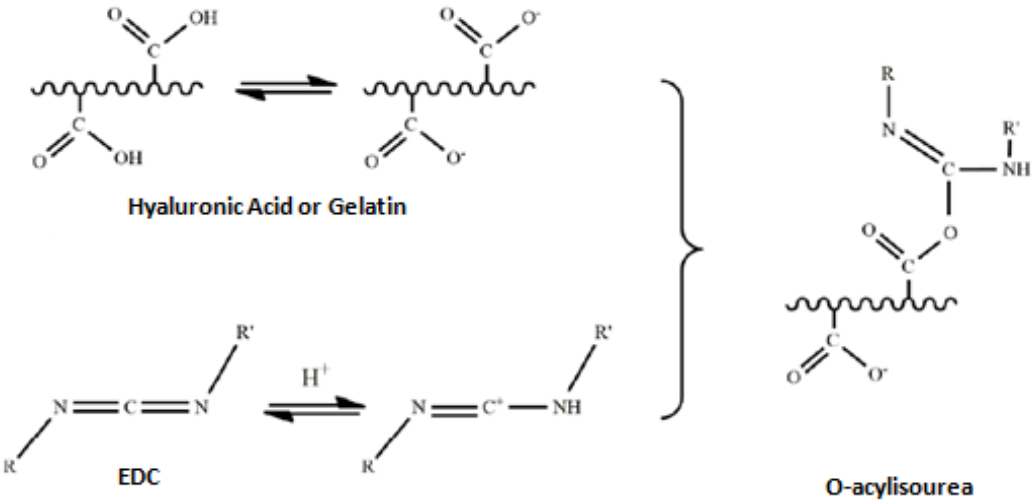

Figure 6. Scheme of the reaction of hyaluronic acid and gelatin with the EDC giving rise to the formation of O-acylisourea. [69]

Then, O-acylisourea reacts with tyramine and NHS to form an amide bond giving rise to the modification of hyaluronic acid and gelatin chains with phenol groups which will allow the subsequent cross-linking of these chains for the formation of in situ hydrogels (**Figure 7**).

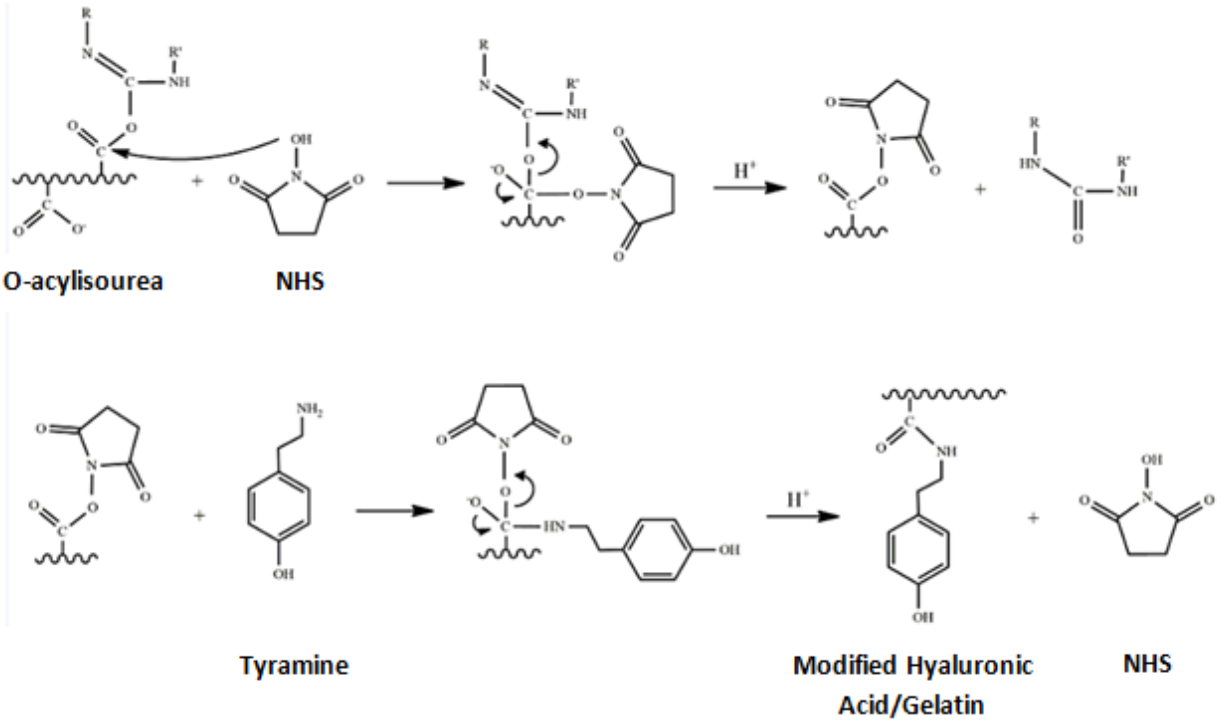

Figure 7. Scheme of the reaction of O-acylisourea with NHS and tyramine giving rise to the tyramine graft in the chains of hyaluronic acid and gelatin. [69]

The chemical crosslinking of the HA/Gel hydrogels is carried out by an oxidative coupling reaction using the enzyme HRP and hydrogen peroxide (H_2O_2). This reaction takes place in two stages. Firstly, the HRP is oxidized in the presence of H_2O_2 to form an intermediate which then oxidizes the phenol groups of the tyramine grafted into the hyaluronic acid and the gelatin resulting in the cross-linking of the hydrogel. [70] A schematic of the chemical structure of the hydrogel obtained after the enzymatic reaction with HRP and hydrogen peroxide has been performed is shown in **Figure 8**.

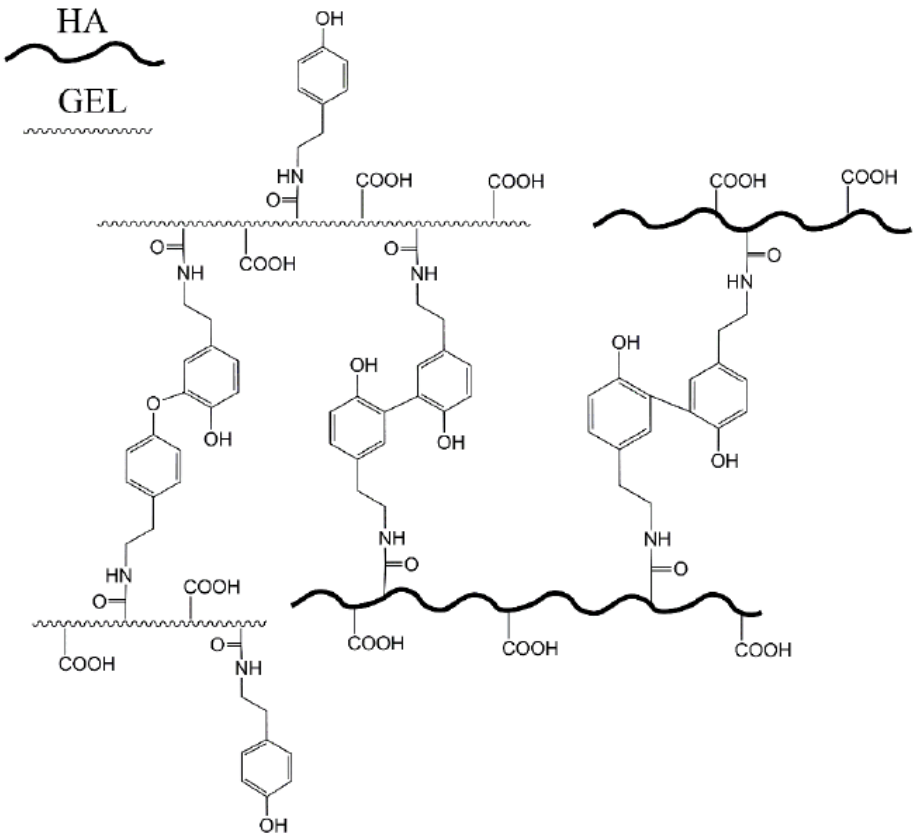

Figure 8. Scheme of the chemical structure of a HA/Gel hydrogel after the enzymatic crosslinking in the presence of HRP and H_2O_2. [71]

3.5. Water states in polymer hydrogels

Hydrogels are materials capable of absorbing large amounts of water. The amount of water absorbed by a hydrogel as well as water-hydrogel interactions will define some of the properties of the hydrogel, such as nutrient and waste transport capacity or the biocompatibility of the hydrogel. [23], [72]

The understanding of the interactions of water with the materials of which the hydrogel is composed is a phenomenon that has not been explained in depth yet. [73] One of the main objectives of this project was the characterization and explanation of different water-hydrogel interactions in gelatin, hyaluronic acid and their mixtures.

Any set of conditions and properties that water may present in a hydrogel is defined as water states. In general, four types of water behaviours have been described in a hydrogel: [23], [74], [75], [76]

1. Primary bound water: Generally, when a dry hydrogel absorbs water, the first water molecules that enter the hydrogel matrix interact with the hydrophilic groups of the hydrogel forming what is called the first layer of water or primary bound water. This water is strongly interacted with the hydrogel chains.

2. Secondary bound water: Once all the hydrophilic groups have been hydrated, it will be the apolar groups of the hydrogel and the water molecules from the first layer that will interact with the water molecules forming the second layer of water or secondary bound water, whose interaction will be weaker than in the case of the primary bound layer. The set of these two layers of water that interacts directly with the chains of the hydrogel is called total bound water.

3. Clusters domains or free water: Once the layers of bound water are formed, water molecules entering to the hydrogel will interact with them forming clusters domains. As this layer does not interact directly with the polymer chains, the interaction is much weaker than in the case of bound water.

4. Pure bulk water: After the clusters are formed, the hydrogel absorbs more water due to the osmotic motive force of the network chains towards infinite dilution to reach the equilibrium water content. This water is called pure bulk water and presents the same properties as pure water. Bulk water is present in the hydrogel when the water activity is equal to one (a_w=1) and the hydrogel presents cavities between its networks to accommodate it.

However, it is difficult to find these four behaviours independently in a polymer. Usually a mixture of them appears.

The amount of water absorbed by the hydrogel is a balance between the thermodynamic strength of the mixture hydrogel-water, which depends mainly on the retraction force of the three-dimensional network, which is given by the number of cross-links connecting the polymer chains forming a three-dimensional network and the hydrophilicity of the hydrogel (characterized by the polymer-solvent interaction parameter, χ). [24]

Different methods are used to estimate the amounts of bound water and free water present in a hydrogel. These include the use of molecular probes, DSC and proton NMR. At this point, it is worth noticing that NMR method classifies water molecules according to their observed mobility, whereas, the thermal method of DSC distinguishes among water molecules that are able to phase separated at sub-zero temperatures or not. Thus, DSC classifies, usually, water molecules as crystallized and non-crystallized molecules. Therefore, conclusions extracted from the DSC scans by analysing the thermal transitions in hydrogels need to take into account not only the interaction between the polymer chains and water, but also the diffusion problems when the temperature is decreased. In this project the DSC test was used to characterize the hydrogels at different relative humidities, and the thermal transitions in the hydrogels were explained based on the temperature-composition diagram. For a better understanding of the processes observed with this technique, the following section explains the phase diagram in polymer hydrogels as well as the curves observed in the DSC test. [23], [77], [78]

3.6. Phase diagram and DSC thermograms in polymer hydrogels

A hydrogel can be considered as a homogeneous mixture of two species, the polymer of which it is formed and a solvent. The phase diagram shows the different thermal processes that can occur in a polymer when a change in temperature occurs as a function of the solvent concentration present in the polymer. This diagram is formed by three curves as shown in **Figure 9**. [79], [80]

The first corresponds to the glass transition temperature (T_g). From this temperature a structural change of the amorphous part of the polymer takes place. At temperatures above Tg the molecules have enough energy to overcome the attraction forces and move. However, below the Tg the material is in a glassy state and molecules do not have sufficient energy being almost negligible the movement of the chains.

The second curve refers to the crystallization temperature (T_c). Crystallization is the process that occurs by lowering the temperature of the polymer to the crystallization temperature, where the molecules can be sorted into crystals. This process is exothermic since secondary bonds are formed and, therefore, energy is released.

Finally, the melting temperature (Tm) curve is found. Said process takes place when the temperature of the polymer is raised to the melting temperature and the secondary bonds formed during the crystallization process melt. Fusion is an endothermic process since secondary bonds are broken, so extra energy is needed for the process to take place. [81], [82]

In general, it can be observed that, as the water fraction in the polymer increases, glass transition temperature decreases and melting and crystallization temperature increase.

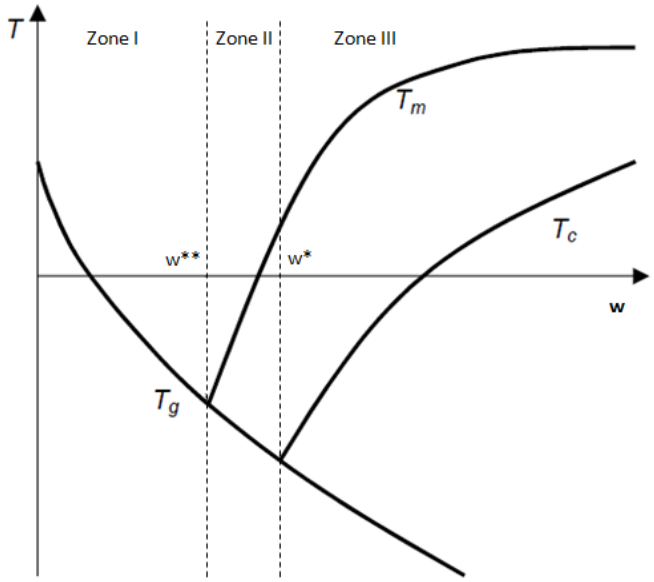

Figure 9. Scheme of a phase diagram of a polymer hydrogel. 'Y' axis shows temperature (T) and 'X' axis shows solvent concentration (w). Tg corresponds with the glass transition curve, Tm is the melting curve, Tc is the crystallization curve and w is the fraction of water in the hydrogel. [79]

When a thermal change in a hydrogel is performed, different processes can be found depending on the area of the graph in which it is. Generally, this graph can be divided into three zones from the fraction of solvent in which the curves of the graph coincide. It will be called w** the solvent fraction in which Tg coincides with Tm and w * the solvent fraction in which Tg coincides with Tc. [83], [84]

- **Zone I: Solvent fractions below w** (w < w**)**

When the temperature decreases in this zone, glass transition curve is found before crystallization and melting curves. Below the Tg, the chains of the polymer do not have mobility since the material is in a glassy state, reason why they do not allow the migration of the solvent and the crystallization processes do not take place. Therefore, it is said that this fraction of solvent present in the hydrogel is non-freezable. Consequently, only the glass transition process will appear in the DSC test as it is shown in **Figure 10**.

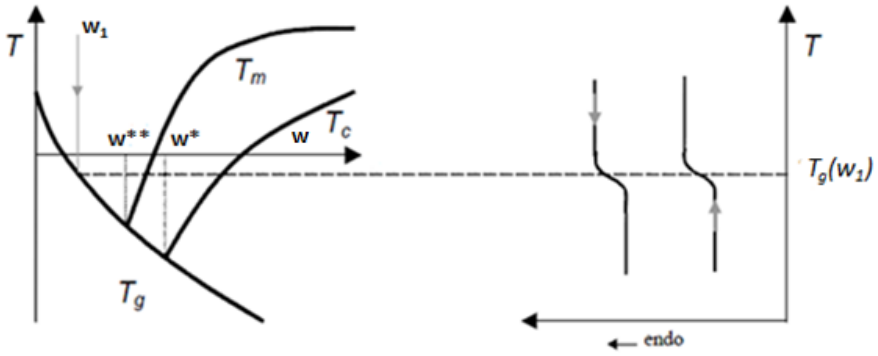

Figure 10. Schematic of a typical phase diagram (left) and thermogram (right) of a polymer swollen in a solvent with a solvent fraction below w.** [85]

- **Zone II: Solvent fractions between w** and w* (w** < w < w*)**

In this zone, like the previous one, when a hydrogel is subjected to a cooling process, the glass transition process is found before the crystallization whereby the solvent remains non-crystallizable on cooling. This is because the formation of crystals is given by two processes: the formation of a nucleus of a critical size and its subsequent growth, which cannot take place without the first stage being completed. The cooling process adversely affects crystal formation because the nucleation rate is increased and, in addition, the viscosity of the system is increased so that solvent migration is not allowed for the formation of nucleus of a critical size. Therefore, only the thermal break due to the glass transition process is observed in the DSC test on cooling (**Figure 11**).

However, when the heating process is carried out and the Tg is reached, the viscosity of the system decreases allowing the migration of the solvent towards the embryos formed in the cooling process producing cold crystallization, that is to say, crystal formation in the hydrogel during the heating process. If the temperature is further increased, the melting of the crystals formed during cold crystallization will take place. This is why in the case of the heating process

shown in **Figure 11**, an exothermic and then an endothermic peak is observed in the DSC thermogram due to cold crystallization and melting processes respectively.

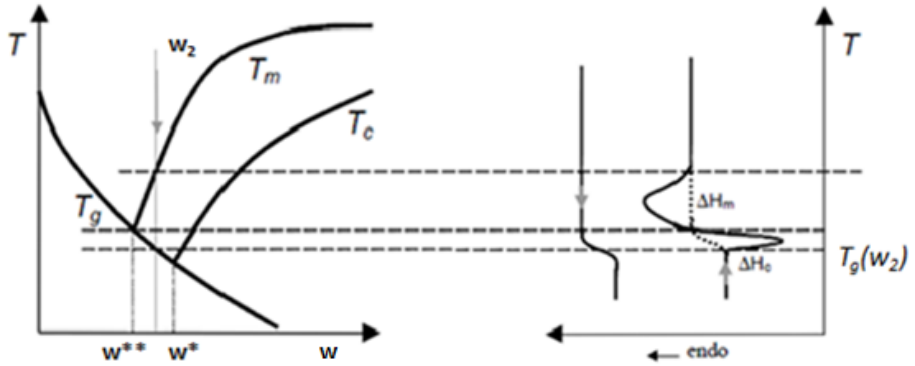

Figure 11. Schematic of a typical phase diagram (left) and thermogram (right) of a polymer swollen in a solvent with a solvent fraction between w* and w.** [85]

- **Zone III: Solvent fractions above w* (w > w*)**

In this case, when the cooling process is performed, crystallization curve is found before the glass transition curve in the phase diagram whereby the formation of crystals takes place and an exothermic peak appears in the DSC thermogram. The formation of crystals leads to the loss of solvent in the hydrogel until the concentration w* is reached. At this point, glass transition temperature is reached, resulting in the loss of mobility of the chains and, consequently, the formation of crystals is not allowed.

In the heating process, cold crystallization process takes place as described above once the glass transition temperature has been exceeded. If the temperature continues to increase, melting process will occur and the crystals formed during cooling and heating processes will melt reaching the initial composition of the solvent. All these processes are collected in **Figure 12**.

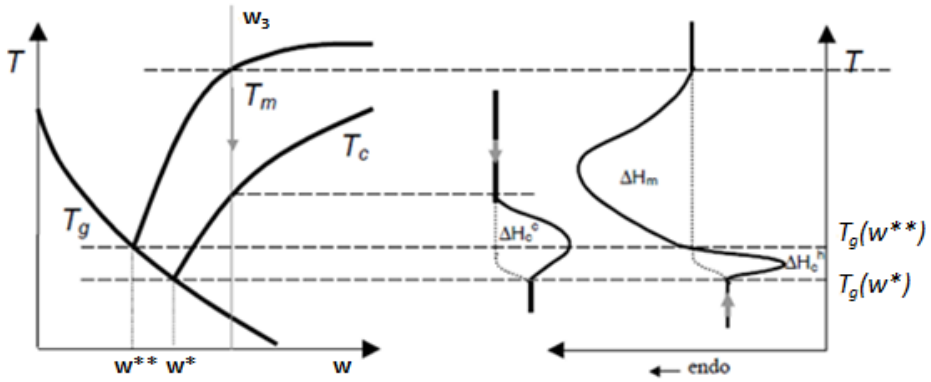

Figure 12. Schematic of a typical phase diagram (left) and thermogram (right) of a polymer swollen in a solvent with a solvent fraction above w*. [85]

4. JUSTIFICATION

This project is based on the development of hydrogels able to mimic the extracellular matrix allowing tissue regeneration. With this, it tries to give solution to problems of the field of medicine such as loss of tissue or terminal organ failure. This new technique of tissue regeneration presents numerous advantages over the limitations present in the conventional techniques. It is for this reason that during the last years numerous investigations have been carried out to develop and optimize these materials in order to find the most suitable characteristics for the regeneration of the different tissues present in the human body.

Specifically, in this project series of hyaluronic acid and gelatin hydrogels were developed with three different cross-linking molar ratios in order to study the effect of cross-linking and the compatibility of mixtures in a larger collaboration with the University of Athens. In the present work we show the results concerning the characterization of the miscibility of the series of materials with the lowest cross-linking molar ratio. In the next future, the other compositions will be analysed in collaboration with the researchers in Athens. The tasks I performed were to prepare the materials with the different cross-linking ratios and optimize the measuring conditions with the DSC, by analysing the series of materials with the lower crosslinking degree at different relative humidities. By placing the hydrogels at different relative humidities, it was intended to simulate the different moist environments in which the cells can be found in the tissue. This is because the tissue is formed by a mixture of water and salts, creating an environment with an activity below the unit. In this way, physicochemical characteristics of this series of materials at macroscopic and microscopic level were evaluated to know thoroughly their behaviour and viability in the field of tissue engineering for regeneration of soft tissues.

Furthermore, it was necessary to carry out the acidic degradation of the hyaluronic acid in order to decrease its molecular weight and to avoid the separation of phases in the mixtures, as has been seen in other works.

In addition, it was proposed to work with injectable hydrogels that allow greater adaptation to the shape of the defect and a simpler cell encapsulation, also guaranteeing that the hydrogels crosslinking reaction is not cytotoxic.

5. LEGISLATION AND REGULATION

All the works developed in this project must comply with the current legislation in Spain and in Greece. Since the work developed focuses on laboratory tasks, the standard to be considered are mainly based on classification and treatment of hazardous substances, labelling and waste management, as well as safety and hygiene regulations at work.

Specifically, the Spanish legislation applicable to the work developed during the achievement of this project is:

- Ley 21/2015. *Prevención y Control Integrados de la Contaminación* y *Residuos y suelos contaminados*.
- Ley 31/1995. *Prevención de riesgos laborales.*
- Real Decreto 952/1997. *Normativa básica de residuos tóxicos y peligrosos*.
- Real Decreto 664/1997. *Protección de los trabajadores contra los riegos relacionados con la exposición a agentes biológicos durante el trabajo.*
- Real Decreto 374/2001. *Protección de la salud y seguridad de los trabajadores contra los riesgos relacionados con los agentes químicos durante el trabajo.*
- Directiva Europea CE 1272/2008. *Clasificación, etiquetado y envasado de sustancias y mezclas*.

On the other hand, although they are not mandatory regulations, the following preventive technical standards (NTP) should be considered, which serve as a recommendation for good practices in the development of work:

- NTP 635. *Clasificación, envasado y etiquetado de las sustancias peligrosas.*
- NTP 663. *Propiedades fisicoquímicas relevantes en la prevención del riesgo químico*.
- NTP 902. *Riesgo biológico: evaluación y prevención en trabajos con cultivos celulares.*

The characterization of the hydrogels in Greece was carried out following the equivalent Greek legislation.

6. MATERIALS AND METHODS

6.1. Reagents

For the synthesis process of low molecular weight hyaluronic acid and the tyramine grafting in hyaluronic acid and gelatin, HA sodium salt from *Streptococcus equi*, Gel from porcine skin (gel strength 300, Type A), 2-(*N*-Morpholino)ethanesulfonic acid (>99%, MES), tyramine hydrochloride (98%), *N*-Hydroxysuccinimide (98%, NHS) and dialysis tubing (3500 and 12400 MWCO) from Sigma-Aldrich (Germany) were used. *N*-(3-Dimethylaminopropyl)- *N*′-ethylcarbodiimide hydrochloride (EDC) were purchased by Iris Biotech GmbH, Marktredwitz (Germany). Sodium chloride, sodium hydroxide, hydrochloric acidand silica gel with orange moisture indicatorwere from Scharlab (Spain).

For the synthesis of injectable hydrogels hydrogen peroxide solution (30% w/w in H_2O, with stabilizer), peroxidase from horseradish Type VI (HRP), 4-(2-hydroxyethyl) piperazine-1-ethanesulphonicacid (HEPES), potassium dihydrogen phosphate, potassium chloride (for molecularbiology), Dulbecco's phosphate buffered saline (DPBS), sodium azide (>99.5%, ReagentPlus) were supplied by Sigma-Aldrich (Germany).

The maintenance of the samples at different relative humidities was carried out using phosphorus oxide III, cobalt chloride, potassium chloride and potassium sulphate for relative humidities 0%, 65%, 85% and 98% respectively from the commercial house Sigma-Aldrich (USA).

6.2. Synthesis of low molecular weight hyaluronic acid (HA-LMW)

As it is shown in other works [71], in order to equalize the gelation times of gelatin and hyaluronic acid and avoid phase separation, it was necessary firstly to carry out the degradation of hyaluronic acid with the aim of resembling the molecular weight of the two components. Low molecular weight hyaluronic acid was obtained following the process of acid degradation of high molecular weight hyaluronic acid. [86]

To do this, 500 mg of high molecular weight hyaluronic acid were added in 50 mL of milliQ water and the pH of the solution was adjusted to 0.5 adding concentrated hydrochloric acid. Then, the solution was kept under stirring for 24 h at room temperature and 200-250 rpm. During this time, the acid degradation of hyaluronic acid takes place.

After, the solution was neutralized to pH 7 with NaOH and introduced into a dialysis membrane of 3500 MWCO. The dialysis process, carried out with the aim of purifying the product, was performed in deionized water for 3 days with 3 changes of water per day.

Finally, it was frozen and lyophilized for 4 days to remove the water and to obtain the product dried and prepared for the subsequent synthesis of tyramine conjugates.

Throughout the whole synthesis process of low molecular weight hyaluronic acid, it was necessary to cover all the vials where the solution was with aluminium foil in order to avoid the contact of light with hyaluronic acid, as it is photosensible.

6.3. Synthesis of hyaluronic acid tyramine grafting (HA-Tyr)

Tyramine grafting in hyaluronic acid chains is a necessary process for obtaining phenol end groups in such chains, which will be able to react in situ and give rise to the formation of injectable hydrogels. The grafting reaction was carried out is shown in **Figure 13**. It consists of the reaction of carboxyl groups of hyaluronic acid with amine groups of tyramine, creating an amide bond and leaving as terminal groups the phenol groups of tyramine.

The reaction takes place in the presence of EDC (N- (3-Dimethylaminopropyl)-N'-ethylcarbodiimide hydrochloride), which acts as an activator of carboxyl groups of HA, and NHS (N-Hydroxysuccinimide), which acts as a catalyst of the reaction facilitating and minimizing possible side reactions.

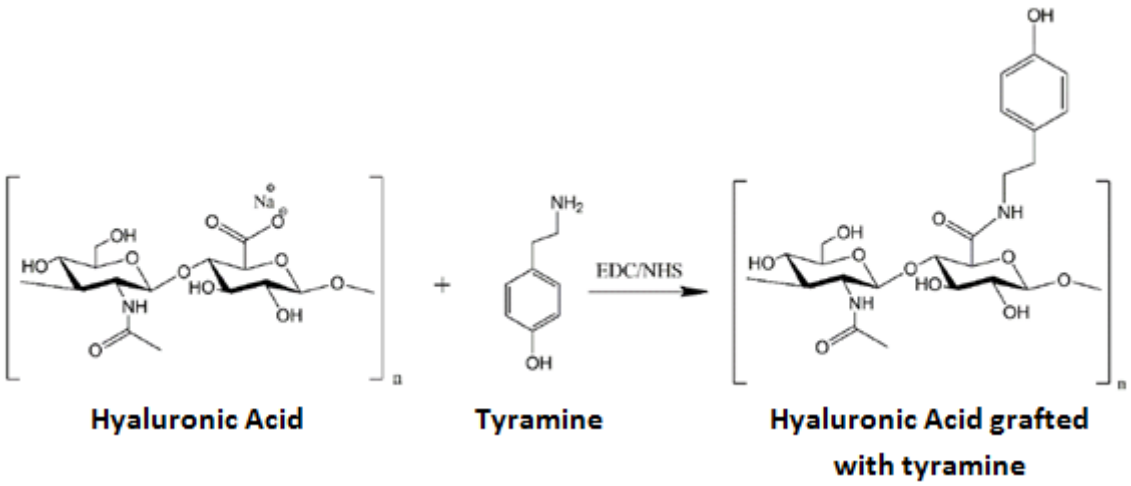

Figure 13. Tyramine graft reaction in hyaluronic acid chains. Reaction between carboxyl groups of hyaluronic acid and amine group of tyramine leading to amide bond. NHS and EDC act as a catalyst and activator of the reaction respectively.

The synthesis of hyaluronic acid with tyramine graft (HA-Tyr) was performed using three different molar ratios taking into account the quantities of hyaluronic acid, tyramine, EDC and NHS. **Table 1** shows the ratios used, where COOH refers to the carboxyl groups of hyaluronic acid.

Table 1. Molar ratios of hyaluronic acid, tyramine, EDC (catalyst) and NHS (activator) used for HA-Tyr grafting. COOH: carboxyl groups of hyaluronic acid.

Ratios	Tyr:COOH	EDC:COOH	EDC:Tyr	NHS:EDC
HA:Tyr 1:1	2:1	1:1	1:2	1:10
HA:Tyr 1:2	2:1	2:1	1:1	1:10
HA:Tyr 1:3	3:1	3:1	1:1	1:10

Based on 100 mg of HA and starting from the molecular weights of the reactants (M_{HA} = 401 g/mol, M_{Tyr}= 173.4 g/mol, M_{EDC} = 191.9 g/mol, M_{NHS} = 115.09 g/mol), the necessary quantities of each reagent were calculated for each of the ratios used. The results are shown in **Table 2.**

Table 2. Quantities of HA, tyramine, EDC and NHS for the synthesis of HA-Tyr grafting for each of the molar ratios used.

Ratios	HA (mg)	Tyr (mg)	EDC (mg)	NHS (mg)
HA:Tyr 1:1	100	86.54	47.77	2.87
HA:Tyr 1:2	100	86.54	95.57	5.73
HA:Tyr 1:3	100	129.86	143.36	8.60

The synthesis of hyaluronic acid tyramine grafting was performed following the procedure described by Darr and Calabro [60], with the molar ratios described in **Table 1**.

First, a solution of sodium chloride 150 mM was prepared in 20 mL of milliQ water. Then, 1.08 g of MES (0.276 mM in the final solution) and 0.3 mL of NaOH 5 M (75 mM in the final solution) were added. MES is a biological buffer that helps maintain the pH of the reaction.

The pH of the solution was adjusted to 5.75 and 100 mg of low molecular weight hyaluronic acid synthesized by acid degradation (0.05% w/v) was added. The solution was subsequently stirred at 500 rpm at room temperature for two hours to ensure dissolution of the hyaluronic acid.

After dissolution of the hyaluronic acid, the required amount of tyramine hydrochloride (Tyr·HCl) was added and the solution was kept under stirring for 20 minutes. The pH was then readjusted to 5.75 and the amount of NHS needed was added. After stirring the solution for about 30 minutes the EDC was added. The amounts of Tyr·HCl, NHS and EDC used, which depend on the molar ratio to be prepared, are given in **Table 2**.

Once all reagents were added, the solution was allowed to stir for 24 hours at 37 °C for the reaction to take place.

When the reaction was completed, the solution was introduced into a 3500 MWCO dialysis membrane. The purification of the product by the dialysis process was performed for two days with three daily washes, the first day with a solution of NaCl 150 mM and the second day with deionized water. Finally, the product was frozen and lyophilized for four days in order to remove the water.

The entire process of synthesis was done by covering with aluminium foil all the vials containing the solution, avoiding any contact of them with the light because of the photosensitivity of hyaluronic acid.

6.4. Synthesis of gelatin tyramine grafting (Gel-Tyr)

Gelatin tyramine grafting has the same purpose than hyaluronic acid tyramine grafting, to obtain terminal phenol groups capable of crosslinking in situ to give rise to the formation of injectable hydrogels.

The chemistry of the reaction is also the same. Carboxyl groups of gelatin react with amine groups of tyramine forming amide bond. Thus, the tyramine is grafted onto the gelatin leaving the phenol groups of the tyramine as terminal groups. A schematic of the reaction taking place is shown in **Figure 14**. In this case EDC is also used as the activator of the carboxyl groups of gelatin and NHS as the reaction catalyst.

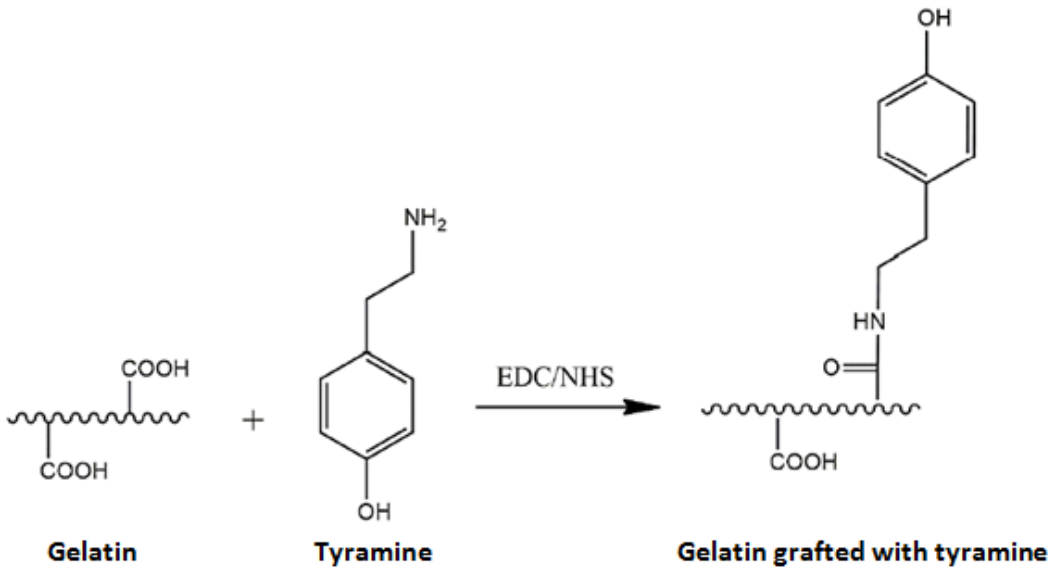

Figure 14. Gelatin tyramine grafting reaction. Reaction between carboxyl groups of gelatin and amine group of tyramine forming amide bond. NHS acts as a reaction catalyst and EDC as a reaction activator.

The synthesis of gelatin with tyramine graft was performed according to the procedure described by Sakai *et al* [87] introducing some modifications. The molar ratios used are shown in **Table 3**, where COOH refers to the carboxyl groups of gelatin.

Table 3. Molar ratios of gelatin, tyramine, EDC and NHS used for the gelatin tyramine grafting (Gel-Tyr).

Tyr:COOH	EDC:COOH	EDC:Tyr	NHS:EDC
2:1	2:1	1:1	1:10

For the synthesis of the Gel-Tyr graft, 0.4 g of gelatin (2 % w/v) and 19.24 mg of MES (50 mM) were first dissolved in 20 mL of water. MES is a biological buffer that helps maintain the pH of the reaction. The solution was kept under stirring for 30 min at 60 °C.

Once the solution was cooled to room temperature, 111.13 mg of tyramine hydrochloride (Tyr·HCl) were added and kept under stirring for 20 min ensuring complete dissolution of the reagent.

Then, the pH was adjusted to 6 and 7.36 mg of NHS were added and kept under stirring for 30 min. Finally, 122.68 mg of EDC were added and the solution was stirred at 37 °C for 24 hours for the grafting reaction to take place.

When the reaction was completed, the dialysis process was performed for the purpose of purifying the product by introducing the solution into a 12400 MWCO dialysis membrane. The process was carried out for 2 days performing three daily washes with deionized water.

Finally, the solution was frozen and lyophilized for four days in order to obtain a dried product for the subsequent synthesis of hydrogels.

6.5. Determination of molecular weight

After the synthesis process of low molecular weight hyaluronic acid as well as the synthesis process of this and gelatin with tyramine graft, it was necessary to determine the molecular weight of the products obtained in order to verify that the synthesis processes were carried out correctly.

The determination of the molecular weight was carried out by the Gel Permeation Chromatography (GPC) assay. The test was performed with the unit GPC Waters Breeze, consisting of waters 1525 binary HPLC pump, waters 2707 autosamples, waters 2489 UV/visible detector and waters 2414 refractive index detector from Waters corporation, Massachusetts.

The test was performed using columns of water at 35 °C with a flow rate of 1 mL/min of a solution of sodium chloride 150 mM and 0.05 % w/v sodium azide. The volume of the injections was 10 µL. The calibration curve was done from polyethylene glycol standards of known molecular weight. The procedure for calculating the molecular weight of the samples analysed after the performance of this test is presented in *Appendix I: Determination of molecular weight by gel permeation chromatography*.

6.6. Determination of tyramine grafting

Quantification of tyramine grafting in low molecular weight hyaluronic acid and gelatin was performed by spectroscopy assay using the dual visible/UV spectrophotometer Cecil CE9200 Super Aquarius, Buck Scientific, UK.

For this, the absorbance of the samples and the standards were measured in solutions 0.1% w/v in milliQ water using a wavelength of 275 nm, characteristic wavelength of the phenol groups. The procedure for calculating the degree of grafting of the samples analysed after the performance of this test is described in *Appendix I: Determination of tyramine graft degree.*

6.7. Synthesis of hyaluronic acid and/or gelatin injectable hydrogels (HA/Gel)

In this project, the synthesis of injectable hydrogels of hyaluronic acid and gelatin chemically crosslinked was carried out by an enzymatic reaction using the enzyme HRP and hydrogen peroxide (H_2O_2).

For their synthesis, the preparation of a buffer was firstly necessary. This buffer was later used for the preparation of different solutions from which the subsequent formation of the hydrogels would take place. The buffer used was the Calcium Free Krebs Ringer Buffer (CF-KRB), which was prepared in milliQ water and its composition in salts is shown in **Table 4**.

Table 4. Salts concentration of Calcium Free Krebs Ringer Buffer.

Salt	Concentration (mM)
NaCl	115
KCl	5
KH_2PO_4	1
HEPES	25

The solutions to be prepared are shown below:

i. **Gel-Tyr (2% w/v):** The solution is prepared to the desired concentration and left for 30 minutes in the oven at 37 °C to ensure dissolution of the gelatin in the buffer.

ii. **HA-Tyr (2% w/v):** The solution is prepared to the desired concentration and maintained for 24 h in a refrigerator at 4 °C to ensure dissolution of the hyaluronic acid in the buffer.

iii. **HRP (12.5 U/mL):** This solution is prepared to the required concentration just before being used for the formation of hydrogels, in order to avoid possible inactivation of the enzyme.

iv. **H_2O_2 (20mM):** The solution is prepared to the required concentration just prior to the synthesis of hydrogels so the solution used is fresh. In order to obtain this solution, a 100 mM aliquot of $H_2O_2$is prepared fist and the necessary volume of it is taken for the preparation of 20 mM hydrogen peroxide solution.

The composition of the hydrogels prepared was:

- 80% v/v of previously prepared solutions of HA-Tyr (2% w/v) or/and Gel-Tyr (2% w/v).
- 10% v/v of HRP solution (12.5 U/mL).
- 10% v/v of H_2O_2 solution (20 mM).

The hydrogels were synthesized in well plates with two different sizes depending on the final required sample size. 48-well plates were used for the preparation of samples with a

volume of 300 µL and 24-well plates for a volume of 750 µL. The gelatin/hyaluronic acid ratios in percent selected for the preparation of hydrogels were 0/100, 30/70, 50/50, 70/30, 100/0.

Once the solutions were prepared, the required amount of HA-Tyr (2% w/v) was added to the well plate first and then the Gel-Tyr solution (2% w/v). After that, the HRP solution was added and the mixture was homogenized. Finally, the H_2O_2 solution was added taking place the cross-linking reaction and resulting in the formation of the hydrogel in few minutes.

After that time, with the help of a spatula the gel was firstly detached from the walls and after from the base of the well, placed in a vial with deionized water and stored in a refrigerator in order to avoid the growth of microorganisms and bacteria in the hydrogel.

6.8. Preparation of samples for the analysis

With the purpose of studying the behaviour of hydrogels at different relative humidities, it was first necessary to remove the water from the hydrogels with the freeze extraction method, dry them and then place them in environments with different relative humidities. Here below we explain the phases of the procedure applied.

6.8.1. Freeze extraction method and drying phase

In the drying phase, once the hydrogels were synthesized and placed overnight in deionized water, the freeze extraction process was performed to remove water from the hydrogel and obtain a porous material.

The freeze extraction process is a phase separation method that aims to obtain a porous structure material under freezing conditions. The principle of this method is based on the extraction of a solvent through a non-solvent, in our case the water and ethanol. [88]In this way, the frozen water will dissolve in the ethanol at low temperature and the spaces occupied by water in the hydrogel will now be occupied by ethanol. Once all the solvent has been replaced in the hydrogel by the non-solvent, the elimination of this one can be carried out leaving the spaces where the ethanol was as the pores of the hydrogel.

To carry out this process, the hydrogels were frozen for 2 hours at -20 ° C. Washing is then performed on the hydrogels with ethanol at -20 °C every 45 minutes for three hours, to ensure that all the water frozen in the hydrogels was dissolved in the ethanol. Finally, the hydrogels were introduced into a vacuum oven at room temperature for 48 hours to remove the ethanol.

6.8.2. Placing of materials at different relative humidities

After the hydrogels were dried, they were weighted and placed in hermetically sealed jars into which a solution of a saturated salt had been previously introduced and equilibrated. The solutions of saturated salts present a critical relative humidity to which the salt begins to absorb the humidity of the medium. This relative humidity is a unique property of salt and

depends mainly on temperature. Therefore, by using different salts at a certain temperature, known values of relative humidity can be achieved in the closed environment of the jars. **Figure 15** shows a scheme of a relative humidity jar into which the samples and the required saturated solution were placed.

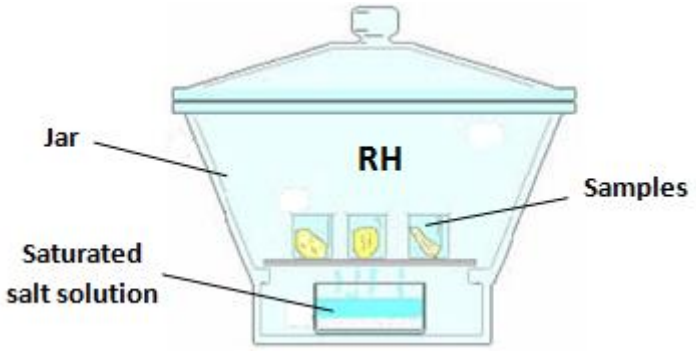

Figure 15. Scheme of a relative humidity jar.

Table 5 shows the relative humidities and solutions used to reach these humidities. Samples were held for 7 days at these humidities in order to achieve equilibrium water content.

Table 5. Relative humidities and solutions used.

Relative Humidity (%)	Solution
0	P_2O_5
65	$CoCl_2$
85	KCl
98	K_2SO_4

Samples with 100% relative humidity were also prepared. For this, directly after drying the samples in a vacuum oven at room temperature for two days, they were immersed overnight in distilled water. These samples were only used for the measurement of the equilibrium water content and the water fraction and the comparison of the freeze-extraction and freeze-drying method, which is explained below.

6.8.3. Freeze-drying method

Another method that was used for the preparation of the samples once hydrogels were synthesized is freeze-drying method. This method was only used for the comparison of the two methods in terms of equilibrium water content and water fraction obtained from the samples when they are directly submerged in distilled water.

To perform this method, once the hydrogels were synthesized according to section 6.7, they were immersed in distilled water overnight and then the freeze-drying method was carried out, which consisted in freezing the hydrogels for three hours at -80 °C and then sublimate the water by lyophilizing them with a LyoQuest equipment (Telstar Life Science Solutions, Japan).

6.9. Morphology

The morphology and microstructure of the synthesized hydrogels was observed through Field Emission Scanning Electron Microscopy (FESEM).

To do this, the freeze dried hydrogels were dried in a vacuum oven and cut with the aid of a blade to observe its internal structure. The sections obtained were coated with platinum at 40 mA for 90 seconds and observed using a JEM 2100F (JEOL Ltd., Japan) microscope at a working voltage of 2 kV.

6.10. Equilibrium water content

As explained in section 6.8, equilibrium water content of the hydrogels was measured from hydrogels synthesized by freeze-extraction method and freeze drying method. The following explains how it was calculated for each of the methods used.

In the case of freeze extraction method, once the hydrogels were synthesized and the drying phase was performed, they were weighed in a precision balance to obtain the dry weight (m_d).

They were then placed in hermetically sealed jars into which a solution of a saturated salt solution had previously been introduced to achieve a specific relative humidity (RH). Samples were maintained for 7 days to reach equilibrium water content. After this period, they were weighed to obtain the wet weight (m_w). For the samples at 100% relative humidity, instead of maintaining them in relative humidity jars for 7 days, they were submerged in distilled water overnight in a refrigerator at 4 °C and were weighed to obtain the wet weight (m_w).

For the samples synthesized by freeze-drying method, the samples were introduced directly after being synthesized in vials with distilled water and kept overnight in a refrigerator at 4 °C until reaching equilibrium water content. After that time, they were removed from the vials, the excess water was removed from the surface of the hydrogels with a paper and the hydrogels were weighed to obtain the wet weight (m_w).

After that, samples were frozen for three hours at - 80 °C and lyophilized for one day in order to remove the water. Then, they were weighed in a precision balance to obtain the dry weight (m_d).

Finally, the equilibrium water content (EWC) and the water fraction (hw) were calculated by the Equation 1 and Equation 2 respectively. All data on wet mass, dry mass, equilibrium water content and water fraction of the samples tested are shown in *Appendix III: Determination of water fraction and equilibrium water content.*

$$EWC\ (\%) = \frac{m_w - m_d}{m_d} \cdot 100 \qquad (1)$$

$$hw\ (\%) = \frac{m_w - m_d}{m_w} \cdot 100 \quad (2)$$

6.11. DSC Measurements

Among the thermal analysis techniques, Differential Scanning Calorimetry(DSC) is the most versatile since it covers many aspects such as qualitative and quantitative identification of materials, the study of thermal processes such as phase changes or glass transition or the study of degradation. [81]

In this technique, when a sample and an inert reference material are heated or cooled at a constant rate, energy changes that the sample undergoes with respect to the reference material are recorded. These results give direct information of the processes observed in the material and, therefore, of the behaviour of this one. In this way, as shown in **Figure 16**, glass transition process appears as a heat capacity step and phase processes as a peak. Specifically, an endothermic peak will be found in the case of melting process and an exothermic peak in the case of crystallization process.

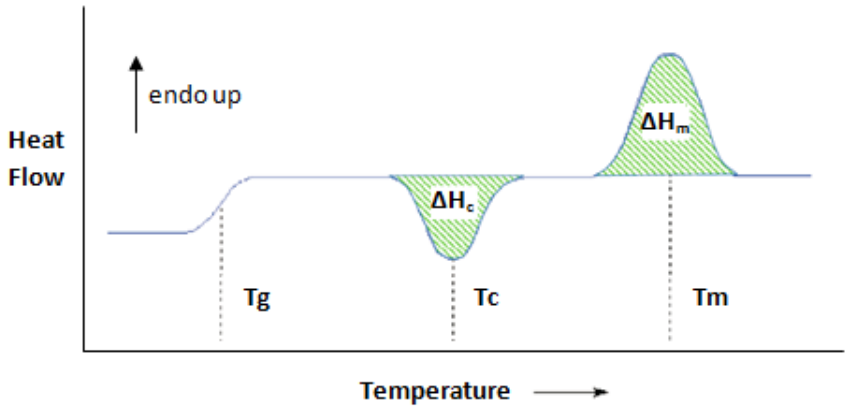

Figure 16. Thermogram with the typical thermal processes observed in a polymer. From left to right, glass transition, crystallization and melting process are shown.

Heat flow results were normalized dividing by heating rate and mass of the sample according to Equation 3.

$$H_n = \frac{H}{m \cdot r} \quad (3)$$

Where H_n is the normalized heat flow in J/g·K, H is the measured heat flow in mW, m is the sample mass in mg and r is the cooling or heating rate in K/min.

Each measurement was performed in a TA Q200 Modulated Differential Scanning Calorimeter instrument (TA Instruments), using liquid nitrogen to control the temperature and

helium as a purge gas with a rate of 25 ml/min. The samples were introduced in Tzero Low Mass Hermetic Aluminium pans (TA Instruments).

Two thermal cycles were performed for each measurement. The first cycle consisted of a cooling from 20 °C to - 150 °C and a heating from - 150 °C to 130 °C. The second cycle was carried out with a cooling from 130 °C to - 150 °C and a heating of - 150 °C to 130 °C. Both cycles were performed with a constant heating rate of 10 °C/min.

6.12. Statistic analysis

Statistical analysis of the results was performed to determine the significance of the differences observed between them. For this, the analysis of variance and multiple rank tests with a p-value < 0.05 was used with Statgraphic software.

7. RESULTS AND DISCUSSION

7.1. Quantification of HA and Gelatin molecular weight

In order to improve the mixing of gelatin and hyaluronic acid in the synthesis of hydrogels, the first step in the synthesis process is based on the reduction of the molecular weight of hyaluronic acid by acid degradation. With this process the viscosity and molecular weight of hyaluronic acid are reduced to a value similar to gelatin.

To ensure that such degradation was carried out suitably, the molecular weight of hyaluronic acid before and after the degradation process (HA and HA-LMW respectively) and gelatin was measured by the GPC test. The results are shown in **Figure 17**. The procedure carried out for the determination of molecular weights is explained in detail in *Appendix I: Determination of molecular weight by gel permeation chromatography*.

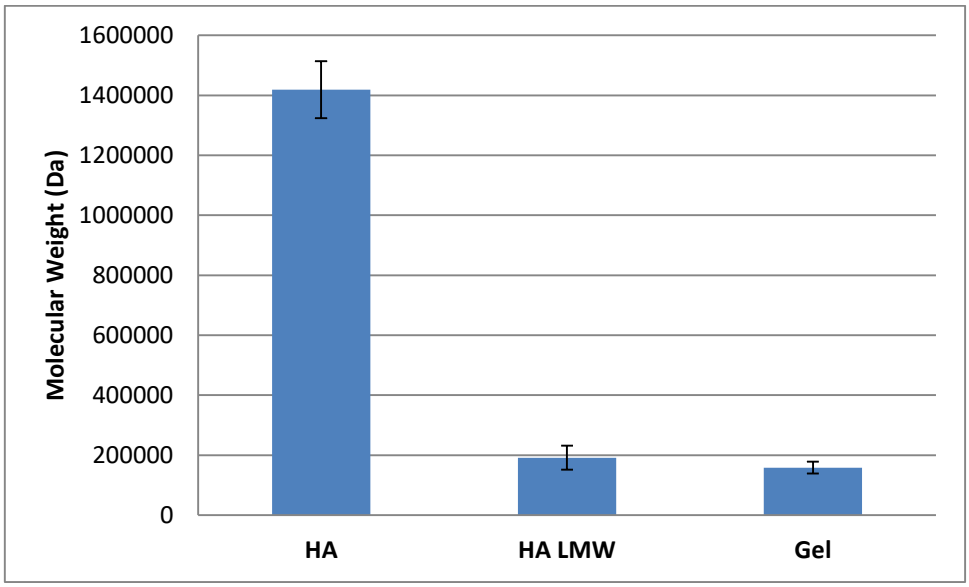

Figure 17. Molecular weight of hyaluronic acid (HA), gelatin (Gel) and hyaluronic acid synthesized by the acid degradation process (HA-LMW) measured by GPC test. Four samples of each component were measured (n=4).

After the GPC test, a molecular weight of 159,000 Da was obtained for gelatin and 1.410,000 Da and 192,000 Da for hyaluronic acid before and after degradation respectively. According to the obtained results, it can be corroborated that the degradation carried out in a suitable way since the reduction of the molecular weight of the hyaluronic acid can be reported, obtaining a value higher but close to the value of the gelatin.

Once the molecular weight of the hyaluronic acid was reduced, tyramine (Tyr) grafting was performed on the HA chains for HA:Tyr molar ratios 1:1, 1:2, 1:3 (explained in section 6.3) and gelatin chains for a molar ratio Gel: Tyr 1: 2 (section 6.4). After such synthesis processes, the GPC test was also performed to notify if any relevant changes in the molecular weight of the samples had taken place. The results obtained are shown in **Figure 18**.

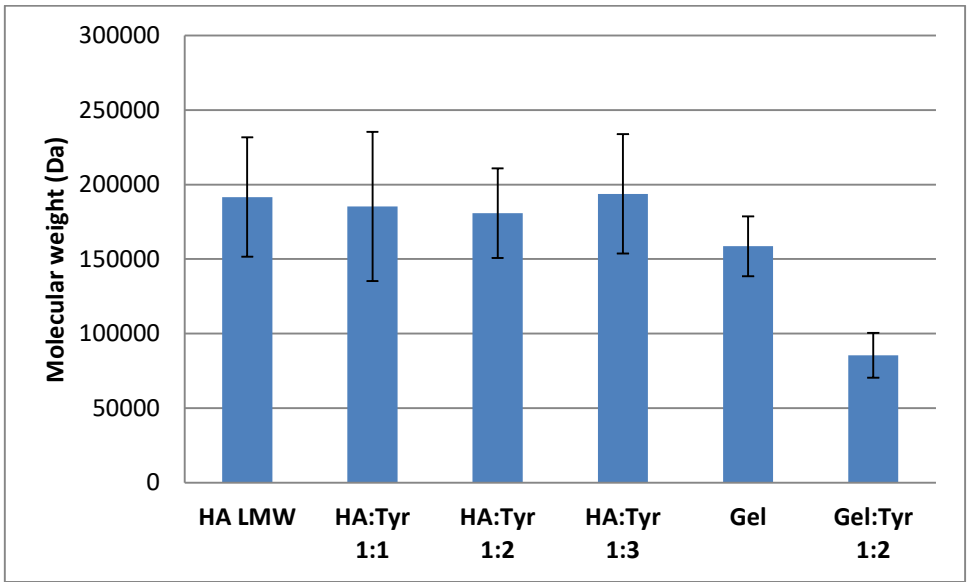

Figure 18. Molecular weight of hyaluronic acid after degradation (HA LMW), gelatin (Gel), hyaluronic acid with tyramine graft for HA:Tyr 1:1, 1:2, 1:3 molar ratios and gelatin with tyramine graft for Gel:Tyr 1:2 molar ratio measured by GPC test. Four samples of each component were measured (n=4).

The molecular weight obtained after the tyramine graft in hyaluronic acid is 185,000 Da for the molar ratio HA:Tyr 1:1, 181,000 Da for HA:Tyr 1:2 and 194,000 Da for HA:Tyr 1:3. These values are quite similar to the molecular weight of the HA prior to the tyramine grafting, so the tyramine graft does not significantly affect the molecular weight of the samples.

As for gelatin, the tyramine grafting produced a decrease in the molecular weight of the sample from 159,000 Da to 85,000 Da after the grafting. Although the grafting reaction incorporates new molecules into the gelatin chains, which could increase its molecular weight, a decrease is observed due to the hydrolysis and the possible degradation of the gelatin chains because of a second stage of synthesis for the incorporation of tyramine molecules.

7.2. Quantification of tyramine grafting

After the synthesis of hyaluronic acid and gelatin with tyramine graft, the quantification of the degree of grafting was necessary to know how many carboxyl groups of hyaluronic acid and gelatin had been substituted by the phenol groups of tyramine.

For this purpose, UV spectroscopy test was performed at 275 nm, characteristic wavelength of the phenol groups of tyramine. The process carried out for the preparation of the samples and the standard curve required for the calculation of results is explained in detail in *Appendix II: Determination of tyramine graft degree.*

The synthesis of HA-Tyr grafted was carried out at three different molar ratios in order to compare the results to obtain a degree of substitution similar to that obtained for gelatin.

Table 6 shows the results achieved for the three molar ratios used for hyaluronic acid as well as that used for gelatin.

Table 6. Tyramine grafting in hyaluronic acid and gelatin expressed in mg/mL, mol/mL and substitution degree.

Molar ratio	Tyramine Injerted (mg/mL)	Tyramine Injerted (mol/mL)	Substitution degree (%)
HA:Tyr 1:1	0,0192 ± 7.3E-4	$1{,}40 \cdot 10^{-7} \pm$ 1.3E-9	10,11 ± 1.2
HA:Tyr 1:2	0,0268 ± 4.2E-5	$1{,}95 \cdot 10^{-7} \pm$ 7.3E-10	14,10 ± 0.9
HA:Tyr 1:3	0,0271 ± 8.9E-5	$1{,}97 \cdot 10^{-7} \pm$ 4.4E-10	14,23 ± 1.0
Gel:Tyr 1:2	0,0261 ± 3.7E-3	$2{,}26 \cdot 10^{-7} \pm$ 2.7E-8	28,55 ± 2.4

As it can be seen, the higher degree of substitution is obtained for gelatin. As for hyaluronic acid, the degree of substitution increases as the molar ratio increases. However, the most notable change is observed between the use of a 1:1 and 1:2 ratios, being the result obtained for 1:2 or 1:3 ratio almost similar.

With the results obtained on the degree of tyramine grafting for the different molar ratios of hyaluronic acid, it was decided to characterize the HA/Gel hydrogel series with molar ratios HA:Tyr 1:1 and 1:2. The molar ratio HA:Tyr 1:3 was excluded due to the similar results obtained with respect to 1:2. In the following sections of results will be shown the results obtained for the HA/Gel hydrogel series with molar ratio 1:1. The series HA:Tyr 1:2 will be carried out later in collaboration with the University of Athens.

7.3. Morphology of HA/Gel hydrogels

The synthesis of hydrogels was performed following the procedure described in section 6.7. Hydrogels were synthesized over the entire range of HA/Gel compositions from a pure gelatin hydrogel (100/0) to a pure hyaluronic acid hydrogel (0/100). The macroscopic and microscopic (FESEM) appearance of the hydrogels obtained can be seen in **Figure 19**.

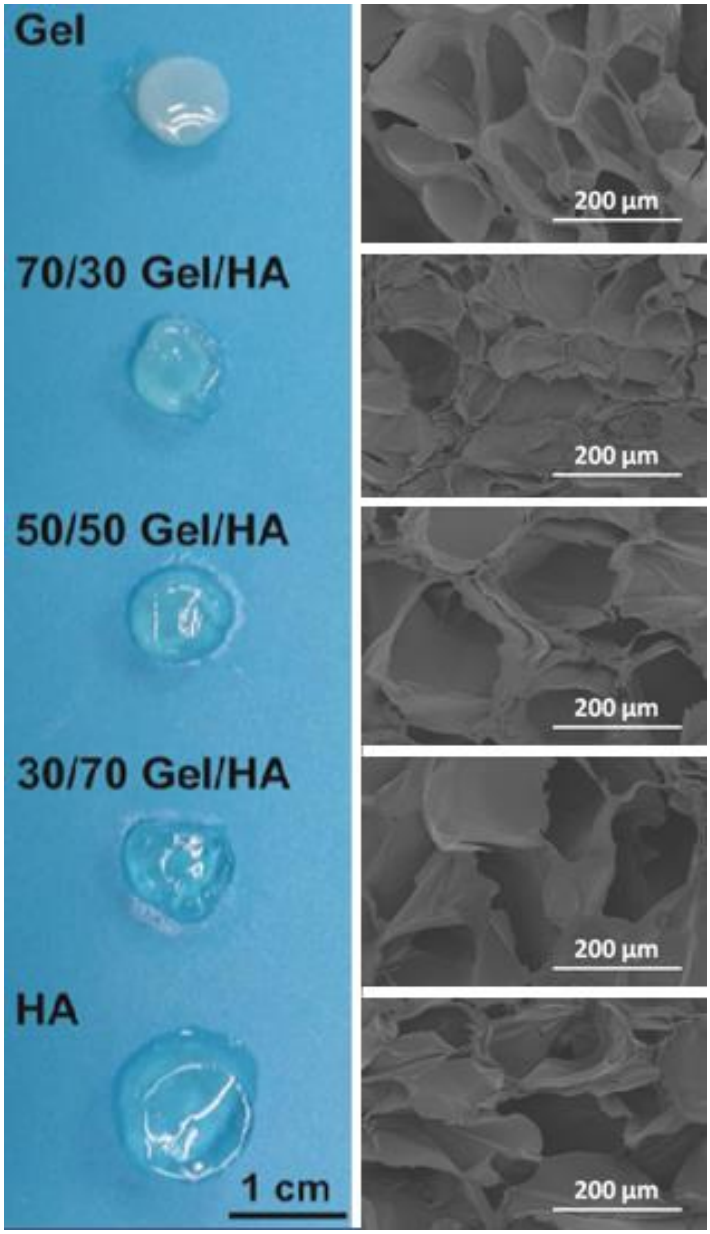

Figure 19. Series of HA/Gel hydrogels. Macroscopic appearance after 24 h of swelling in water (left) and cross-sectional microstructure observed by FESEM after performing freeze extraction method and drying them in an oven for 2 days at room temperature (right).

As to its macroscopic appearance, it is observed that, after gelation, pure gelatin hydrogels have a whiter and opaque coloration whereas pure hyaluronic acid hydrogels are transparent. Hydrogels containing both components (HA/Gel: 70/30, 50/50 and 30/70) have an intermediate blend coloration, with a greater or lesser degree of opacity depending on their gelatin content.

On the other hand, it is possible to emphasize the differences of size present in the synthesized hydrogels. As it is shown in the section 6.8, after synthesizing the hydrogels, they were either dried in an oven with vacuum and then placed at different relative humidities or directly immersed in distilled water overnight. In both cases, the size of the hydrogels containing a higher proportion of hyaluronic acid was appreciably higher than the hydrogels which

possessed higher content in gelatin. This fact is due to the higher hydrophilicity of the hyaluronic acid chains and hence the greater water retention capacity of them.

Finally, it was also possible to ascertain macroscopically that the appearance of the hydrogels was homogeneous, without observing phase separation of the components. This hypothesis can also be verified with greater certainty from the images of the microstructure of the hydrogels obtained by Field Emission Scanning Electron Microscopy (FESEM) of **Figure 19**. These images show a honeycomb microstructure of pores with a homogeneous size distribution for each of the samples. However, the pores are not fully interconnected as Poveda-reyes *et. al* show [71]. This may be due to the use of a different method of preparing the hydrogel. Thus, while they use the freez-drying method, in this case freeze-extraction method was used, which could lead to partial collapse of the pores of the samples during the removal phase of ethanol.

To measure the pore size, three replicates of each composition were analysed by ImageJ program, counting the pores of three images of each replicate (approximately 150 pores per composition). The results can be seen in **Table 7**.

Table 7. Average pore size obtained for HA/Gel hydrogels series from FESEM images using ImageJ software. Three replicates of each composition were analysed, counting the pores of 3 images of each replicate (approximately 150 pores per composition).

HA/Gel	Pore size (µm)
0/100	71.8 ± 3.6
30/70	73.8 ± 5.4
50/50	78.0 ± 7.2
70/30	81.6 ± 9.3
100/0	78.1 ± 8.2

According to the results, it is verified that the addition of hyaluronic acid to pure gelatin hydrogels causes an increase in the size of the internal pores of its microstructure. Again, this fact may be related to the greater water retention capacity of hyaluronic acid. As the section of the hydrogels observed has been previously frozen, the pore size and internal cavities of the hydrogels may be due to the removal of the previously formed water crystals. Thus, since hyaluronic acid is able to retain a greater amount of water, the water domains and water crystals inside it are larger, generating larger cavities and pores when the water is frozen.

The statistical analysis of the results obtained shows two distinct groups. On the one hand, the HA/Gel 0/100, and 30/70 hydrogels do not present statistically significant differences in mean pore size, obtaining an average size of 72 µm. On the other hand, the HA/Gel 50/50, 70/30 and 100/0 hydrogels, whose main component is hyaluronic acid, have an average size of 79 µm. The difference in mean pore size of both groups is statistically significant.

Regarding the pore size, pore sizes around 75 µm have been obtained. These results are higher than other studies presented in the literature for similar hydrogel systems. [71], [89], [90] This may be because the freeze extraction method was used in this project to prepare the hydrogels while in the other studies the samples were directly lyophilized.

In any case, the pore structure the synthesized hydrogels present allows diffusion through the material which facilitates the transport of nutrients necessary for cellular viability.

7.4. HA/Gel hydrogels equilibrium water content

7.4.1. Comparison of the equilibrium water content at different relatives humidities

Water fraction (hw) and equilibrium water content (EWC) of HA/Gel hydrogels systems at different relative humidities were calculated as described in section 6.10. For this, 3 replicates of each composition were measured. The results of EWC and hw of the different HA/Gel compositions with a molar ratio HA:Tyr 1:1 at 65%, 85% and 98% relative humidity and in immersion are shown in **Figure 20** and **Figure 21.**

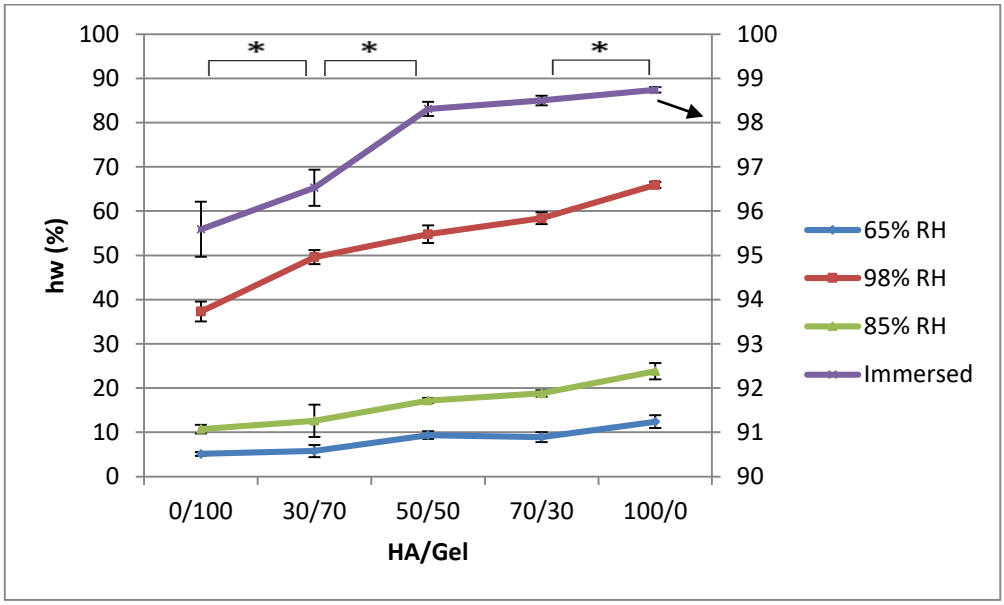

Figure 20. Water fraction (hw) of the different HA/Gel compositions at 65%, 85% and 98% RH and immersion of samples with molar ratio HA:Tyr 1:1.The values of the HA/Gel compositions at 65%, 85% and 98% RH are shown in the main axis while the values of HA/Gel compositions immersed in distilled water (purple line) are shown in the secondary axis. Three samples of each component were measured (n=3). * indicates statistically significant difference between groups marked.

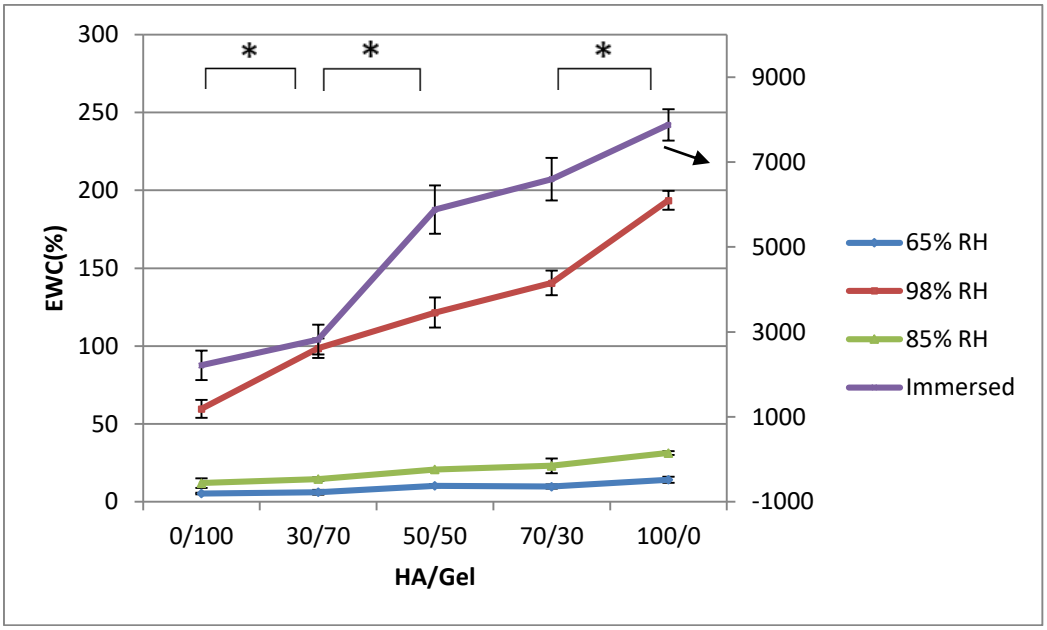

Figure 21. Equilibrium water content (EWC) of the different HA/Gel compositions at 65%, 85% and 98% RH and immersion of samples with molar ratio HA:Tyr 1:1.The values of the HA/Gel compositions at 65%, 85% and 98% RH are shown in the main axis while the values of HA/Gel compositions immersed in distilled water (purple line) are shown in the secondary axis. Three samples of each component were measured (n=3). * indicates statistically significant difference between groups marked.

In **Figure 20**, two main conclusions can be drawn about the water fraction present in the synthesized hydrogels. On the one hand, it can be seen that, for each of the relative humidities, water fraction increases as the amount of hyaluronic acid present in the hydrogel increases. This is because, as already explained above, hyaluronic acid has a higher hydrophilicity than gelatin and can retain larger amounts of water. Furthermore, the degree of tyramine substitution for HA is lower than for gelatin and consequently the crosslinking degree of HA gels is lower than for gelatin, giving rise to hydrogel networks with higher capacity to absorb water. It should be noticed that there is a significant difference between the water fractions for each HA/Gel compositions analysed except in the case of the compositions HA/Gel 50/50 and 70/30, where the values obtained were very similar independently of the relative humidity used.

On the other hand, an increase in the water fraction of the samples can be observed as the relative humidity of the medium in which they were placed increases. For the samples that were at 65% RH, a water fraction of 10 % was obtained. When these were placed at 85 % RH, a water fraction of 20 % was reached, twice as much as in the previous case. When the relative humidity was increased to 98 %, the fraction of water obtained in the samples increased considerably to about 55 %. Finally, when they were introduced directly into distilled water, more than 96 % of their mass corresponded to the water housed inside of them. Note that the values of immersion are represented in the secondary Y axis, and are quite different from those at the other relative humidities.

Figure 21 shows the equilibrium water content of the synthesized hydrogels in relation to their dry mass. While EWC of pure gelatin hydrogels is 5.4 %, 12.05 %, 59.71 % and 2214.53 % for 65 % RH, 85 % RH, 98 % RH and immersion respectively, EWC of pure hyaluronic acid

hydrogels have a value of 14.19 %, 31.39 %, 193.56 % and 7875.94 %. EWC values of the mixtures are between the values obtained for the two pure components. Thereby, hyaluronic acid is a more hygroscopic material and is less crosslinked so that hydrogels with higher content in HA are able to retain a greater amount of water in equilibrium which is related to the larger pore size observed for these hydrogels.

The equilibrium water contents at immersion are much higher than those at the different relative humidities because of two facts. On the one hand, this is the only environment that allows the existence of pure or bulk water domains within the networks completely filling the pores generated at freeze-extraction. On the other hand, in this environment the networks are more extended than in the other conditions, having the possibility to lodge larger amounts of water in them than at relative humidities lower than 100%.

7.4.2. Comparison of freeze-extraction and freeze-drying method

Water fraction (hw) and equilibrium water content (EWC) of HA/Gel hydrogels systems immersed in distilled water using freeze-extraction and freeze-drying method were calculated as described in section 6.10. For this, 5 replicates of each composition were measured. The results are shown in **Figure 22** and **Figure 23**.

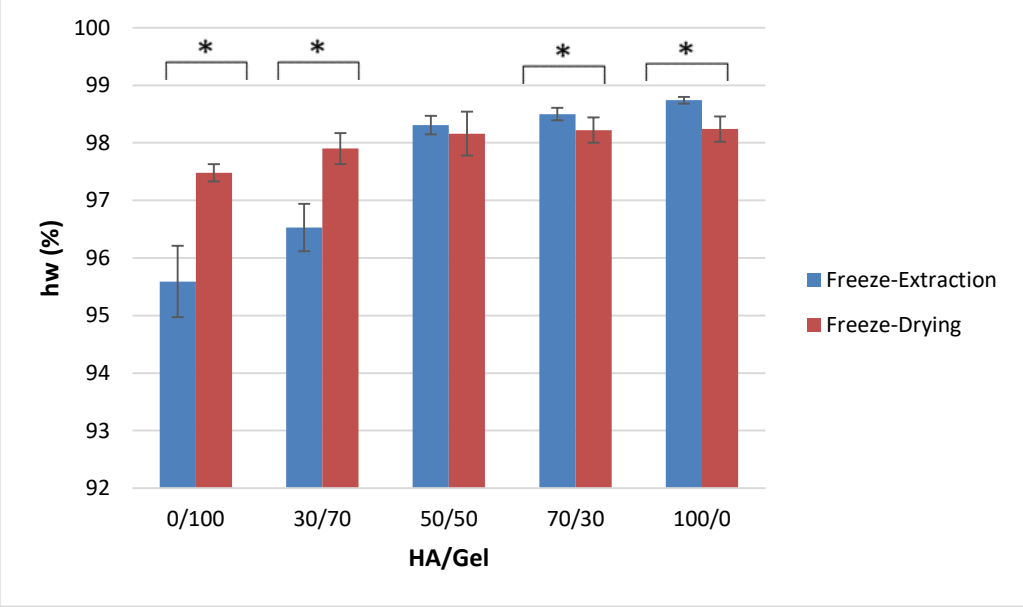

Figure 22. Water fraction (hw) of the different HA/Gel compositions with molar ratio HA:Tyr 1:1 immersed directly in distilled water using freeze-extraction method and freeze-drying method. Three samples of each component were measured (n=3). * indicates statistically significant difference between groups marked.

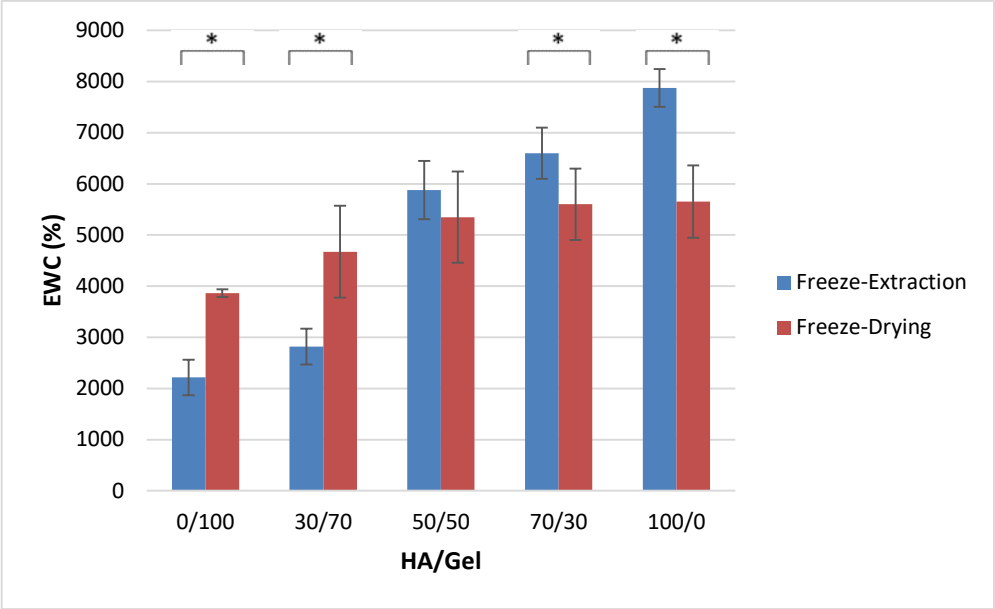

Figure 23. Equilibrium water content (EWC) of the different HA/Gel compositions with molar ratio HA:Tyr 1:1 immersed directly in distilled water using freeze-extraction method and freeze-drying method. Three samples of each component were measured (n=3). * indicates statistically significant difference between groups marked.

In **Figure 22** it can be seen that when samples are immersed in distilled water using freeze-extraction or freeze-drying method, they reach a water fraction above 95% in all cases, being this value higher as the content of hyaluronic acid in the hydrogel increases. In this way, samples of pure hyaluronic acid reached a water fraction of 98.74 % when the freeze-extraction method was used and 98.24 % when freeze-drying method was used.

For HA/Gel compositions containing at least 50 % of hyaluronic acid, it can be observed that water fraction obtained with freeze-extraction method is higher than using freeze-drying method, although the difference obtained for the composition 50/50 using either method is not significant. However, for pure gelatin hydrogels or those with 70% of this component, a very pronounced decrease of the water content is observed when freeze-extraction method is used. This reduction in the amount of water retained by the hydrogels is associated with the fact that mechanical modulus of gelatin is lower than hyaluronic acid modulus and the structure of these hydrogels collapses to the conditions under which freeze-extraction method was performed. In freeze-extraction method, samples were frozen at -20 °C and then dried at room temperature. In contrast, this collapse is not as pronounced in the case of the use of the freeze-drying method since this process was carried out at - 80 ° C, a lower temperature. The collapse of the networks is not completely recuperated when placing them in immersion, and the equilibrium water content is lower. A similar result was observed in [91] when gelatin equilibrium water content of dried samples at room conditions was compared with that of lyophilized samples.

As for the equilibrium water content shown in **Figure 23**, values of 2214.53 % and 3865.83 % for pure gelatin and 7875.94 % and 5653.80 % for the pure HA were obtained for the freeze extraction and freeze drying method respectively. For the mixtures, intermediate values were obtained between the two pure components. The results obtained were consistent with other studies that appear in the literature. [39], [21], [92] For example, Lee *et al*. obtained HA-

Tyr hydrogels with equilibrium water content between 3000 % and 6000 % varying the concentration of hydrogen peroxide. [93] On the other hand, Wang *et al*. presented HRP crosslinked gelatin hydrogels with a EWC of 3000%. [94]

7.5. DSC of HA/Gel hydrogels

In order to study the interactions of the polymer with the water they are able to absorb and the miscibility between hyaluronic acid and gelatin, DSC measurements were performed on the series HA/Gel with a molar ratio HA:Tyr 1:1.

To do this, the samples were placed at different relative humidities in order to simulate the environment in which they would be found in the different tissues. The tissues are composed mainly of a mixture of water and salts, having a water activity less than one and being the amount of water present in them greater or lesser depending on the type of tissue. Samples were studied at 0%, 65%, 85% and 98% relatives humidities. The results are shown below.

- **0% RH (DRY)**

First of all, DSC test of dry samples was performed. **Figure 24** and **Figure 25** show the thermograms obtained for second cooling and heating processes respectively.

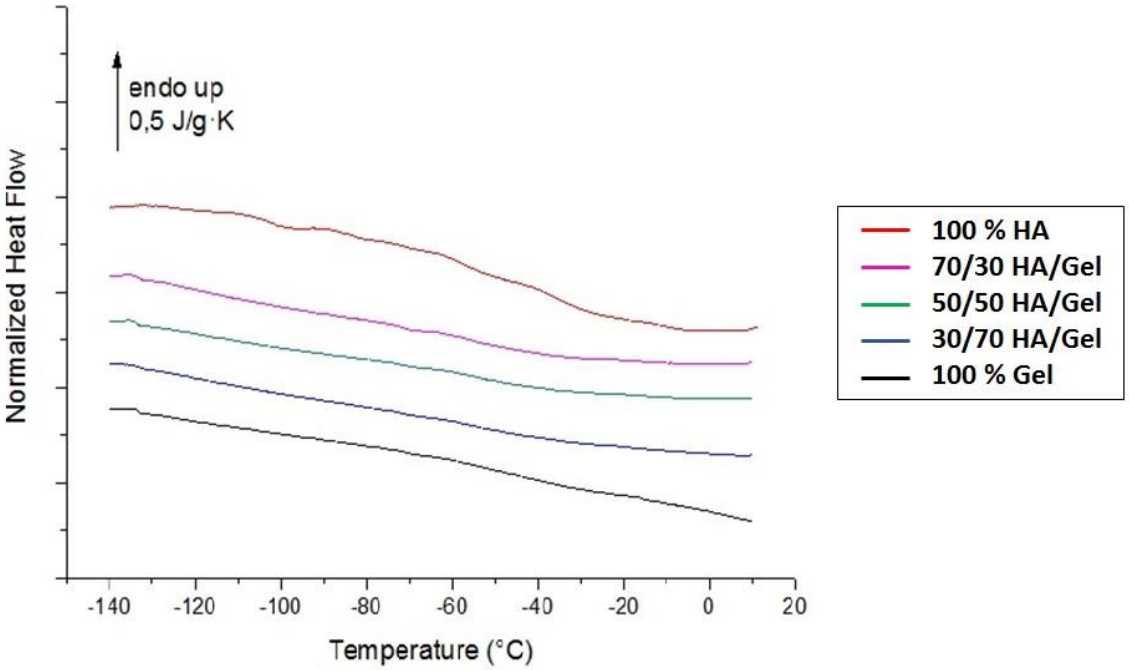

Figure 24. DSC thermogram during second cooling at a heating rate of 10 °C/min for the series HA/Gel hydrogels with molar ratio HA:Tyr 1:1 at 0% RH. 'Y' axis shows the heat flow in J/g·K and 'X' axis shows temperature in °C.

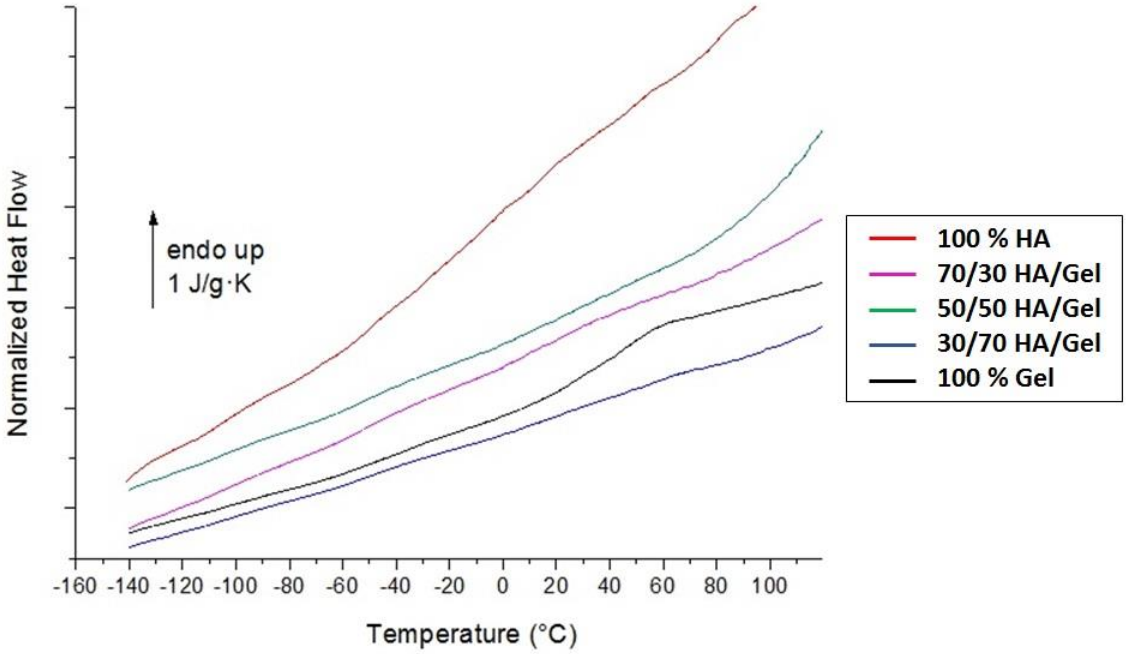

Figure 25. DSC thermogram during second heating at a heating rate of 10 °C/min for the series HA/Gel hydrogels with molar ratio HA:Tyr 1:1 at 0% RH. 'Y' axis shows the normalized heat flow in J/g·K and 'X' axis shows temperature in °C.

For the determination of the glass transition temperature, the first derivative of the normalized heat flow with respect to the temperature was plotted (dH_n/dT) and the maximum was taken as glass transition temperature (Tg). Then, the baselines of the thermogram before and after the transition step were extrapolated and a vertical line at Tg was drawn. The jump measured between the intersection of the vertical line at Tg and the baselines was considered to calculate the change in the heat capacity (ΔCp). [95]

Due to the rigidity of hyaluronic acid chains, it does not present any glass transition in the dry state. [96] However, P_2O_5 salt solution is not able to keep 0% humidity and the few traces of water present in the jars make the samples to absorb a small amount of water that is sufficient to plasticize the HA chains giving rise to a subtle glass Tg at a very low temperature, -48.5˚C. Gelatin shows a clear glass transition at 43 ˚C.

At this relative humidity, only a glass transition of the two pure components was found in the heating process. Glass transition temperature and increment of the heat capacity between the glass and rubber states for the pure hydrogels are shown in **Table 8**.

Table 8. Glass transition temperature (Tg) and increment of the heat capacity (ΔCp) seen during second heating at a heating rate of 10 ˚C/min for the HA/Gel series with molar ratio HA:Tyr 1:1 at 0% RH.

	Tg (°C)	ΔCp (J/g·K)
Gel	43	0.36
HA	- 48.5	0.33

When a polymeric mixture is homogeneously mixed a single broad glass transition between that of the pure components is observed. Completely phase separated mixtures, with domains larger than the minimum size for cooperative motion, present two glass transition

temperatures at the same temperature as the pure components. Partially separated mixtures can present two glass transitions slightly moved to the temperatures between those of pure components. [79], [97], [98] In our case no glass transition of domains rich in hyaluronic acid and gelatin was found in the mixtures, which allows us to conclude that they present a good miscibility between the two components. Besides that, we cannot see a clear glass transition between those of pure components for the hydrogels mixtures, probably due to the rigidity of hyaluronic chains at this relative humidity that constrain the movement of the perfectly mixed domains.

On the other hand, no crystallization or melting process due to water was observed. This is logical since the hydrogels were very dry and only traces of non-crystallisable water can be present in the polymer networks.

- **65% RH**

After having samples for 7 days at 65% relative humidity, water fraction and equilibrium water content obtained in each sample is shown in **Table 9**.

Table 9. Equilibrium water content (EWC) and water fraction (hw) of HA/Gel series with molar ratio HA:Tyr 1:1 at 65% RH.

HA/Gel	EWC(%)	hw(%)
0/100	5.4 ± 0.49	5.12 ± 0.45
30/70	6.16 ± 1.55	5.78 ± 1.39
50/50	10.35 ± 1.04	9.37 ± 0.85
70/30	9.81 ± 1.37	8.92 ± 1.13
100/0	14.19 ± 1.87	12.41 ± 1.45

The thermograms obtained for the second cooling and heating processes are showed in **Figure 26** and **Figure 27** respectively.

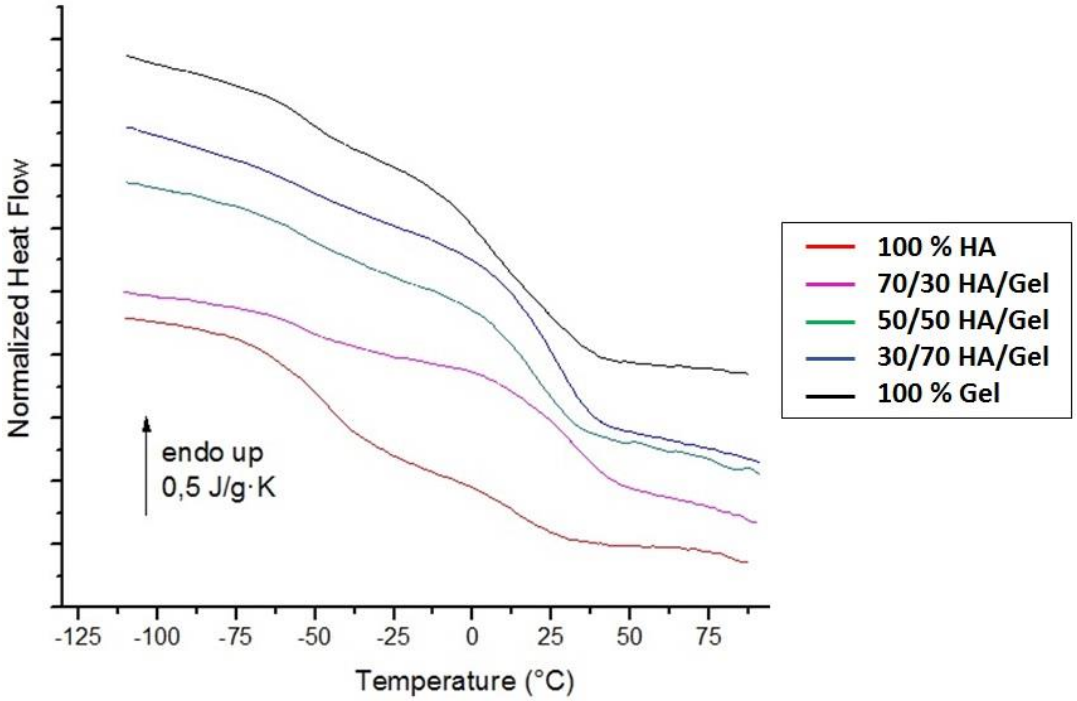

Figure 26. DSC thermogram during cooling at a heating rate of 10 °C/min for the series HA/Gel hydrogels with molar ratio HA:Tyr 1:1 at 65% RH. 'Y' axis shows the normalized heat flow in J/g·K and 'X' axis shows temperature in °C.

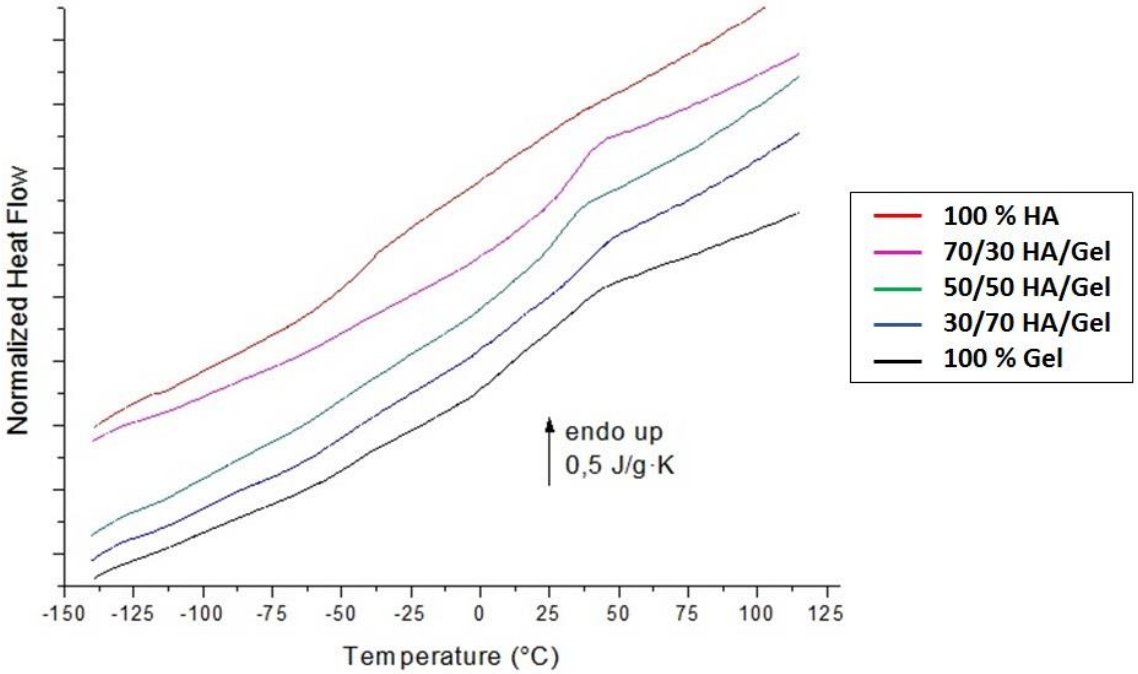

Figure 27. DSC thermogram during heating at a heating rate of 10 °C/min for the series HA/Gel hydrogels with molar ratio HA:Tyr 1:1 at 65% RH. 'Y' axis shows the normalized heat flow in J/g·K and 'X' axis shows temperature in °C.

In this case, a glass transition was observed both in the pure components and in the mixtures. In the case of the mixtures, also a subtle glass transition at temperatures close to that of hyaluronic acid seems to be observed, but was not considered for the calculus as is very

subtle. The value of Tg and ΔCp of these processes were quantified from the thermogram obtained in the second heating process (**Table 10**).

Table 10. Glass transition temperature (Tg) and increment of the capacity (ΔCp) seen during second heating at a heating rate of 10 °C/min for the series HA/Gel hydrogels with molar ratio HA:Tyr 1:1 at 65% RH.

HA/Gel (%)	Tg (°C)	ΔCp (J/g·K)
0/100	36	0.38
30/70	35	0.30
50/50	29	0.22
70/30	26	0.28
100/0	-38	0.25

When the samples are equilibrated in 65% relative humidity, water molecules absorb in the polymeric chains and provoke their movement, a phenomenon known as plasticization. In this situation, gelatin chains tend to join together and also hyaluronic acid ones, due to their chemical affinity. This provokes a certain phase separation in the mixtures giving rise to a clear glass transition of the domains rich in gelatin and a very slight (almost incalculable) glass transition of the formed hyaluronic acid domains. As in the case of dry mixtures samples, the glass transition of hyaluronic acid cannot be calculated in the heating process and is very subtle, because the unrelaxing domains of gelatin constrain their relaxation and movement. However, it is possible to see the glass transition of gelatin since, having previously relaxed the hyaluronic acid domains, mobility of gelatin is not constrained.

On the other hand, if we look at the values obtained for Tg for each HA/Gel composition, a decrease in Tg can be observed as the amount of hyaluronic acid is increased. This is because hyaluronic acid is more hydrophilic than gelatin, so the amount of water that it can absorb at the same relative humidity is higher and, according to the phase diagram in polymers, as the water fraction present in the polymer increases the Tg decreases.

Finally, for the water fractions obtained for each composition in the series of samples analysed after being at 65% RH, no crystallization on cooling or crystallization on heating and fusion process is observed. This is due to two phenomena, on the one hand the water located in the gelatin phase cannot crystallize, as the Tg is above the expected crystallization temperatures of water. The water located in the HA phase is not able to diffuse from the hydrogel network probably due to the viscosity reached at low temperatures, quite close to the Tg of the HA phase. Therefore, it can be concluded that all the water present in the hydrogel is non-freezable water. As water cannot migrate from the chains to form crystals no melting is observed at higher temperatures.

- **85% RH**

Results of equilibrium water content and water fraction of HA/Gel hydrogels at 85% RH are shown in **Table 11**.

Table 11. Equilibrium water content (EWC) and water fraction (hw) of HA/Gel series with molar ratio HA:Tyr 1:1 at 85% RH.

HA/Gel	EWC(%)	hw(%)
0/100	12.05 ± 1.21	10.74 ± 0.97
30/70	14.64 ± 4.76	12.62 ± 3.66
50/50	20.77 ± 0.82	17.19 ± 0.56
70/30	23.15 ± 1.09	18.79 ± 0.72
100/0	31.39 ±3.14	23.84 ± 1.84

The thermograms obtained for the second cooling and heating processes are shown in **Figure 28** and **Figure 29** respectively.

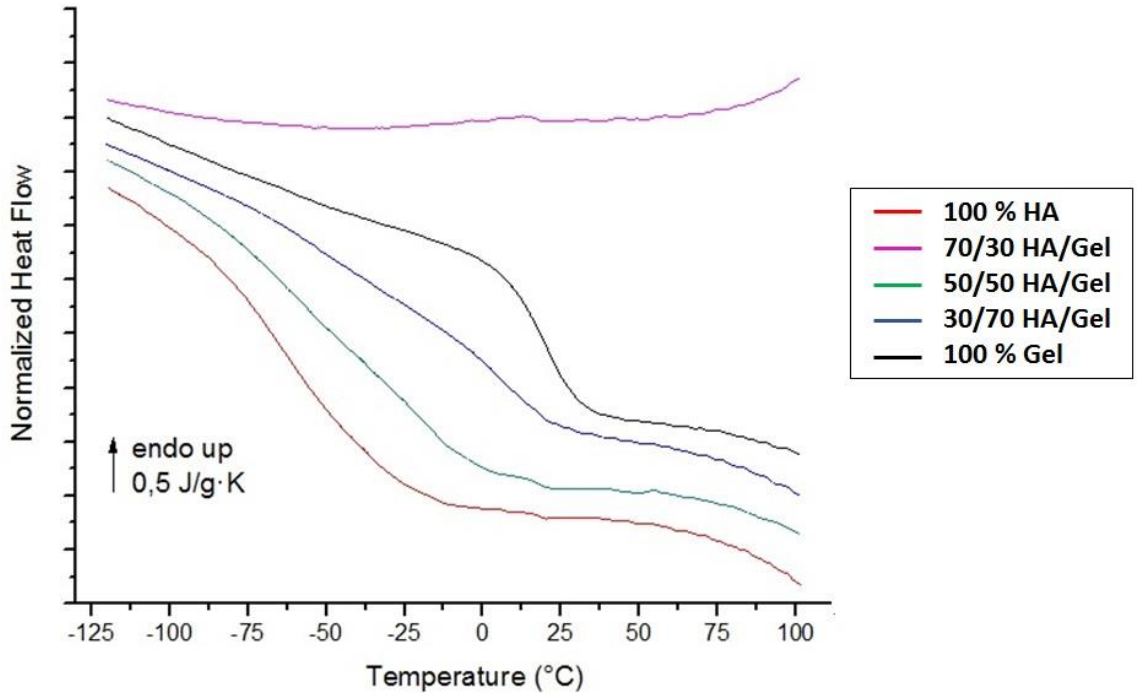

Figure 28. DSC thermogram during second cooling at a heating rate of 10 °C/min for the series HA/Gel hydrogels with molar ratio HA:Tyr 1:1 at 85% RH. 'Y' axis shows the normalized heat flow in J/g·K and 'X' axis shows temperature in °C.

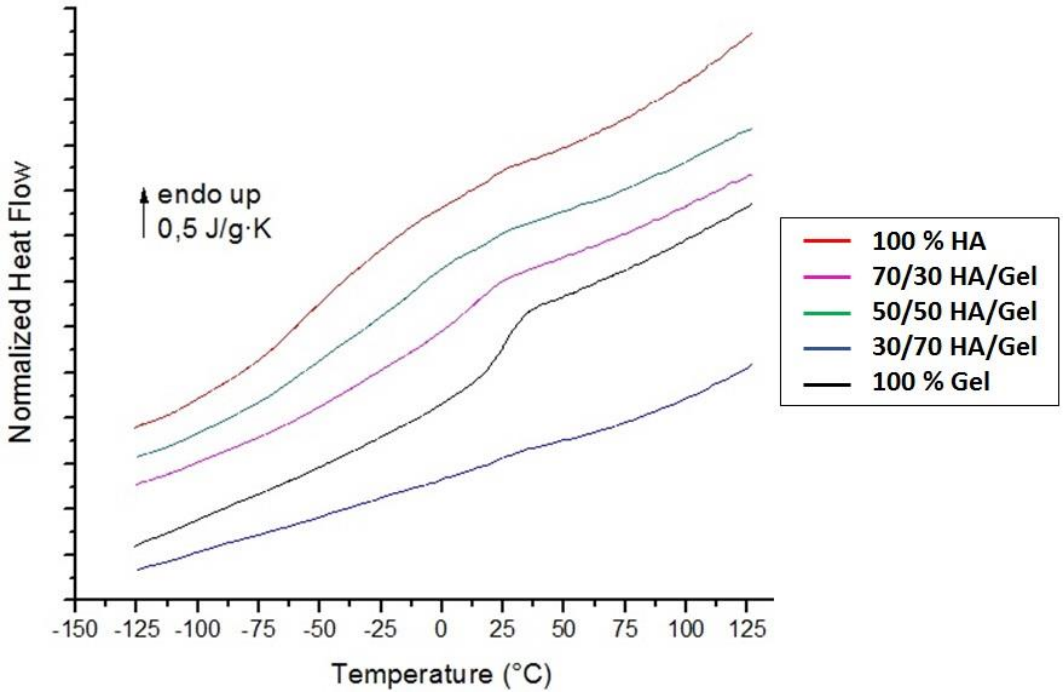

Figure 29. DSC thermogram during second heating at heating rate 10 °C/min for the series HA/Gel hydrogels with molar ratio HA:Tyr 1:1 at 85% RH. 'Y' axis shows the normalized heat flow in J/g·K and 'X' axis shows temperature in ºC.

At this relative humidity, the glass transition process can be observed in the whole series of samples analysed. The results are shown in **Table 12**.

Table 12. Glass transition temperature (Tg) and calorific capacity (ΔCp) seen during heating at a heating rate of 10 °C/min for the series HA/Gel hydrogels with molar ratio HA:Tyr 1:1 at 85 % RH.

HA/Gel (%)	Tg (°C)	ΔCp (J/g·K)
0/100	27	0.45
30/70	22	0.11
50/50	20	0.09
70/30	13	0.18
100/0	- 58	0.45

As with 0% and 65% RH, it was possible to observe the glass transition process of the pure components at 27 °C for gelatin and - 58 °C for hyaluronic acid. As for the mixtures, the relaxation of the gelatin domains separated in the mixtures due to the plasticization of water was seen in the heating process for the same reasons explained for 65% RH.

In addition, a decrease in the Tg can be observed as the hyaluronic acid content of the samples increases. This phenomenon is due to the water fraction obtained for each sample, which increases as the hyaluronic acid content does due to its hydrophilicity and less crosslinking density and, according to the polymer phase diagram, as the amount of water present in the hydrogel increases, Tg decreases.

Eventually, no fusion or crystallization process could be seen. Thus, we conclude that when placing the samples at 85% RH, the entire fraction of water absorbed by the samples is non-freezable water that cannot migrate to crystallize or melt.

- **98% RH**

Finally, DSC measurements of samples at 98 % RH was performed. Results of equilibrium water content and water fraction of HA/Gel hydrogels at 98% RH are shown in **Table 13**.

Table 13. Equilibrium water content (EWC) and water fraction (hw) of HA/Gel series with molar ratio HA:Tyr 1:1 at 98% RH.

HA/Gel	EWC(%)	hw(%)
0/100	59.71 ± 5.74	37.31 ± 2.24
30/70	98.62 ± 6.21	49.60 ± 1.58
50/50	121.53 ± 9.71	54.77 ± 2.01
70/30	140.55 ± 7.90	58.38 ± 1.35
100/0	193.56 ± 6.03	65.92 ± 0.69

Figure 30 and **Figure 31** show the thermograms obtained for the second cooling and heating processes respectively.

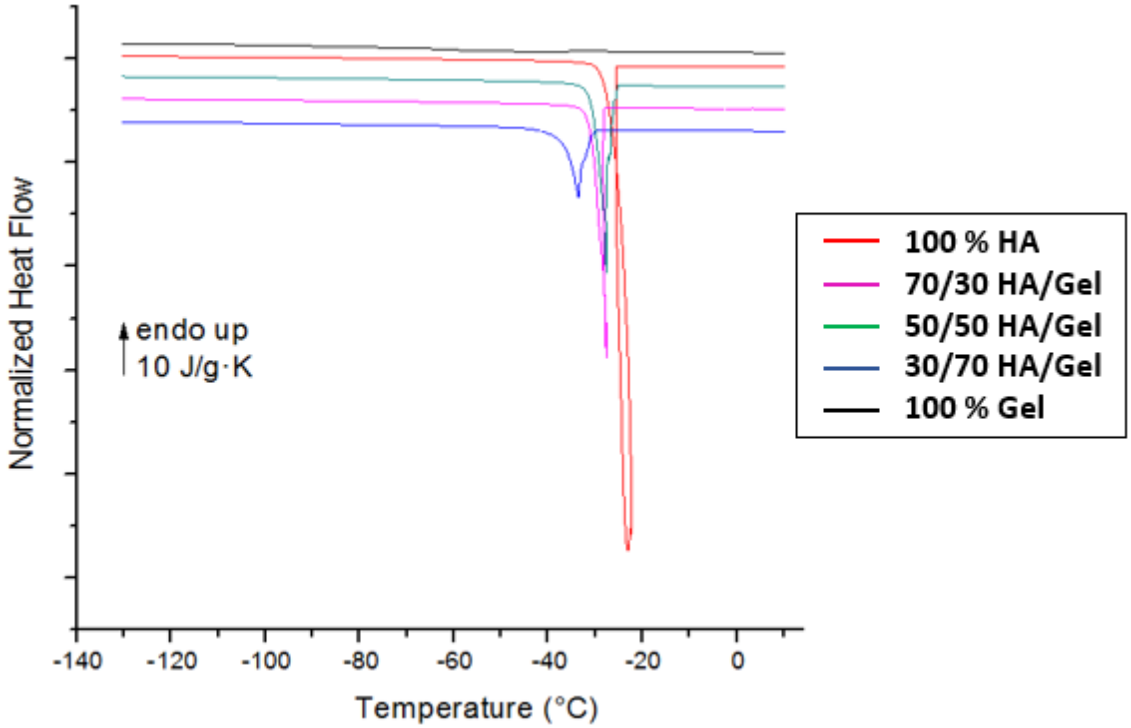

Figure 30.DSC thermogram during second cooling at a heating rate of 10 ºC/min for the series HA/Gel hydrogels with molar ratio HA:Tyr 1:1 at 98% RH. 'Y' axis shows the normalized heat flow in J/g·K and 'X' axis shows temperature in °C.

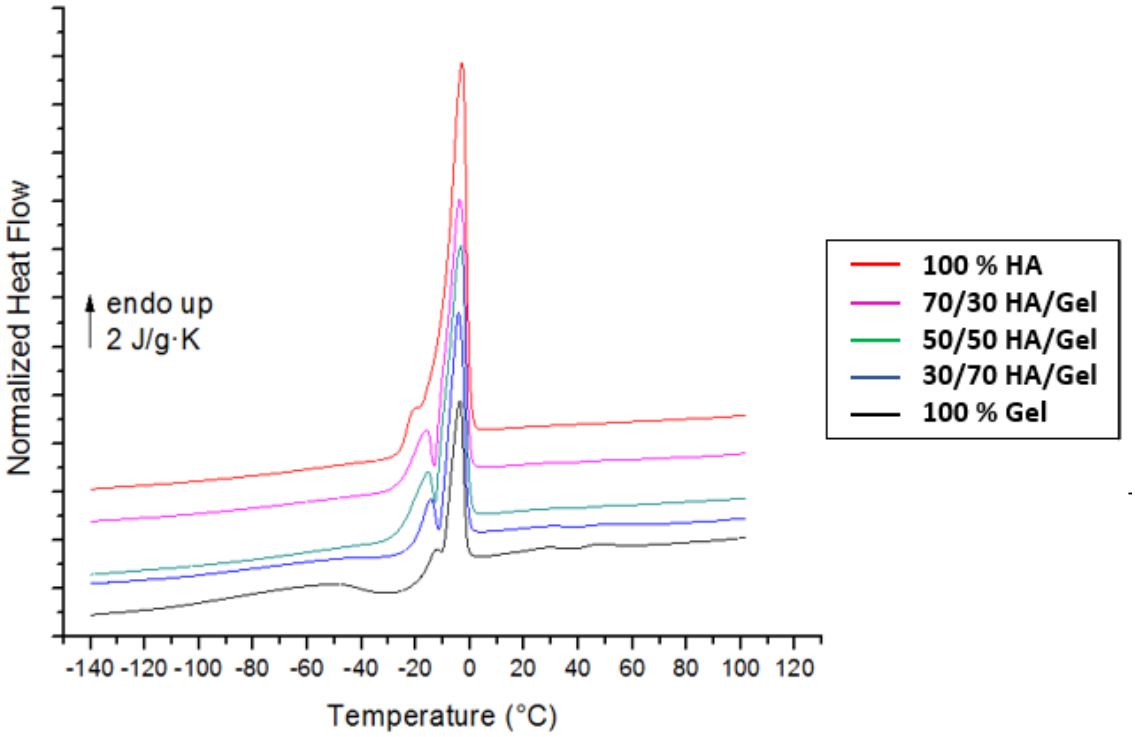

Figure 31.DSC thermogram during second heating at a heating rate of 10 ºC/min for the series HA/Gel hydrogels with molar ratio HA:Tyr 1:1 at 98% RH. 'Y' axis shows the normalized heat flow in J/g·K and 'X' axis shows temperature in °C.

In this case, crystallization process during cooling and melting process during heating of the samples could be observed in the whole HA/Gel hydrogel series. Specifically, a double melting peak was found in all samples, being smaller the peak found at lower temperature (first peak) than the one found at larger temperature (second peak). The appearance of two different peaks is attributed to the formation of two types of crystals depending on the type of water present in the hydrogel forming the crystals. On the one hand, bound water, which is more confined, forms cubic ice which melts at temperatures below the melting temperature of bulk water. This behaviour is attributed to the first peak. On the other hand, free water forms hexagonal ice, which melts around 0 ˚C, and is attributed to the second peak. [99], [100] These peaks can be seen more clearly in **Figure 32**.

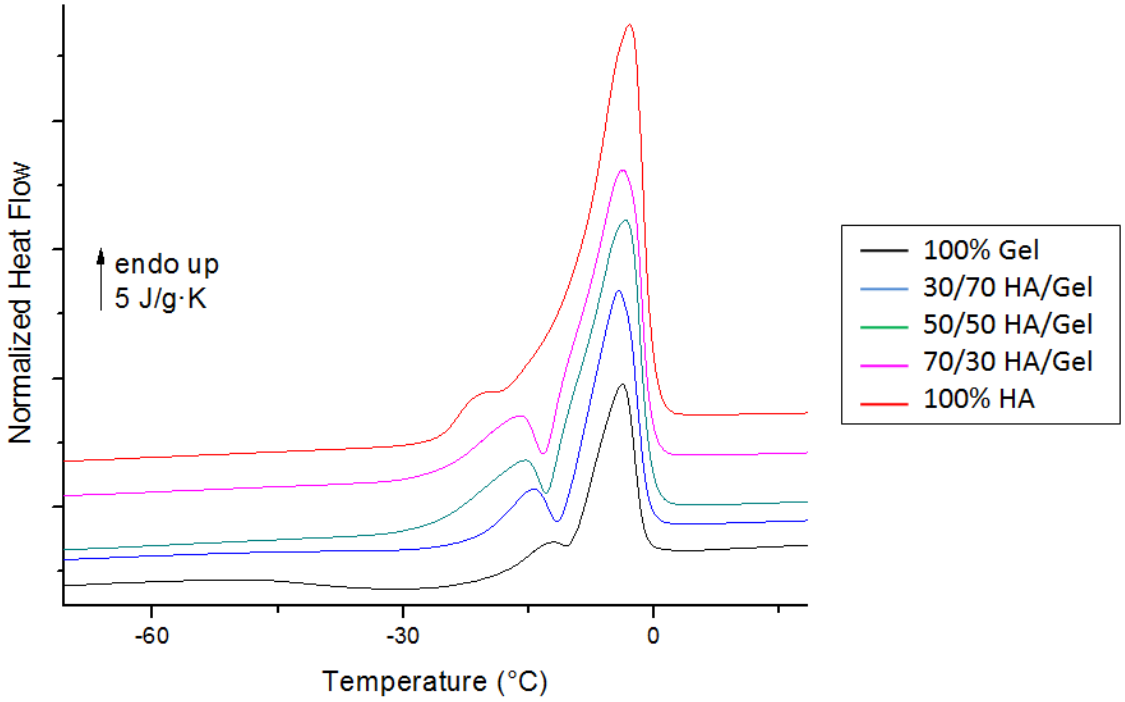

Figure 32. Zoom of the DSC thermogram during heating at a heating rate of 10 °C/min for the series HA/Gel hydrogels with molar ratio HA:Tyr 1:1 at 98% RH. 'Y' axis shows the normalized heat flow in J/g·K and 'X' axis shows temperature in °C.

The peaks observed during the heating process of the samples were analysed directly with the TA Universal Analysis software. The results obtained from the melting temperature (Tm) and the melting enthalpy (ΔHm) are shown in **Table 14**. In addition, in the case of pure gelatin, cold crystallization process can be clearly observed, which begins once the Tg of the gelatine is reached at - 52 °C. In the case of the composition HA/Gel 30/70, this process can also be appreciated more subtly, starting at the same temperature as in the case of pure gelatin.

Table 14. Melting temperature (Tm) and melting enthalpy (ΔHm) seen during heating at heating rate 10 °C/min for the series HA/Gel hydrogels at 98 % RH. First peak corresponds to the peak at lower temperature and second peak corresponds to the peak at higher temperature.

HA/Gel	First Peak		Second peak		Total
	Tm (°C)	ΔHm (J/g)	Tm (°C)	ΔHm (J/g)	ΔHm (J/g)
0/100	-11.91	1.53	-3.79	30.17	31.70
30/70	-14.38	7.34	-4.18	53.32	60.66
50/50	-15.41	10.28	-3.30	77.20	87.48
70/30	-15.97	11.31	-3.91	81.32	92.63
100/0	-21.29	13.20	-2.88	133.70	146,90

The values of Tm obtained for both peaks were plotted to analyse the behaviour of these according to the gelatin content present in the hydrogel (**Figure 33**). Thus, while the second peak

shows a constant behaviour of the Tm with respect to the percentage of gelatin present in the hydrogel, the first peak shows an increase of the Tm as the gelatin content increases. The second peak corresponds to the melting of the water crystals formed by free water or water forming part of clusters in the hydrogels. These crystals are easily formed when decreasing the temperature in the equipment (and eventually when increasing the temperature above Tg) and are not very confined by the polymer networks. They can also have higher size than those which melt at lower temperatures, and then melt at a constant temperature independently of the crosslinking degree of the networks and composition and at a temperature typical of the bulk water. This occurs regardless of the greater or lesser amount of gelatin or hyaluronic acid present in the hydrogel. However, in the case of the first peak, being more confined the crystals, they melt at a higher temperature as the gelatin content increases because the gelatin networks are more cross-linked than the hyaluronic ones.

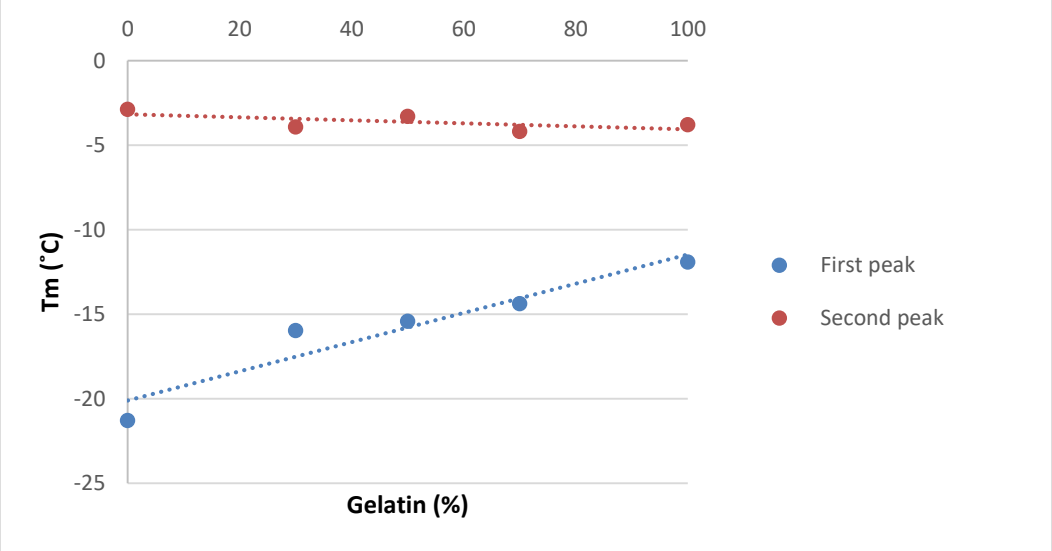

Figure 33. Representation of melting temperatures (Tm) seen during heating for the series HA/Gel hydrogels at 98 % RH versus the percent of gelatin present in the hydrogel.

In addition, an increase in the melting enthalpy at both peaks can be observed as the hyaluronic acid content of the samples increases. This fact is due to the greater water absorption capacity of hyaluronic acid because it has greater hydrophilicity than gelatin. Therefore, more water will crystallize during the cooling process and then, more water will melt during the heating process.

From the melting enthalpy values obtained and according to the literature [99], [101] the different water forms present in the hydrogels were calculated. Although it was previously said that the first endothermic melting peak corresponds to the bound water and the second to free water, we must have in mind that the different types of water present in the hydrogel do not have a totally independent behaviour, but usually a mixture of them appears. Therefore, when calculating the different types of water present in the hydrogel, it is only possible to differentiate between water that can freeze, freezable total water (W_f), and water that cannot freeze, non-freezable water (W_{nf}). **Table 15** shows the results obtained for each of the HA/Gel

compositions. The calculation procedure followed is explained in detail in *Appendix IV: Determination of different water forms present in hydrogel from DSC results.*

Table 15. Water content of HA/Gel hydrogels at 98 % RH. W_{fb} is the freezable bound water, W_{ff} is the free water, W_f is the freezable total water and W_{nf} is the non-freezable water.

HA/Gel	W_f (%)	W_{nf} (%)
0/100	9.51	27,80
30/70	18.19	31,41
50/50	26.23	28,54
70/30	27.78	30,60
100/0	44,05	21,87

In the case of freezable water obtained (W_f), a clear increase is observed as the content of hyaluronic acid in the hydrogel increases. Thus, there is an increase of 30% free water in the case of pure hyaluronic acid with respect to pure gelatin. This fact is due, as already explained above, to the greater water retention capacity of hyaluronic acid with respect to gelatin because of its higher hydrophilic character.

As for non-freezable water, the percentage of water that interacts strongly with the polymer chains not being able to form crystals and hence melting, is considerably higher in the case of pure gelatine than in the case of hyaluronic acid. This is because, although hyaluronic acid is more hydrophilic than gelatin, the higher cross-linking degree of the gelatin chains allows more water molecules to be confined between the networks and cannot migrate to form crystals. As for the mixtures, a higher value is obtained than in the case of pure gelatine.

In the synthesized hydrogels it is intended that the cells be adhered thanks to the RGD sequences present in the gelatin chains. Therefore, an environment as hydrated as possible near the chains and, hence, near the adhesion groups is required to allow the transport of nutrients and metabolic wastes. Thus, the use of the pure gelatin or the mixtures as cellular support material for tissue regeneration will be more appropriate from this point of view.

8. CONCLUSIONS

This project has addressed the synthesis and characterization of hyaluronic acid gelatin injectable hydrogels for their application as biomaterials in the field of soft tissue regeneration.

Firstly, with the previous degradation of the hyaluronic acid, the molecular weights of both components have been adjusted to obtain hyaluronic acid gelatin homogeneous mixtures where no phase separation at macroscopic and microscopic levels has been observed.

After the synthesis of hyaluronic acid tyramine grafting at different molar ratios, raw materials with different grafting degrees have been obtained whose influence on the properties and characteristics of the hyaluronic acid gelatin hydrogels systems.

Regarding the complete study of the series HA/Gel hydrogels with a molar ratio HA:Tyr 1:1, several deductions have been extracted. Considering the morphology, a honeycomb microstructure of pores with a homogeneous size distribution for each of the compositions of the HA/Gel hydrogels series has been obtained, which allows diffusion through the material facilitating the transport of nutrients necessary for cellular viability. In addition, two different pore sizes have been obtained, being the pore size of the pure gelatine and the mixture HA/Gel 30/70 less than the pure hyaluronic acid and the mixtures HA/Gel 50/50 and 70/30.

Concerning the water retention capacity of hydrogels, it has been found that hydrogels containing more hyaluronic acid in their composition can retain more water due to the higher hydrophilicity of this compound and the lower crosslinking degree of their chains with respect to gelatine.

Moreover, the results obtained using the freeze extraction method and the freeze drying method for hydrogels formation have been compared. A greater water retention capacity has been obtained with the freeze extraction method in the case of hydrogels with higher amount of hyaluronic acid due to the larger pore size obtained with the use of this method. However, the opposite behaviour is observed for hydrogels with greater amount of gelatin in their chains because of the collapse of pores with freeze extraction method.

With DSC measurements it has been proven that hyaluronic acid gelatin hydrogels mixtures have a good miscibility in the dry state, being the networks of both compounds well intermixed. However, a phase separation between the two components occurs when the samples are at higher relative humidities, since the presence of water produces the plasticity of the networks and results in the clustering of chains of the same compound due to a higher affinity.

DSC measurements have also allowed to calculate the amount of different types of water present in the hydrogel, concluding that the pure gelatin as well as the mixtures have a greater amount of water strongly bound to the polymer chains, providing a more hydrated environment near the RGD groups of cell adhesion present in the gelatin chains.

The higher degree of hydration and larger pore size than gelatin and greater amount of bound water strongly linked to the chains of the hydrogel, the mixtures present improved characteristics with respect to the pure components. Therefore, they will be able to mimic the extracellular matrix of the soft tissues making them suitable for their use by guaranteeing a correct cell adhesion and proliferation, as well as a good diffusion of nutrients and wastes. The use of one composition or another will depend on the properties required in the hydrogel, which will depend on the particular application to be carried out.

9. REFERENCES

[1] Fuchs, J. R., Nasseri, B. A., Vacanti, J. P., "Tissue Engineering: A 21st Century Solution to Surgical Reconstruction and Transplantation," The Annals of thoracic surgery, vol. 72, no. 2, p. 577-591., 2001.

[2] World Health Organization, Europe. Gateway.Data. Total number of inpatient surgical procedures per year. Total number of inpatient surgical procedures per year. 2016, Recuperado desde: http://gateway.euro.who.int/en/visualizations/line-charts/hfa_539-total-number-of-inpatient-surgical-procedures-per-year/.

[3] Vacanti, J. P., Langer, R., "Tissue engineering: the design and fabrication of living replacement devices for surgical reconstruction and transplantation," The lancet, vol. 354, p. S32-S34, 1999.

[4] Palsson, B. O., Bhatia, S. N., "Tissue Engineering," Pearson Prentice Hall, 2004.

[5] Teitelbaum, S. L., Ross, F. P., "Genetic regulation of osteoclast development and function," Nature Reviews. Genetics, vol. 4, p. 638 -649, 2003.

[6] Boyle, W. J., Simonet, W. S., Lacey, D. L., "Osteoclast differentiation and activation," Nature, vol. 423, no. 6937, p. 337-342, 2003.

[7] A. Mikos, "NWO | Huygens Lecture 2003: Tissue Engineering," Netherlands Organization for Scientific Research, The Hague, 2003.

[8] Sarker, B., Singh, R., Silva, R., Roether, J. A., Kaschta, J., Detsch, R., Boccaccini, A. R., "Evaluation of fibroblasts adhesion and proliferation on alginate-gelatin crosslinked hydrogel," PLoS One, vol. 9, no. 9, p. e107952, 2014.

[9] Annual Report of the US Scientific Registry for Transplant Recipients and the Organ Procurement and Transplantation. Network: Transplantation Data: 2003–2015. US Department of Health and Human Services. Recuperado desde: https://optn.transplant.hrsa.gov/.

[10] Jiankang, H., Dichen, L., Yaxiong, L., Bo, Y., Hanxiang, Z., Qin, L., Yi, L., "Preparation of chitosan–gelatin hybrid scaffolds with well-organized microstructures for hepatic tissue engineering," Acta biomaterialia, vol. 5, no. 1, p. 453-461, 2009.

[11] Cheng, Y., Lu, J., Liu, S., Zhao, P., Lu, G., Chen, J., "The preparation, characterization and evaluation of regenerated cellulose/collagen composite hydrogel films," Carbohydrate polymers, vol. 107, p. 57-64, 2014.

[12] Langer, R., Vacanti, J. P., “Principles of tissue engineering,” Academic press. Fourth Edition. Elsevie, 2011.

[13] Drury, J. L., Mooney, D. J., “Hydrogels for tissue engineering: scaffold design variables and applications,” Biomaterials, vol. 24, no. 24, p. 4337-4351., 2003.

[14] Zhu, C., Fan, D., Duan, Z., Xue, W., Shang, L., Chen, F., Luo, Y., “Initial investigation of novel human-like collagen/chitosan scaffold for vascular tissue engineering,” Journal of biomedical materials research Part A, vol. 89, no. 3, pp. 829–840, 2009.

[15] Vavken, P., Joshi, S., Murray, M. M., “TRITON-X is most effective among three decellularization agents for ACL tissue engineering,” Journal of orthopaedic research: official publication of the Orthopaedic Research Society, vol. 27, no. 12, p. 1612, 2009.

[16] Levett, P. A., Melchels, F. P., Schrobback, K., Hutmacher, D. W., Malda, J., Klein, T. J., “Chondrocyte redifferentiation and construct mechanical property development in single-component photocrosslinkable hydrogels,” Journal of Biomedical Materials Research Part A, vol. 102, no. 8, p. 2544–2553, 2014.

[17] Cohen, N. P., Foster, R. J., Mow, V. C., “Composition and dynamics of articular cartilage: structure, function, and maintaining healthy state,” Journal of Orthopaedic & Sports Physical Therapy, vol. 28, no. 4, p. 203–215, 1998.

[18] Suri, S., Schmidt, C. E., “Photopatterned collagen–hyaluronic acid interpenetrating polymer network hydrogels,” Acta biomaterialia, vol. 5, no. 7, p. 2385-2397, 2009.

[19] Chopra, A., Lin, V., McCollough, A., Atzet, S., Prestwich, G. D., Wechsler, A. S., Janmey, P. A., “Reprogramming cardiomyocyte mechanosensing by crosstalk between integrins and hyaluronic acid receptors,” Journal of biomechanics, vol. 45, no. 5, p. 824–831, 2012.

[20] Du, M., Liang, H., Mou, C., Li, X., Sun, J., Zhuang, Y., Dai, J., “Regulation of human mesenchymal stem cells differentiation into chondrocytes in extracellular matrix-based hydrogel scaffolds,” Colloids and Surfaces B: Biointerfaces, vol. 114, p. 316–323, 2014.

[21] Shu, X. Z., Liu, Y., Palumbo, F., Prestwich, G. D., “Disulfide-crosslinked hyaluronan-gelatin hydrogel films: a covalent mimic of the extracellular matrix for in vitro cell growth,” Biomaterials, vol. 24, no. 21, p. 3825–3834, 2003.

[22] Huang, X., Zhang, Y., Zhang, X., Xu, L., Chen, X., Wei, S., “Influence of radiation crosslinked carboxymethyl-chitosan/gelatin hydrogel on cutaneous wound healing,” Materials Science and Engineering: C, vol. 33, no. 8, p. 4816–4824, 2013.

[23] A. S. Hoffman, “Hydrogels for biomedical applications,” Advanced drug delivery reviews, vol. 64, p. 18–23, 2012.

[24] Kopeček, J., Yang, J., “Hydrogels as smart biomaterials,” Polymer International, vol. 56, no. 9, p. 1078–1098, 2007.

[25] J. Kopeček, “Hydrogel biomaterials: a smart future?,” Biomaterials, vol. 28, no. 34, p. 5185-5192, 2007.

[26] Furth, M. E., Atala, A., Van Dyke, M. E., “Smart biomaterials design for tissue engineering and regenerative medicine,” Biomaterials, vol. 28, no, 34, p. 5068-5073, 2007.

[27] S. J. A. K. S. Bryant, “Hydrogel properties influence ECM production by chondrocytes photoencapsulated in poly (ethylene glycol) hydrogels,” Journal of Biomedical Materials Research Part A, 59(1), p. 63-72, 2002.

[28] S. Van Vlierberghe, D. Dubruel, E. Schacht., “Biopolymer-Based Hydrogels as Scaffolds for Tissue Engineering Applications: A Review,” Polymer Chemistry & Biomaterials Research Group, 2011.

[29] Zhao, W., Jin, X., Cong, Y., Liu, Y., Fu, J., “Degradable natural polymer hydrogels for articular cartilage tissue engineering,” Journal of Chemical Technology and Biotechnology, vol. 88, no. 3, p. 327-339, 2013.

[30] Lee, Y., Bae, J. W., Oh, D. H., Park, K. M., Chun, Y. W., Sung, H. J., Park, K. D., “In situ forming gelatin-based tissue adhesives and their phenolic content-driven properties,” Journal of Materials Chemistry B, vol. 1, no. 18, p. 2407-2414, 2013.

[31] Liu, Y., Ren, L., Wang, Y., “Crosslinked collagen–gelatin–hyaluronic acid biomimetic film for cornea tissue engineering applications,” Materials Science and Engineering: C, vol. 33, no. 1, p. 196-201, 2013.

[32] Arfat, Y. A., Ahmed, J., Hiremath, N., Auras, R., Joseph, A., “Thermo-mechanical, rheological, structural and antimicrobial properties of bionanocomposite films based on fish skin gelatin and silver-copper nanoparticles,” Food Hydrocolloids, vol. 62, p. 19, 2017.

[33] G. H. GMIA, “Gelatin Handbook,” Gelatin Manufacturers Institute of America, 2012.

[34] Zhou, Z., Chen, J., Peng, C., Huang, T., Zhou, H., Ou, B., Huang, H., “Fabrication and physical properties of gelatin/sodium alginate/hyaluronic acid composite wound dressing hydrogel,” Journal of Macromolecular Science, Part A, vol. 51, no. 4, p. 318-325, 2014.

[35] Li, Y., Jia, H., Cheng, Q., Pan, F., Jiang, Z., “Sodium alginate–gelatin polyelectrolyte complex membranes with both high water vapor permeance and high permselectivity,” Journal of membrane science, vol. 375, no. 1, p. 304-312, 2011.

[36] da Silva, M. A., Bode, F., Grillo, I., Dreiss, C. A., “Exploring the kinetics of gelation and final architecture of enzymatically cross-linked chitosan/gelatin gels,” Biomacromolecules, vol. 16, no. 4, p. 1401-1409, 2015.

[37] Liu, Y., Ren, L., Wang, Y., “Crosslinked collagen–gelatin–hyaluronic acid biomimetic film for cornea tissue engineering applications,” Materials Science and Engineering: C, vol. 33, no. 1, p. 196-201, 2013.

[38] Young, S., Wong, M., Tabata, Y., Mikos, A. G., “Gelatin as a delivery vehicle for the controlled release of bioactive molecules,” Journal of controlled release, vol. 109, no. 1, p. 256-274, 2005.

[39] Zhou, Z., Yang, Z., Kong, L., Liu, L., Liu, Q., Zhao, Y., Cao, D., “Preparation and characterization of hyaluronic acid hydrogel blends with gelatin,” Journal of Macromolecular Science, Part B, vol. 51, no. 12, p. 2392-2400, 2012.

[40] Kuijpers, A. J., Van Wachem, P. B., Van Luyn, M. J. A., Engbers, G. H. M., Krijgsveld, J., Zaat, S. A. J., Feijen, J., “In vivo and in vitro release of lysozyme from cross-linked gelatin hydrogels: a model system for the delivery of antibacterial proteins from prosthetic heart valves,” Journal of controlled release, vol. 67, no. 2, p. 323-336, 2000.

[41] Sarker, B., Singh, R., Silva, R., Roether, J. A., Kaschta, J., Detsch, R., Boccaccini, A. R., “Evaluation of fibroblasts adhesion and proliferation on alginate-gelatin crosslinked hydrogel,” PloS one, vol. 9, no. 9, e107952, 2014.

[42] R. O. Hynes, “Integrins: bidirectional, allosteric signaling machines,” Cell, vol. 110, no. 6, p. 673-687, 2002.

[43] Taubenberger, A. V., Woodruff, M. A., Bai, H., Muller, D. J., Hutmacher, D. W., “The effect of unlocking RGD-motifs in collagen I on pre-osteoblast adhesion and differentiation,” Biomaterials, vol. 31, no. 10, p. 2827-2835, 2010.

[44] Mogoşanu, G. D., Grumezescu, A. M. , “Natural and synthetic polymers for wounds and burns dressing,” International journal of pharmaceutics, vol. 463, no. 2, p. 127-136, 2014.

[45] G. D. Prestwich, “Hyaluronic acid-based clinical biomaterials derived for cell and molecule delivery in regenerative medicine,” Journal of controlled release, vol. 155, no. 2, p. 193-199, 2011.

[46] Girish, K. S., Kemparaju, K., “The magic glue hyaluronan and its eraser hyaluronidase: a biological overview,” Life sciences, vol. 80, no. 21, p. 1921-1943, 2007.

[47] Tang, S., Vickers, S. M., Hsu, H. P., Spector, M., “Fabrication and characterization of porous hyaluronic acid–collagen composite scaffolds,” Journal of Biomedical Materials Research Part A, vol. 82, no. 2, p. 323-335, 2007.

[48] Fraser, J. R. E., Laurent, T. C., Laurent, U. B. G., “Hyaluronan: its nature, distribution, functions and turnover,” Journal of internal medicine, vol. 242, no. 1, p. 27-33, 1997.

[49] Ishida, O., Tanaka, Y., Morimoto, I., Takigawa, M., Eto, S., “Chondrocytes are regulated by cellular adhesion through CD44 and hyaluronic acid pathway,” Journal of Bone and Mineral Research, 12(10), 1657-1663., 1997.

[50] Jiang, H., Peterson, R. S., Wang, W., Bartnik, E., Knudson, C. B., Knudson, W., “A requirement for the CD44 cytoplasmic domain for hyaluronan binding, pericellular matrix assembly, and receptor-mediated endocytosis in COS-7 cells,” Journal of Biological Chemistry, vol. 277, no. 12, p. 10531-10538, 2002.

[51] Tan, H., Chu, C. R., Payne, K. A., Marra, K. G., “Injectable in situ forming biodegradable chitosan–hyaluronic acid based hydrogels for cartilage tissue engineering,” Biomaterials, vol. 30, no. 13, p. 2499-2506, 2009.

[52] Lee, F., Chung, J. E., Kurisawa, M., “An injectable hyaluronic acid–tyramine hydrogel system for protein delivery,” Journal of Controlled Release, vol. 134, no. 3, p. 186-193, 2009.

[53] Sakai, S., Hirose, K., Taguchi, K., Ogushi, Y., Kawakami, K., “An injectable, in situ enzymatically gellable, gelatin derivative for drug delivery and tissue engineering,” Biomaterials, vol. 30, no. 20, p. 3371-3377, 2009.

[54] Sun, Y., Deng, Z., Tian, Y., Lin, C., “Horseradish peroxidase-mediated in situ forming hydrogels from degradable tyramine-based poly (amido amine)s,” Journal of Applied Polymer Science, vol. 127, no. 1, p. 40-48, 2013.

[55] Hennink, W. E., Van Nostrum, C., “Novel crosslinking methods to design hydrogels,” Advanced drug delivery reviews, vol. 64, p. 223-236, 2012.

[56] R. Jin, “In-situ forming biomimetic hydrogels for tissue regeneration,” INTECH Open Access Publisher, 2012.

[57] Wang, L. S., Du, C., Chung, J. E., Kurisawa, M., “Enzymatically cross-linked gelatin-phenol hydrogels with a broader stiffness range for osteogenic differentiation of human mesenchymal stem cells,” Acta biomaterialia, vol. 8, no. 5, p. 1826-1837, 2012.

[58] Weng, L., Pan, H., Chen, W., “Self-crosslinkable hydrogels composed of partially oxidized hyaluronan and gelatin: In vitro and in vivo responses,” Journal of Biomedical Materials Research Part A, vol. 85, no. 2, p. 352-365, 2008.

[59] Chen, Y. C., Su, W. Y., Yang, S. H., Gefen, A., Lin, F. H., “In situ forming hydrogels composed of oxidized high molecular weight hyaluronic acid and gelatin for nucleus pulposus regeneration,” Acta biomaterialia, vol. 9, no. 2, p. 5181-5193, 2013.

[60] Darr, A., Calabro, A., “Synthesis and characterization of tyramine-based hyaluronan hydrogels,” Journal of Materials Science: Materials in Medicine, vol. 20, no. 1, p. 33-44, 2009.

[61] Davis, N. E., Ding, S., Forster, R. E., Pinkas, D. M., Barron, A. E., “Modular enzymatically crosslinked protein polymer hydrogels for in situ gelation,” Biomaterials, vol. 3, no. 28, p. 7288-7297, 2010.

[62] Jin, R., Teixeira, L. S. M., Dijkstra, P. J., van Blitterswijk, C. A., Karperien, M., Feijen, J., “Chondrogenesis in injectable enzymatically crosslinked heparin/dextran hydrogels,” Journal of controlled release, vol. 152, no. 1, p. 186-195, 2011.

[63] Teixeira, L. S. M., Feijen, J., van Blitterswijk, C. A., Dijkstra, P. J., Karperien, M., “Enzyme-catalyzed crosslinkable hydrogels: emerging strategies for tissue engineering,” Biomaterials, vol. 33, no. 5, p. 1281-1290, 2012.

[64] Lee, S. H., Lee, Y., Lee, S. W., Ji, H. Y., Lee, J. H., Lee, D. S., Park, T. G., “Enzyme-mediated cross-linking of Pluronic copolymer micelles for injectable and in situ forming hydrogels,” Acta biomaterialia, vol. 7, no. 4, p. 1468-1476, 2011.

[65] Roberts, J. J., Naudiyal, P., Lim, K. S., Poole-Warren, L. A., Martens, P. J., “A comparative study of enzyme initiators for crosslinking phenol-functionalized hydrogels for cell encapsulation,” Biomaterials Research, vol. 20, no. 1, p. 30, 2016.

[66] Chen, T., Embree, H. D., Brown, E. M., Taylor, M. M., Payne, G. F., “Enzyme-catalyzed gel formation of gelatin and chitosan: potential for in situ applications,” Biomaterials, vol. 24, no. 17, p. 2831-2841, 2003.

[67] N. C. Veitch, “Horseradish peroxidase: a modern view of a classic enzyme,” Phytochemistry, vol. 65, no. 3, p. 249-259, 2004.

[68] Ryan, B. J., Carolan, N., Ó’Fágáin, C., “Horseradish and soybean peroxidases: comparable tools for alternative niches?,” Trends in biotechnology, vol. 24, no. 8, p. 355-363, 2006.

[69] Hoare, D. T., Koshland, D. E., “A method for the quantitative modification and estimation of carboxylic acid groups in proteins,” Journal of Biological Chemistry, vol. 242, no.10, p. 2447-2453, 1976.

[70] Lee, F., Chung, J. E., Kurisawa, M., “An injectable enzymatically crosslinked hyaluronic acid–tyramine hydrogel system with independent tuning of mechanical strength and gelation rate,” Soft Matter, vol. 4, no. 4, p. 880-887, 2008.

[71] Poveda-Reyes, S., Moulisova, V., Sanmartín-Masiá, E., Quintanilla-Sierra, L., Salmerón-Sánchez, M., Ferrer, G. G., “Gelatin—Hyaluronic Acid Hydrogels with Tuned Stiffness to

Counterbalance Cellular Forces and Promote Cell Differentiation," Macromolecular bioscience, vol. 16, no. 9, p. 1311-1324, 2016.

[72] Vallés-Lluch, A., Poveda-Reyes, S., Amorós, P., Beltran, D., Monleón Pradas, M., "Hyaluronic Acid–Silica Nanohybrid Gels," Biomacromolecules, vol. 14, no. 12, p. 4217-4225, 2013.

[73] Konsta, A. A., Daoukaki, D., Pissis, P., Vartzeli, K., "Hydration and conductivity studies of polymer–water interactions in polyacrylamide hydrogels," Solid State Ionics, vol. 125, no. 1, p. 235-241, 1999.

[74] Sasaki, K., Panagopoulou, A., Kita, R., Shinyashiki, N., Yagihara, S., Kyritsis, A., Pissis, P., "Dynamics of Uncrystallized Water, Ice, and Hydrated Protein in Partially Crystallized Gelatin-Water Mixtures Studied by Broadband Dielectric Spectroscopy," The Journal of Physical Chemistry B, 2016.

[75] L. O. Cervelló, "Study of molecular and water dynamics in hyaluronic acid (HA) and HA+ CNTS and HA+ SIO2 (Doctoral dissertation)," National Technical University of Athens, Greece, 2015.

[76] A. K. Panagopoulou, "Molecular dynamics and phase transitions in protein-water systems. (Doctoral dissertation)," National Technical University of Athens, 2014.

[77] Panagopoulou, A., Kyritsis, A., Shinyashiki, N., Pissis, P., "Protein and water dynamics in bovine serum albumin–water mixtures over wide ranges of composition," The Journal of Physical Chemistry B, vol. 116, no. 15, p. 4593-4602, 2012.

[78] Panagopoulou, A., Kyritsis, A., Aravantinou, A. M., Nanopoulos, D., i Serra, R. S., Ribelles, J. L. G., Pissis, P., "Glass transition and dynamics in lysozyme–water mixtures over wide ranges of composition," Food Biophysics, vol. 6, no. 2, p. 199-209, 2011.

[79] Pissis, P., Kyritsis, A. , "Hydration studies in polymer hydrogels," Journal of Polymer Science Part B: Polymer Physics, vol. 51, no. 3, p. 159-175, 2013.

[80] Enrione, J., Díaz-Calderón, P., Weinstein-Oppenheimer, C. R., Sánchez, E., Fuentes, M. A., Brown, D. I., Acevedo, C. A., "Designing a gelatin/chitosan/hyaluronic acid biopolymer using a thermophysical approach for use in tissue engineering," Bioprocess and biosystems engineering, vol. 36, no. 12, p. 1947-1956, 2013.

[81] Balart, R., López, J., García, D., Parres, F., "Técnicas experimentales de análisis térmico de polímeros," 2003.

[82] Hatakeyama, T., Quinn, F. X., "Thermal analysis: fundamentals and applications to polymer science," [sl], 1999.

[83] Salmerón Sánchez, M., Ferrer, G. G., Monleón Pradas, M., Gómez Ribelles, J. L., "Influence of the hydrophobic phase on the thermal transitions of water sorbed in

polymer hydrogel based on interpenetration of a hydrophilic and a hydrophobic network," Macromolecules, vol. 36, no. 3, p. 860-866, 2003.

[84] Sánchez, M. S., Pradas, M. M., Ribelles, J. L. G., "Thermal transitions in PHEA hydrogels by thermomechanical analysis. A comparison with DSC data," European polymer journal, vol. 40, no. 2, p. 329-334, 2004.

[85] M. S. Sánchez, On the nature of thermal transitions in acrylic polymer gels. (Doctoral dissertation), Universidad Politécnica de Valencia, 2002.

[86] Shu, X. Z., Liu, Y., Luo, Y., Roberts, M. C., Prestwich, G. D., "Disulfide cross-linked hyaluronan hydrogels," Biomacromolecules, vol. 3, no. 6, p. 1304-1311, 2002.

[87] Sakai, S., Hirose, K., Taguchi, K., Ogushi, Y., Kawakami, K., "An injectable, in situ enzymatically gellable, gelatin derivative for drug delivery and tissue engineering," Biomaterials, vol. 30, no. 20, p. 3371-3377, 2009.

[88] Y. I., "Tissue engineering: fundamentals and applications," Elsevier Ltd.Oxford, UK, 2006.

[89] Choi, Y. S., Hong, S. R., Lee, Y. M., Song, K. W., Park, M. H., Nam, Y. S., "Studies on gelatin-containing artificial skin: II. Preparation and characterization of cross-linked gelatin-hyaluronate sponge," Journal of Biomedical Materials Research Part A, vol. 48, no. 5, p. 631-639, 1999.

[90] Xu, K., Narayanan, K., Lee, F., Bae, K. H., Gao, S., Kurisawa, M., "Enzyme-mediated hyaluronic acid–tyramine hydrogels for the propagation of human embryonic stem cells in 3D," Acta biomaterialia, vol. 24, no. 159-171, 2015.

[91] Poveda-Reyes, S., Mellera-Oglialoro, L. R., Martínez-Haya, R., Gamboa-Martínez, T. C., Gómez Ribelles, J. L., Gallego Ferrer, G. , "Reinforcing an injectable gelatin hydrogel with PLLA microfibers: two routes for short fiber production," Macromolecular Materials and Engineering, vol. 300, no. 10, p. 977-988, 2015.

[92] Choi, Y. S., Hong, S. R., Lee, Y. M., Song, K. W., Park, M. H., Nam, Y. S., "Studies on gelatin-containing artificial skin: II. Preparation and characterization of cross-linked gelatin-hyaluronate sponge," Journal of Biomedical Materials Research Part A, vol. 48, no. 5, p. 631-639, 1999.

[93] Lee, F., Chung, J. E., Kurisawa, M., "An injectable enzymatically crosslinked hyaluronic acid–tyramine hydrogel system with independent tuning of mechanical strength and gelation rate," Soft Matter, vol. 4, no. 4, p. 880-887, 2008.

[94] Wang, L. S., Chung, J. E., Chan, P. P. Y., Kurisawa, M., "Injectable biodegradable hydrogels with tunable mechanical properties for the stimulation of neurogenesic

differentiation of human mesenchymal stem cells in 3D culture," Biomaterials, vol. 31, no. 6, p. 1148-1157, 2010.

[95] W. J. Sichina, "Measurement of Tg by DSC," Thermal Analysis: Application Note. Perkin Elmer ZDA: Norwalk, CT, 2000.

[96] Panagopoulou, A., Molina, J. V., Kyritsis, A., Pradas, M. M., Lluch, A. V., Ferrer, G. G., Pissis, P., "Glass transition and water dynamics in hyaluronic acid hydrogels," Food biophysics, vol. 8, no. 3, p. 192, 2013.

[97] Noel, T. R., Parker, R., Ring, S. G., "Effect of molecular structure and water content on the dielectric relaxation behaviour of amorphous low molecular weight carbohydrates above and below their glass transition," Carbohydrate Research, vol. 329, no. 4, p. 83, 2000.

[98] Orford, P. D., Parker, R., Ring, S. G., "Aspects of the glass transition behaviour of mixtures of carbohydrates of low molecular weight," Carbohydrate Research, vol. 196, p. 11-18, 1990.

[99] "Thermal analysis to determine various forms of water present in hydrogels," TA Instruments. TA384.

[100] Seidl, M., Elsaesser, M. S., Winkel, K., Zifferer, G., Mayer, E., Loerting, T., "Volumetric study consistent with a glass-to-liquid transition in amorphous ices under pressure," Physical Review B, vol. 83, no. 10, p. 100201, 2011.

[101] Aktas, N., Tülek, Y., Gökalp, H. Y., "Determination of freezable water content of beef semimembranous muscle DSC study," Journal of Thermal Analysis and Calorimetry, vol. 48, no. 2, p. 259-266, 1997.

[102] J. E. Mark, "Polymer data handbook," Oxford University Press, 199.

[103] Mendichi, R., Šoltés, L., Giacometti Schieroni, A., "Evaluation of radius of gyration and intrinsic viscosity molar mass dependence and stiffness of hyaluronan," Biomacromolecules, vol. 4, no. 6, p. 1805-1810, 2003.

[104] H. H. Perkampus, "UV-VIS Spectroscopy and its Applications," Berlin: Springer-Verlag, p. 220-22, 1992.

APPENDICES

APPENDIX I: DETERMINATION OF MOLECULAR WEIGHT BY GEL PERMEATION CHROMATOGRAPHY

Gel Permeation Chromatography (GPC) is a polymer characterization technique that provides the complete molecular weight distribution of a sample and its different averages.

This analytical technique is based on separating dissolved macromolecules by size based on their elution in columns filled with a porous gel. The smaller molecules, which have lower molecular weight, can enter more easily into the pores so they can be retained in the microporosity of the spheres that make up the columns achieving higher retention times. In contrast, higher molecular weight molecules will be eluted earlier because they will not pass through the microporosity of the spheres but through the interstices remaining between spheres, achieving shorter retention times.

For the determination of molecular weights of the samples studied, a calibration curve must first be calculated from compounds which molecular weight is known versus the retention time obtained in the GPC test. Once the calibration curve is obtained, the molecular weight of the samples will be calculated through the retention times obtained in the GPC.

The following is an example of the calculation of molecular weight of one of the compounds analysed.

Calibration curve

The calibration curve was obtained from polyethylene glycol (PEG) solutions of known molecular weight in a buffer 150 mM sodium chloride and 0,05% w/v sodium azide. These solutions were injected into the equipment in water columns. The molecular weights of the patterns used as well as the retention times obtained after performing the GPC test are presented in **Table 16**.

Table16. Molecular weights and retention times of the PEG patterns used to obtain the GPC calibration curve.

Pattern	Molecular weight (Da)	Retention time (min)
1	871000	21,88
2	599000	22,58
3	328000	23,56
4	177000	24,71
5	81300	26,43
6	41300	27,97

From the results gathered in **Table 15** the calibration curve was constructed representing the molecular weight of the different PEG patterns versus the retention times obtained after the GPC test (**Figure 34**).

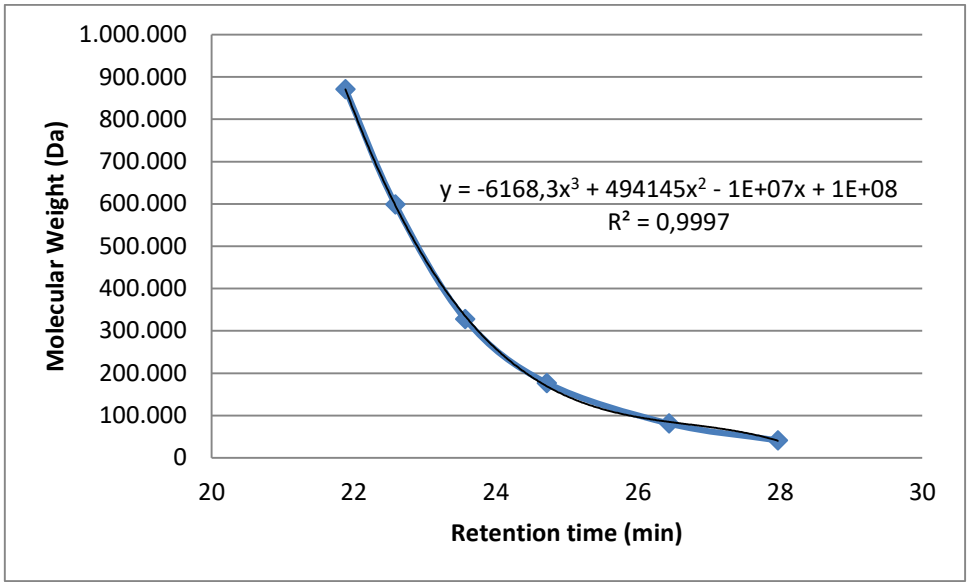

Figure34. Representation of calibration curve from PEG patterns obtained by GPC test. 'Y' axis shows the molecular weight in Dalton and 'X' axis shows retention time in minutes.

Calculation of molecular weight of the samples

From the injection of the sample in the GPC test a graph is obtained in which the retention time of the sample is plotted against the intensity of the output signal. **Figure 35** shows the graph obtained after analysing a sample of low molecular weight hyaluronic acid.

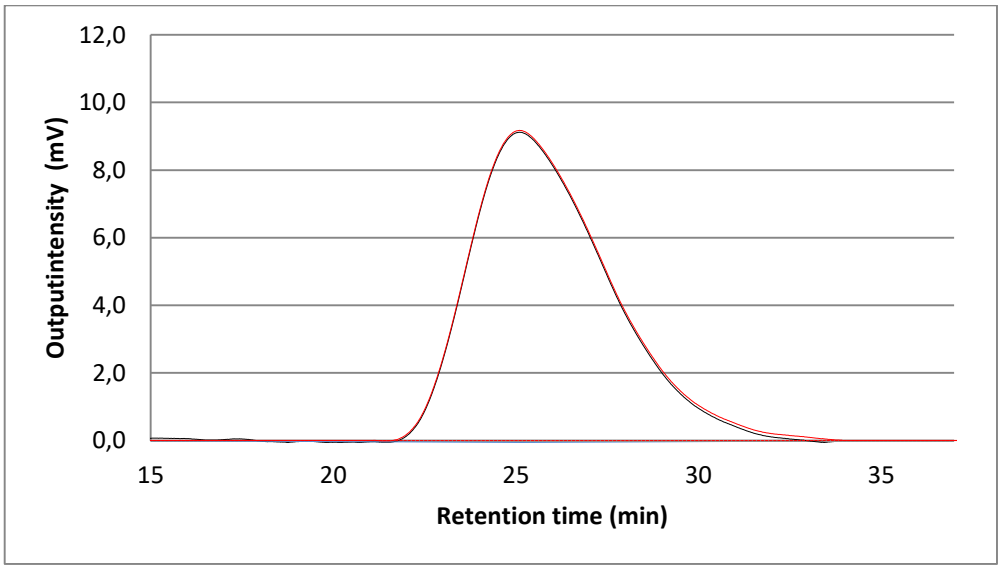

Figure35. Representation of the output intensity in millivolts versus retention time in minutes obtained in the GPC test for a sample of low molecular weight hyaluronic acid.

The higher the intensity of the output signal at a certain time, the more fraction of the sample will emerge at that time and, therefore, the more polymer fraction will have a molecular weight corresponding to that retention time. To relate the corresponding molecular weight with the retention time found, the previously calculated calibration curve was used.

However, the calculated calibration curve was obtained from samples of polyethylene glycol and not from the compound to be measured. Therefore, in order to apply this equation to the samples used, the molecular weight obtained must be readjusted by the Mark-Houwink equation (Equation 4).

$$K_1 \cdot M_1^{1+\alpha_1} = K_2 \cdot M_2^{1+\alpha_2} \quad (4)$$

where K_1 and α_1 are the Mark-Houwink parameters of the compound used in the calibration curve (in our case the PEG), K_2 andα_2 are the Mark-Houwink parameters of the compound of interest to be analysed (gelatin or hyaluronic acid) and M_1 and M_2 are the molecular weights of the compound of the calibration curve and the compound of interest respectively.

The Mark-Houwink parameters for PEG, gelatin and hyaluronic acid obtained from the literature [102], [103] are shown in **Table 17**.

Table17. α and K Mark-Houwink parameters for PEG, hyaluronic acid and gelatin.

Compound	α	K (mL/g)
PEG	0,820	$6,4x10^{-3}$
HA	0,778	$3,39x10^{-2}$
Gelatin	0,740	$1,1x10^{-4}$

Therefore, from the retention times obtained in the GPC test of the analyzed sample and using the equation of the calibration curve and the Mark-Houwink equation, it can be finally found the molecular weight of the analyzed sample (M_2). From the obtained results the molecular weight distribution curve is constructed. **Figure 36** shows the curve for low molecular weight hyaluronic acid.

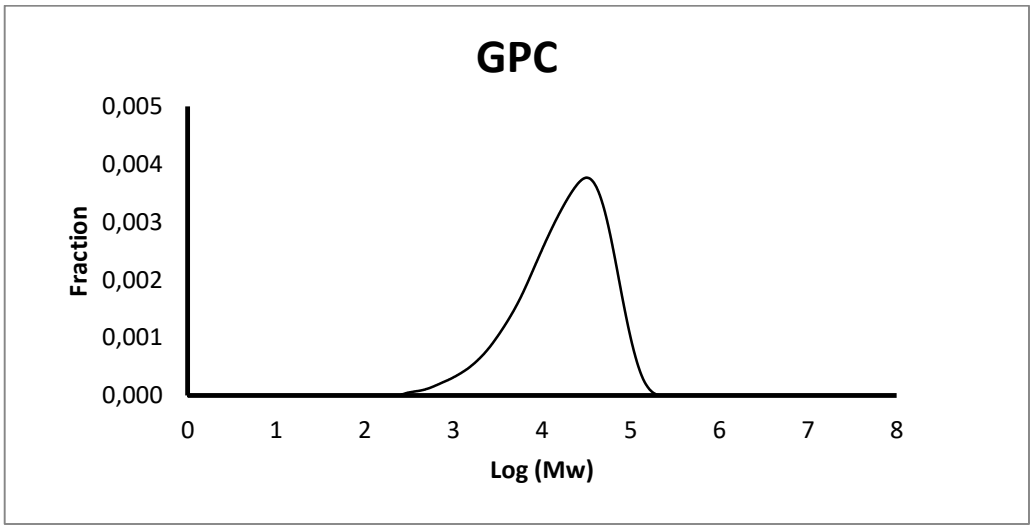

Figure 36. Molecular weight distribution curve obtained for a sample of low molecular weight hyaluronic acid by the GPC test. 'Y' axis shows the polymer fraction and 'X' axis shows the logarithm of the molecular weight.

From the curve obtained the mass average molecular weight of the sample was calculated as the weighted sum of the polymer fraction multiplied by the molecular weight (equation 5).

$$M_w = \sum_i x_i \cdot M_i \quad (5)$$

Four GPC assays were performed for each of the compounds. For the low molecular weight hyaluronic acid, the mass average molecular weight was 192,000 Da.

APPENDIX II: DETERMINATION OF TYRAMINE GRAFT DEGREE

After the synthesis of low molecular weight hyaluronic acid and gelatin with tyramine, it was necessary to quantify the degree of grafting of tyramine in both substances to get an idea of the number of tyramine groups grafted per carboxyl group.

This measurement was carried out by the spectroscopy test. This test is based on the measurement of the absorbance of the sample, in other words, the amount of light that the sample is capable of absorbing at a given wavelength. [104]

For the quantification of the grafted tyramine, the calibration line was obtained previously from the measurement of the absorbance of patterns with a known concentration of tyramine. Then, once the calibration line was obtained and the spectroscopy test was performed to the samples, the tyramine concentration of the samples could be calculated.

Calibration line

The calibration line was obtained from solutions of tyramine of known concentration in mQ water. **Table 18** shows the concentrations of tyramine used to obtain the calibration line as well as the absorbance obtained after performing the spectroscopy test. From the results reported in **Table 18**, the calibration line was constructed (**Figure 37**).

Table18. Concentration of tyramine and absorbance of the patterns used to obtain the calibration line in the spectrophotometry test.

Pattern	[Tyr] (mg/ml)	Absorbance
1	0,00625	0,048
2	0,0125	0,103
3	0,025	0,197
4	0,05	0,418
5	0,1	0,822

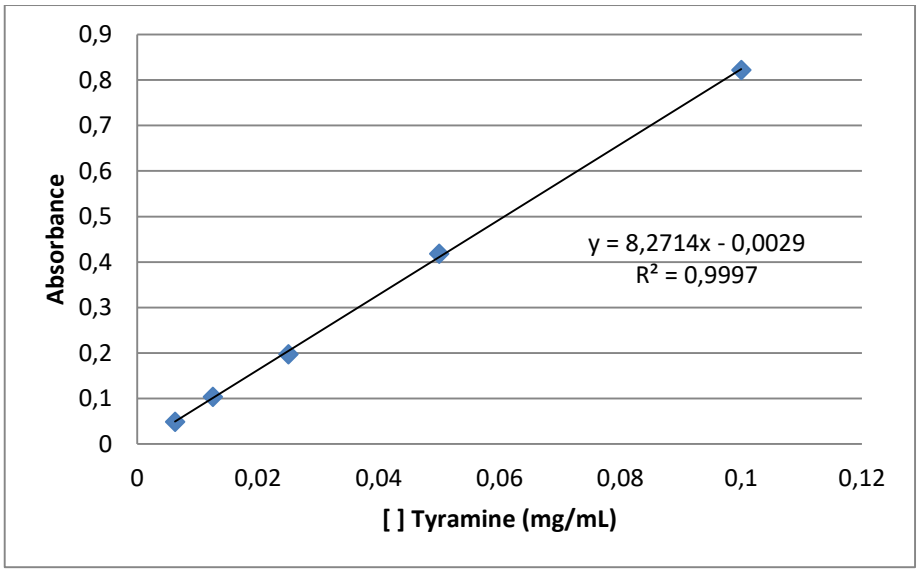

Figure37. Calibration line from tyramine patterns. 'Y' axis shows absorbance and 'X' the tyramine concentration in mg/mL.

Grafting degree of samples

To measure the grafting degree of the samples, 0.1 % w/v solutions of the synthesized product were prepared in 1.5 mL of milliQ wate.

After measuring the absorbance of the samples in the spectrophotometer, the tyramine concentration was quantified from the calibration line and the molecular weight of tyramine (137.18 g/mol). The results obtained are shown in section 7.2.

APPENDIX III: DETERMINATION OF WATER FRACTION AND EQUILIBRIUM WATER CONTENT

To determine the amount of water that the hydrogel is able to absorb is necessary to know its weight in the swollen state and its dry weight. In this way, the mass of water that the hydrogel is able to retain can be calculated.

Thus, following the procedure set forth in section 6.10, mass values were taken in the swollen and in the dry state for each of the hydrogels tested and the percentage of equilibrium water content and water fraction were determined by equation 1 and equation 2 respectively. For the calculation of the EWC and hw, 3 replicates of each of the HA/Gel hydrogel compositions were tested.

The masses obtained from the swollen and dry hydrogels as well as the equilibrium water content (EWC) and the water fraction (hw) are presented for each of the replicates tested in the following tables.

65% RH

Table 19. Wet mass, dry mass, equilibrium water content and water fraction of the samples tested at 65% RH.

Pattern HA/Gel	m_{dry} (mg)	m_{wet} (mg)	EWC (%)	hw (%)
0/100 no. 1	2,39	2,51	5,02	4,78
0/100 no. 2	2,13	2,26	6,10	5,75
0/100 no. 3	4,53	4,76	5,08	4,83
30/70 no. 1	3,76	4,02	6,91	6,47
30/70 no. 2	1,72	1,85	7,56	7,03
30/70 no. 3	2,5	2,6	4,00	3,85
50/50 no. 1	2,83	3,11	9,89	9,00
50/50 no. 2	2,12	2,37	11,79	10,55
50/50 no. 3	1,6	1,75	9,37	8,57
70/30 no. 1	2,46	2,7	9,76	8,89
70/30 no. 2	2,78	3,1	11,51	10,32
70/30 no. 3	2,7	2,92	8,15	7,53
100/0 no. 1	3,58	4,12	15,08	13,11
100/0 no. 2	2,64	3,06	15,91	13,73
100/0 no. 3	6,47	7,22	11,59	10,39

85% RH

Table 20. Wet mass, dry mass, equilibrium water content and water fraction of the samples tested at 85% RH.

Pattern HA/Gel	m_{dry} (mg)	m_{wet} (mg)	EWC (%)	hw (%)
0/100 no. 1	11,45	12,98	13,36	11,79
0/100 no. 2	2,3	2,54	10,43	9,45
0/100 no. 3	4,21	4,73	12,35	10,99
30/70 no. 1	11,86	13,66	15,18	13,18
30/70 no. 2	7,38	8,87	20,19	16,80
30/70 no. 3	2,57	2,79	8,56	7,89
50/50 no. 1	11,06	13,26	19,89	16,59
50/50 no. 2	2,58	3,11	20,54	17,04
50/50 no. 3	1,6	1,95	21,88	17,95
70/30 no. 1	10,87	13,22	21,62	17,78
70/30 no. 2	3,11	3,86	24,12	19,43
70/30 no. 3	2,7	3,34	23,70	19,16
100/0 no. 1	2,05	2,71	32,20	24,35
100/0 no. 2	1,25	1,59	27,20	21,38
100/0 no. 3	4,89	6,59	34,76	25,80

98% RH

Table 21. Wet mass, dry mass, equilibrium water content and water fraction of the samples tested at 98% RH.

Pattern HA/Gel	m_{dry} (mg)	m_{wet} (mg)	EWC (%)	hw (%)
0/100 no. 1	2,43	4,06	67,08	40,15
0/100 no. 2	2,22	3,53	59,01	37,11
0/100 no. 3	2,13	3,26	53,05	34,66
30/70 no. 1	2,83	5,4	90,81	47,59
30/70 no. 2	2,11	4,2	99,05	49,76
30/70 no. 3	2,5	5,15	106,00	51,46
50/50 no. 1	2,8	6,26	123,57	55,27
50/50 no. 2	1,89	4,39	132,28	56,95
50/50 no. 3	1,6	3,34	108,75	52,10
70/30 no. 1	2,2	5,1	131,82	56,86
70/30 no. 2	1,57	3,94	150,96	60,15
70/30 no. 3	2,7	6,45	138,89	58,14
100/0 no. 1	2,25	6,52	189,78	65,49
100/0 no. 2	3,58	10,34	188,83	65,38
100/0 no. 3	2,91	8,79	202,06	66,89

Immersed (freeze-extraction method)

Table 22. Wet mass, dry mass, equilibrium water content and water fraction of the samples tested in immersion by freeze-extraction method.

Pattern HA/Gel	m_{dry} (mg)	m_{wet} (mg)	EWC (%)	hw (%)
0/100 no. 1	2,51	54,3	2063,35	95,38
0/100 no. 2	1,32	36,92	2696,97	96,42
0/100 no. 3	2,99	59,3	1883,28	94,96
30/70 no. 1	1,85	52,65	2745,95	96,49
30/70 no. 2	1,22	41,25	3281,15	97,04
30/70 no. 3	2,5	63,3	2432,00	96,05
50/50 no. 1	2,37	141,55	5872,57	98,33
50/50 no. 2	1,52	101,52	6578,95	98,50
50/50 no. 3	2,3	121,55	5184,78	98,11
70/30 no. 1	3,1	206,1	6548,39	98,50
70/30 no. 2	2,46	180,32	7230,08	98,64
70/30 no. 3	3,61	220,63	6011,63	98,36
100/0 no. 1	3,06	241,49	7791,83	98,73
100/0 no. 2	2,99	226,35	7470,23	98,68
100/0 no. 3	2,54	215,03	8365,75	98,82

Immersed (freeze-drying method)

Table 23. Wet mass, dry mass, equilibrium water content and water fraction of the samples tested in immersion by freeze-drying method.

Pattern HA/Gel	m_{dry} (mg)	m_{wet} (mg)	EWC (%)	hw (%)
0/100 no. 1	10,72	433,17	3940,76	97,53
0/100 no. 2	10,87	422,94	3790,89	97,43
0/100 no. 3	10,53	416,85	3858,69	97,47
30/70 no. 1	11,24	536,35	4671,80	97,90
30/70 no. 2	9,1	506,98	5471,21	98,21
30/70 no. 3	5,9	409,75	6844,92	98,56
50/50 no. 1	21,33	579,83	2618,38	96,32
50/50 no. 2	7,17	525,33	7226,78	98,64
50/50 no. 3	10,2	555,7	5348,04	98,16
70/30 no. 1	3,95	586,34	4744,05	99,33
70/30 no. 2	11,82	591,57	4904,82	98,00
70/30 no. 3	8,37	535,36	6296,18	98,44
100/0 no. 1	12,26	634,95	5079,04	98,07
100/0 no. 2	19,80	1239,56	6160,40	98,40
100/0 no. 3	15,51	1028,23	6529,46	98,49

APPENDIX IV: DETERMINATION OF DIFFERENT WATER FORMS PRESENT IN HYDROGEL FROM DSC RESULTS

Calculations of the different water forms present in a hydrogel were done from the melting enthalpies obtained in the heating and cooling process from the DSC measurements.

First, it is necessary to calculate the total melting enthalpy ($\Delta H_{m,t}$) from the sum of the melting enthalpies obtained from the two endothermic peaks observed during the heating process as shown in equation 6.

$$\Delta H_{m,t} = \Delta H_{m,1} + \Delta H_{m,2} \quad (6)$$

Where $\Delta \mathrm{H}_{\mathrm{m},1}$ is the melting enthalpy of the first peak and $\Delta \mathrm{H}_{\mathrm{m},2}$ is the melting enthalpy of the second peak.

Thus, and dividing this value by the melting enthalpy of ice under normal conditions ($\Delta \mathrm{H}^{\circ}_{\mathrm{m},\mathrm{H_2O}} = 333.5\ \mathrm{kJ/kg}$), the freezable water fraction (W_f) present in the hydrogel can be calculated (equation 7).

$$W_f = \frac{\Delta H_{m,t}}{\Delta H^{\circ}_{m,H_2O}} \quad (7)$$

Finally, from the total freezable water and knowing the water fraction of the polymer, which is calculated according to equation 1, the non-freezable bound water (W_{nf}) can be calculated according to equation 8.

$$W_{nf} = hw - W_f \quad (8)$$

GLOSSARY

LIST OF ACRONYMS

α:	Mark-Houwink's parameter
ΔCp:	Heat capacity increment
CF-KRB:	Calcium Free Krebs Ringer Buffer
$CoCl_2$:	Cobalt Chloride
DSC:	Differential scanning calorimetry
DRS:	Dielectric relaxation spectroscopy
ECM:	Extracellular matrix
EDC:	N-(3-Dimethylaminopropyl)-N'-ethylcarbodiimide hydrochloride
EWC:	Equilibrium water content
DPBS:	Dulbecco´s phosphate buffered saline
Gel:	Gelatin
Gel-Tyr:	Gelatin with tyramine graft
GPC:	Gel permeation chromatography
H_2O_2:	Hydrogen peroxide
HA:	Hyaluronic acid
HA-LMW:	Low molecular weight hyaluronic acid
HA-Tyr:	Hyaluronic acid with tyramine graft
HCl:	Hydrochloric acid
HEPES:	4-(2-hydroxiethyl)piperazine-1-ethanesulphonic acid
HRP:	Horseradishperoxidase
K:	Mark-Houwink's parameter
KCl:	Potassium chloride
KH_2PO_4:	Potassium dihydrogen phosphate
m_d:	Dry weight
m_w:	Wet weight
mQ:	Milli-Q
M:	Mass molecular weight
MES:	2-(N-Morpholino)ethanesulfonic acid
M_w:	Average mass molecular weight
NaCl:	Sodium chloride
NaOH:	Sodium hydroxide
NHS:	N-Hydroxysuccinimide
P_2O_5:	Phosphorus Oxide III
PEG:	Polyethylene glycol
RH:	Relative Humidity
Tc:	Crystallization temperature
Tcc:	Cold crystallization temperature
Tg:	Glass transition temperature
Tm:	Melting temperature
Tyr·HCl:	Tyramine hydrochloride
UV:	Ultraviolet
x:	Molar fraction

LIST OF FIGURES

Figure 20. Water fraction (hw) of the different HA/Gel compositions at 65%, 85% and 98% RH and immersion of samples with molar ratio HA:Tyr 1:1.The values of the HA/Gel compositions at 65%, 85% and 98% RH are shown in the main axis while the values of HA/Gel compositions immersed in distilled water (purple line) are shown in the secondary axis. Three samples of each component were measured (n=3). * indicates statistically significant difference between groups marked.

Figure 21. Equilibrium water content (EWC) of the different HA/Gel compositions at 65%, 85% and 98% RH and immersion of samples with molar ratio HA:Tyr 1:1.The values of the HA/Gel compositions at 65%, 85% and 98% RH are shown in the main axis while the values of HA/Gel compositions immersed in distilled water (purple line) are shown in the secondary axis. Three samples of each component were measured (n=3). * indicates statistically significant difference between groups marked.

Figure 22. Water fraction (hw) of the different HA/Gel compositions with molar ratio HA:Tyr 1:1 immersed directly in distilled water using freeze-extraction method and freeze-drying method. Three samples of each component were measured (n=3). * indicates statistically significant difference between groups marked.

Figure 23. Equilibrium water content (EWC) of the different HA/Gel compositions with molar ratio HA:Tyr 1:1 immersed directly in distilled water using freeze-extraction method and freeze-drying method. Three samples of each component were measured (n=3). * indicates statistically significant difference between groups marked.

Figure 24. DSC thermogram during second cooling at a heating rate of 10 ºC/min for the series HA/Gel hydrogels with molar ratio HA:Tyr 1:1 at 0% RH. 'Y' axis shows the heat flow in J/g·K and 'X' axis shows temperature in °C.

Figure 25. DSC thermogram during second heating at a heating rate of 10 °C/min for the series HA/Gel hydrogels with molar ratio HA:Tyr 1:1 at 0% RH. 'Y' axis shows the normalized heat flow in J/g·K and 'X' axis shows temperature in ºC.

Figure 26. DSC thermogram during cooling at a heating rate of 10 °C/min for the series HA/Gel hydrogels with molar ratio HA:Tyr 1:1 at 65% RH. 'Y' axis shows the normalized heat flow in J/g·K and 'X' axis shows temperature in °C.

Figure 27. DSC thermogram during heating at a heating rate of 10 °C/min for the series HA/Gel hydrogels with molar ratio HA:Tyr 1:1 at 65% RH. 'Y' axis shows the normalized heat flow in J/g·K and 'X' axis shows temperature in °C.

Figure 28. DSC thermogram during second cooling at a heating rate of 10 ºC/min for the series HA/Gel hydrogels with molar ratio HA:Tyr 1:1 at 85% RH. 'Y' axis shows the normalized heat flow in J/g·K and 'X' axis shows temperature in °C.

Figure 29. DSC thermogram during second heating at heating rate 10 °C/min for the series HA/Gel hydrogels with molar ratio HA:Tyr 1:1 at 85% RH. 'Y' axis shows the normalized heat flow in J/g·K and 'X' axis shows temperature in ºC.

Figure 30. DSC thermogram during second cooling at a heating rate of 10 ºC/min for the series HA/Gel hydrogels with molar ratio HA:Tyr 1:1 at 98% RH. 'Y' axis shows the normalized heat flow in J/g·K and 'X' axis shows temperature in °C.

Figure 31.DSC thermogram during second heating at a heating rate of 10 ºC/min for the series HA/Gel hydrogels with molar ratio HA:Tyr 1:1 at 98% RH. 'Y' axis shows the normalized heat flow in J/g·K and 'X' axis shows temperature in °C.

LIST OF TABLES

DOCUMENT II: TECHNICAL SPECIFICATIONS

TECHNICAL SPECIFICATIONS INDEX

1. SCOPE OF THE PROJECT

The project consists of the synthesis and characterization of hydrogels composed of hyaluronic acid and gelatin in order to verify its validity and utility in regenerative soft tissue therapies.

The work is structured in two parts:

1. The synthesis of hyaluronic acid gelatin hydrogels for which the molar ratios and the concentration of the precursor solutions should be chosen.

2. The characterization of the hydrogels performed. The characterization tests performed on the hydrogels are:

a. Equilibrium water content, which will quantify the amount of water they are able to retain in equilibrium.

b. Morphology, which will allow to observe the microscopic and macroscopic structure of the hydrogels.

c. Differential scanning calorimetry measurements, which will help us study the interactions of the polymer chains with the water absorbed, as well as the miscibility of the two components that form the hydrogel.

2. GENERAL CONDITIONS

2.1. Obligations of project parts

i) Project promoters

The promoters of the project are: Dr. Industrial Engineer Mrs. Gloria Gallego Ferrer, Professor at the Universidad Politécnica de Valencia, who is the project tutor and has to follow the regulations of the Universidad Politécnica de Valencia and Escuela Técnica Superior de Ingenieros Industriales; and Dr. in Physics Apostolos Kyritsis, Assistant Professor at National Technical University of Athens, who is project cotutor acting on behalf of the Physics Department of National Technical University of Athens.

As promoters of the project, they have the power to make changes in the project and specifications, although these modifications should not be prejudicial to the work performed by the designer.

The beginning of the works and the execution deadlines of the project will be marked by the promoters, although the pace of work will depend on the time available to the designer, as long as it is justified to the promoters. The completion date of the work will be established by mutual agreement between the promoters and the designer, and finally, undertakes to deliver the project according to the agreed specifications and within the stipulated period.

ii) Obligations and rights of the designer

The project developed is framed within the Master's Final Works, that have the objective of proving that the student who develops them has acquired the necessary competences during the Master's Degree to be awarded the title of Master Engineer.

From his part, the designer has the following obligations:

- Comply with the current legislation and regulations regarding the Final Work of Master that marks the Escuela Técnica Superior de Ingenieros Industriales.
- Acting on the promoters' instructions and informing them of the work progress.
- Discuss possible changes in the work with the project promoters.
- Respect copyright laws.

In addition, the following rights are granted to the designer:

- Have the necessary equipment to carry out the jobs.
- Have the specifications of the equipment used.
- Receive technical assistance if required by contingencies during the course of the trials and not attributable to negligence of the designer.
- Have facilities that guarantee the safety and security conditions that are reflected in the Law of Labor Risk Prevention.

iii) Work accidents

The designer shall adopt the necessary safety and hygiene measures during the work in order to avoid any type of accident.

iii) Termination of contract

The contractual relationship between promoter and designer may be terminated in of the following conditions:

- In the event of excessive delays in the implementation of the project.
- Due to abandonment of the project without justified cause.
- By mutual agreement between the two parts, provided that none of them is harmed.

Finally, any discrepancies or disagreements between the parts shall be resolved according to the statutes of the Universitat Politècnica de València and the National Technical University of Athens.

iv) Trademarks and copyrights

Both the project author and his promoters publicly recognize both registered trademarks as the copyright in the bibliography consulted during the development of the work.

2.2. Economic conditions

Given the nature of the project, an academic project, no fees or any type of remuneration are recognized for the designer.

3. PARTICULAR CONDITIONS

3.1. Equipment datasheets

- **Precision balance**

Table 24. Technical specifications of precision balance.

Brand	IKAMAG (big squid white)
Maximum load	220 g
Accuracy	0.01 mg

Rules of use and installation of equipment:

- Install the balance on a flat and stable surface or place it on a wall console.

- Avoid extreme temperatures that occur if the balance is placed next to a source of heat or exposure to direct sunlight.

- Protect the balance of drafts.

- Protect the balance of aggressive chemical fumes.

- Do not use the balance in hazardous areas.

- Do not expose the balance to extreme humidity.

In addition, the weights should always be made on a suitable container and not directly placed on the balance tray. Moreover, before performing a weight, the equipment shall be pre-calibrated or tared with the vessel where the reagent is going to be measured. The measure will be done by closing the draft shield and waiting for the value to show that the display of the equipment has stabilized.

- **Magnetic stirrer**

Table 25. Technical specifications of magnetic stirrer.

Brand	IKAMAG (big squid white)
Stirring stations	1
Max, Amount to be stirred (H2O)	1 L
Speed range	0-2500 rpm
Surface Dimensions	Ø 160 mm
Power consumption motor	3 W
Energy consumption	300 mA
Type of indication	LED

Rules of use and installation of equipment:

- Do not work in explosive environments.

- The magnetic field effect can erase cards, tapes and affect pacemaker appliances.

- Do not use the equipment at temperatures above 60 ˚C.

- Do not use at relative humidity above 80% for a long time because it would shorten the life of the device considerably.

- **Liophilizer**

Table 26. Technical specifications of liophylizer.

Brand	TELSTAR LyoQuest-85
Ice capacity	8 kg
Condenser end temperature	< -85 ˚C
Number of compressors	2
Weight of base unit	70 kg
Total power	1.4 kW

Terms of use:

- Before introducing the samples to lyophilize, it is necessary to put in freezing the equipment until reaching a temperature of - 80 ° C.

- Introduce the frozen samples at low temperature in a hole that allow sublimation of the water and ensure that the camera is sealed and the vacuum is generated inside.

- Finish the process, put in defrost mode to remove the ice accumulated in the condenser, leaving it ready for a new use.

- **pH meter**

Table 27. Technical specifications of pH meter.

Brand	Eutech Instruments pH 1500 Cyber Scan
Functions	pH, redox, datalogger
Scale	-1.999 – 19.999 pH
Resolution	0.1/0.01/0.001
Accuracy	± 0.002
Display type	LED

Terms of use:

- Rinse the sensor with distilled water to remove residues from the saline solution used to keep it in good condition.

- Calibrate the pH meter with the calibration solutions to obtain a measurement as accurate as possible.

- Keep stirring the solution that will be measured while adjusting the pH.

- Rinse the sensor with distilled water at the end of the measurement and re-enter it in the sheath with the saline solution.

- **Field Emission Scanning Electron Microscopy**

Table 28. Technical specifications of Field Emission Scanning Electron Microscopy.

Brand	JEM-2100F
Resolution	0.1 nm
Acceleration Voltage	200 kV
OL Focal Point	2.3 nm
Minimum Step	1.4 nm
Magnification range	X50 to X1.5M

Terms of Use:

Field Scanning Electron Microscopy is available for use in the service of Microscopy of the Universitat Politècnica de València. The samples you want to observe are precoated by a platinum bath at 40 mA for 90 seconds to be displayed on the computer later.

In addition, all manipulation of the samples will be done with clamps and the cut of the section of the same will be done with a blade.

- **Spectrophotometer**

Table 29. Technical specifications of Spectrophotometer.

Brand	CECIL SuperAquarius CE9200
Working range	190 - 800 nm
Accuracy	± 0.1 nm
Resolution	0.1/0.01/0.001
Accuracy in absorbance measurements	± 0.001 A
Display type	LCD display

Terms of use:

- Handle the side cuvettes in order to avoid leaving any type of mark on the front faces that interferes with the desired measurement.

- Before performing any measurement, it will be necessary to calibrate or zero the measurement using a standard solution.

- After completing the measurements, it is important to wash the cuvettes carefully to avoid damaging them. The washing will be carried out with distilled water and acetone, which will facilitate its drying.

- **Differential Scanning Calorimeter**

Table 30. Technical specifications of Differential Scanning Calorimeter.

Brand	TA Q200
Temperature Range	- 180 ˚C to 725 ˚C
Temp Accuracy	± 0.1 ˚C
Temp Precision	± 0.01 ˚C
Enthalpy Precision	± 0.1 %
Baseline Flatness	< 100 µW
Baseline Repeatability	< 40 µW

Terms of use:

- The equipment works together with computer software that must be connected at the time the equipment is required to be used.

- In this computer software, the calibration of the equipment will be performed, prior to the measurement, and the characteristics and stages of the test will be programmed.

3.2. Working conditions in the laboratory

The work in the laboratory will be carried out using the safety measures necessary to avoid risks and to minimize the consequences in the event that an incident occurs. For this reason, it will be necessary to use Personal Protective Equipment (PPE) during the entire stay in the laboratory. Thus, lab coat, gloves, safety glasses and gas mask will be used when the situation requires it.

As a special requirement during the implementation of this project, provided that work with carbodiimide (EDC) will require the use of a mask to avoid possible inhalation of dust.

Furthermore, the workplace will be protected with filter paper to absorb any spills that may occur and, where necessary, work under an extraction hood.

At the end of the work, all the material used will be washed, dried correctly and located in its corresponding place so that it can be reused later. The washing of the laboratory material will be done with water and soap, rinsing it with deionized water. For drying it will be used paper as a general rule, using acetone to facilitate the drying of glass material, which is difficult to dry with paper and ethanol for the plastic elements.

3.3. Residue management

All residues generated during the process will be managed according to its nature and danger. In this way, different drums and containers are placed in the laboratory where deposit each of the wastes.

During the execution of this project, the following types of residues have been produced that must be properly identified, classified and managed:

- Latex gloves, which will be deposited after use them in an organic trash bin.

- Micropipette tips and other uncontaminated plastic wastes that will be deposited in the plastic waste bin.

- Filter paper and other paper waste used in the drying of laboratory to be deposited in the paper and cardboard wastebasket.

- Acetone and ethanol washing material that is stored in specific drums labelled as non-halogenated solvents.

- Micropipette tips, Eppendorf's and other contaminated plastics that should be treated as contaminated plastic in separate drums.

- Finally, broken glassware will be managed in drums labelled for this cause.

The drums containing the residues will be properly labelled as published in Annex 1 of Royal Decree RD 952/1997. Thus, the code corresponding to each of the generated wastes is collected in **Table 31.**

Table 31. Classification and labelling codes of residues generated in the laboratory that require special management.

Residue	Code
Non-halogenated solvents	Q7//D15//L5//C41//H3A//A871(7)//B0019 LER 070104
Contaminated plastic	Q16//D15//S36//C23/24//H14//A871//B0019 LER 150110

DOCUMENT III: BUDGET

BUDGET INDEX

1. FINANCING

The Centre for Biomaterials and Tissue Engineering of Polytechnic University of Valencia and Department of Applied Physics of National Technical University of Athens have financed this project.

2. BUDGET

2.1. Price chart No. 1: Labor

This section details the part of the project corresponding to the wages of the necessary labor indicating the unit price and the total cost depending on the number of hours dedicated to the project.

No.	Designation	Unit Price (€/h)	Quantity (h)	Total (€)
1.1	Project director	50	30	1500
1.2	Project co-director	50	25	1250
1.3	Investigator	30	55	1650
1.4	Chemical Engineer	30	305	9150
1.5	Physicist	30	105	3150
1.6	Laboratory assistant	15	78	1170
			Total Labor	**17870**

2.2. Price chart No. 2: Material

This section takes into account all the material necessary for the realization of the project including reagents, laboratory equipment and personal protective equipment used as security measures. Thus, the amount and the cost of each of the materials used are reflected in the following price charts.

The material used has been divided into three categories: reagents, lab's material and personal protective equipment (PPE). The following price charts show each of these three categories in detail. Eventually, the material total cost is collected in a last price chart.

2.1. Reagents

No.	Unit	Designation	Unit Price (€)	Quantity	Total (€)
2.1.1	g	HA sodium salt from *Streptococcus equi*	26,30	2,00	52,60
2.1.2	g	Gel from porcine skin (Type A)	0,21	1,20	0,25
2.1.3	g	MES	2,44	8,70	21,23
2.1.4	mg	Tyramine hydrochloride	0,01	1025,71	10,26
2.1.5	mg	NHS	0,01	67,92	0,68
2.1.6	mg	EDC	0,01	1132,60	11,33
2.1.7	g	Sodium chloride (NaCl)	0,02	630,24	12,60

No.	Unit	Designation	Unit Price (€)	Quantity	Total (€)
2.1.8	g	Sodium hydroxide (NaOH)	0,04	0,60	0,02
2.1.9	L	Hydrochloric acid (HCl)	15,16	0,80	12,13
2.1.10	L	Ethanol	0,06	5,00	0,30
2.1.11	mL	H_2O_2	0,37	0,15	0,06
2.1.12	U	HRP	0,04	115,00	4,60
2.1.13	g	HEPES	1,11	2,56	2,84
2.1.14	g	KCl	0,05	0,07	0,00
2.1.15	g	KH_2PO_4	0,15	0,09	0,01
2.1.16	L	MilliQ water	3,00	72,17	216,51
2.1.17	L	Distilled water	2,32	155,00	359,60
2.1.18	L	DPBS	35,90	1,50	53,85
2.1.19	g	Sodium azide	0,36	0,03	0,01
2.1.20	g	Phosphorus oxide III (P_2O_5)	0,12	0,85	0,11
2.1.21	mg	Cobalt chloride ($CoCl_2$)	0,09	250,00	23,70
2.1.22	g	Potassium sulphate (K_2SO_4)	10,20	0,35	3,57
				Total Reagents	**786,26**

2.2. Lab's material

No.	Unit	Designation	Unit Price (€)	Quantity	Total (€)
2.2.1	m	Dialysis membrane (3500 MWCO)	28,00	2,40	67,20
2.2.2	m	Dialysis membrane (12400 MWCO)	4,58	0,60	2,75
2.2.3	u	P24-culture multiple well plate	3,35	4	13,40
2.2.4	u	P48-culture multiple well plate	4,52	3	13,56
2.2.5	u	Relative humidity jar	72,52	3	217,56
2.2.6	u	Tzero low mass hermetic pan	1,9	25	47,50
2.2.7	u	Tzero low mass hermetic lid	1,2	25	30,00
2.2.8	u	Micropipette	110,00	4	440,00
2.2.9	u	Micropipette tip	0,01	450	4,50
2.2.10	u	Volumetric pipette 1 mL	4,50	2	9,00
2.2.11	u	Volumetric pipette 2 mL	4,50	1	4,50
2.2.12	u	Volumetric pipette 10 mL	5,73	2	11,46
2.2.13	u	Volumetric pipette 25 mL	7,65	1	7,65
2.2.14	u	Pasteur Pipet	0,05	4	0,20
2.2.15	u	Beaker 50 mL	3,49	4	13,96
2.2.16	u	Beaker 100 mL	3,59	2	7,18
2.2.17	u	Beaker 250 mL	4,01	3	12,03
2.2.18	u	Beaker 3 L	31,43	1	31,43
2.2.19	u	Glass bottle with screw cap 100 mL	6,25	4	25,00
2.2.20	u	Glass bottle with screw cap 1 L	11,83	3	35,49
2.2.21	u	Eppendorf 1,5 mL	0,01	22	0,22

No.	Unit	Designation	Unit Price (€)	Quantity	Total (€)
2.2.22	u	Vial 30 mL	0,60	15	9,00
2.2.23	u	Petri dish	0,22	8	1,76
2.2.24	u	Tweezer	1,80	3	5,40
2.2.25	u	Spatula	2,25	2	4,50
2.2.26	u	Cutting blade	0,04	1	0,04
2.2.27	u	Scissors	2,22	2	4,44
2.2.28	u	Magnetic stirrer	2,50	3	7,50
2.2.29	u	Needle	0,91	1	0,91
2.2.30	u	Syringe 20 mL	0,24	2	0,48
				Total Lab's Material	**1028,62**

2.3. Personal Protective Equipment (PPE)

No.	Unit	Designation	Unit Price (€)	Quantity	Total (€)
2.3.1	u	Lab coat	15,00	1	15,00
2.3.2	u	Disposable latex gloves	0,05	250	12,50
2.3.3	u	Disposable nitrile gloves	0,27	30	8,10
2.3.4	u	Gas mask	29,50	1	29,50
2.3.5	u	Dust Mask	8,32	1	8,32
2.3.6	u	Safety glasses	2,40	1	2,40
				Total PPE	**75,82**

2. 4. Personal Protective Equipment (PPE)

2.4. Material price chart

No.	Designation	Total (€)
2.1	Reagents	786,26
2.2	Lab's Material	1028,62
2.3	Personal Protective Equipment (PPE)	75,82
	Total Material	**1890,70**

2.3. Price chart No. 3: Equipment and machinery

This section includes the equipment and machinery used during the project.

No.	Unit	Designation	Unit Price (€)	Quantity	Total (€)
3.1	h	Precision balance	0,01	16,00	0,16
3.2	h	Magnetic stirrer	0,01	1440,00	14,40
3.3	h	Stove	0,02	432,00	8,64
3.4	h	pH meter	0,01	3,40	0,03
3.5	h	Lyophilizer	0,12	1080,00	129,60
3.6	h	Gel Permeation Chromatograph	0,61	30,00	18,30
3.7	h	Field Emission Scanning Electron Microscopy	25,00	3,00	75,00
3.8	h	Spectrophotometer	0,14	1,25	0,18
3.9	h	Differential Scanning Calorimeter	0,17	72,00	12,24
3.10	h	Refrigerator	0,01	1256,00	12,56
3.11	h	Freezer	0,09	45,00	4,05
3.12	h	Desiccator	0,02	48,00	0,96
3.13	h	Centrifuge	0,03	0,50	0,02
				Total Equipment and Machinery	**276,13**

2.4. Broken down price chart

The broken down price chart shows the reagents, materials, equipment and labor broken down according to the stage of the process where they were employed. In addition, the classification of resources is detailed by assigning a code based on the nature of the resources. The codes used and the category to which they refer are listed in **Table 32**.

Table 32. Classification codes used according to the different categories of resources.

Code	Category
R	Reagents
MT	Material
EM	Equipment and machinery
PPE	Personal Protective Equipment
L	Labor

Chapter 1. Synthesis of low molecular weight hyaluronic acid (LMW)					
Code	**Unit**	**Quantity**	**Description**	**Unit Price (€)**	**Total (€)**
1.1	u		**Acid degradation process of hyaluronic acid**		

R	g	0,50	HA sodium salt from *Streptococcus equi*	23,60	11,80
R	L	0,20	Hydrochloric acid (HCl)	15,16	3,03
MT	u	1,00	Glass bottle with screw cap 100 mL	6,25	6,25
EM	h	24,00	Magnetic stirrer	0,01	0,24
EM	h	0,50	pH meter	0,01	0,01
L	h	1,00	Chemical Engineer	30,00	30,00
L	h	0,10	Laboratory assistant	15,00	1,50
		0,02	Complementary direct costs		1,06
				Total	**262,73**

Code	Unit	Quantity	Description	Unit Price (€)	Total (€)
1.2	u		**Dialysis and lyophilization of hyaluronic acid**		
R	L	27,00	Distilled water	2,32	62,64
MT	m	0,20	Dialysis membrane (3500 MWCO)	28,00	5,60
EM	h	48,00	Magnetic stirrer	0,01	0,48
EM	h	3,00	Freezer	0,09	0,27
EM	h	48,00	Lyophilizer	0,12	5,76
L	h	1,00	Chemical Engineer	30,00	30,00
L	h	0,05	Laboratory assistant	15,00	0,75
		0,02	Complementary direct costs		2,11
				Total	**107,61**

Chapter 2. Synthesis of tyramine hyaluronic acid grafting (HA-Tyr)

Code	Unit	Quantity	Description	Unit Price (€)	Total (€)
2.1	u		**Preparation of hyaluronic acid solution for subsequent grafting of tyramine groups**		
R	g	9,80	Sodium chloride (NaCl)	0,02	0,20
R	L	2,50	MilliQ water	3,00	7,50
R	g	1,08	MES	2,44	2,64
R	g	0,08	Sodium chloride (NaCl)	0,02	0,00
MT	u	1,00	Glass bottle with screw cap 100 mL	6,25	6,25
EM	h	2,00	Magnetic stirrer	0,01	0,02
EM	h	0,20	pH meter	0,01	0,00
L	h	1,00	Chemical Engineer	30,00	30,00
		0,02	Complementary direct costs		0,93
				Total	**47,54**

Code	Unit	Quantity	Description	Unit Price (€)	Total (€)
2.2	u		**Grafting tyramine groups into hyaluronic acid**		
R	mg	86,47	Tyramine hydrochloride	0,01	0,86
R	mg	37,13	NHS	0,01	0,37
R	mg	2,23	EDC	0,01	0,02
EM	h	24,00	Magnetic stirrer	0,01	0,24
EM	h	0,25	pH meter	0,01	0,00
L	h	2,5	Chemical Engineer	30	75
L	h	0,2	Laboratory assistant	15	3
		0,02	Complementary direct costs		1,59
				Total	**81,09**

Code	Unit	Quantity	Description	Unit Price (€)	Total (€)
2.3	u		**Dialysis and lyophilization of hyaluronic acid modified**		
R	L	3,00	Distilled water	2,32	6,96
MT	m	0,20	Dialysis membrane (12400 MWCO)	28,00	5,60
EM	h	48,00	Magnetic stirrer	0,01	0,48
EM	h	3,00	Freezer	0,09	0,27
EM	h	72,00	Lyophilizer	0,12	8,64
EM	h	0,15	Spectrophotometer	0,14	0,02
L	h	1,00	Chemical Engineer	30,00	30,00
L	h	0,20	Laboratory assistant	15,00	3,00
		0,02	Complementary direct costs		1,10
				Total	**56,07**

Chapter 3. Synthesis of tyramine gelatin grafting (Gel-Tyr)

Code	Unit	Quantity	Description	Unit Price (€)	Total (€)
3.1	u		**Preparation of gelatin solution for subsequent tyramine grafting**		
R	g	0,40	Gel from porcine skin (Type A)	0,21	0,08
R	L	0,03	MilliQ water	3,00	0,09
R	g	0,20	MES	2,44	0,49
MT	u	1,00	Glass bottle with screw cap 100 mL	6,25	6,25
EM	h	1,50	Magnetic stirrer	0,01	0,02
L	h	1,00	Chemical Engineer	30,00	30,00
		0,02	Complementary direct costs		0,74
				Total	**37,67**

Code	Unit	Quantity	Description	Unit Price (€)	Total (€)
3.2	u		**Grafting tyramine groups into gelatin**		
R	mg	111,13	Tyramine hydrochloride	0,01	1,11
R	mg	122,68	NHS	0,01	1,23
R	mg	7,36	EDC	0,01	0,07
EM	h	28,00	Magnetic stirrer	0,01	0,28
EM	h	0,75	pH meter	0,01	0,01
L	h	1,5	Chemical Engineer	30,00	45,00
		0,02	Complementary direct costs		0,95
				Total	**48,65**

Code	Unit	Quantity	Description	Unit Price (€)	Total (€)
3.3	u		**Dialysis and lyophilization of gelatin modified**		
R	L	9,00	Distilled water	2,32	20,88
MT	m	0,20	Dialysis membrane (3500 MWCO)	4,58	0,92
EM	h	48,00	Magnetic stirrer	0,01	0,48
EM	h	3,00	Freezer	0,09	0,27
EM	h	68,00	Lyophilizer	0,12	8,16
EM	h	0,20	Spectrophotometer	0,14	0,03
L	h	0,75	Chemical Engineer	30,00	22,50
L	h	0,15	Laboratory assistant	15,00	2,25
		0,02	Complementary direct costs		1,11
				Total	**56,59**

Chapter 4. Synthesis of hyaluronic acid gelatin hydrogels

Code	Unit	Quantity	Description	Unit Price (€)	Total (€)
4.1	u		**Solutions preparation**		
R	g	3,11	Sodium chloride (NaCl)	0,02	0,06
R	g	2,30	HEPES	1,11	2,55
R	g	0,15	KCl	0,05	0,01
R	g	0,07	KH_2PO_4	0,15	0,01
R	L	0,40	MilliQ water	3,00	1,20
R	mL	0,10	H_2O_2	0,37	0,04
R	U	110,00	HRP	0,04	4,40
MT	u	3,00	Micropipette	110,00	330,00
MT	u	55,00	Micropipette tip	0,01	0,55

MT	u	45,00	Eppendorf 1,5 mL	0,01	0,45
EM	h	1,00	Stove	0,02	0,02
EM	h	710,00	Refrigerator	0,01	7,10
L	h	2,50	Chemical Engineer	30,00	75,00
		0,02	Complementary direct costs		8,43
				Total	**429,76**

Code	Unit	Quantity	Description	Unit Price (€)	Total (€)
4.2	u		**Formation of hydrogels**		
R	L	0,60	DPBS	35,90	21,54
R	g	0,05	Sodium azide	0,36	0,02
R	L	2,30	MilliQ water	3,00	6,90
MT	u	1,00	P24-culture multiple well plate	3,35	3,35
MT	u	1,00	P48-culture multiple well plate	4,52	4,52
MT	u	1,00	Micropipette	110,00	110,00
MT	u	35,00	Micropipette tip	0,01	0,35
MT	u	5,00	Vial 30 mL	0,60	3,00
MT	u	1,00	Needle	0,91	0,91
EM	h	710,00	Refrigerator	0,01	7,10
L	h	1,50	Chemical Engineer	30,00	45,00
		0,02	Complementary direct costs		4,05
				Total	**185,20**

Chapter 5. Preparation of the hydrogels for the characterization

Code	Unit	Quantity	Description	Unit Price (€)	Total (€)
5.1	u		**Drying of samples and freeze extraction method**		
R	L	9,00	Distilled water	2,32	20,88
R	L	1,00	Ethanol	0,06	0,06
EM	h	2,00	Desiccator	0,02	0,04
EM	h	48,00	Stove	0,02	0,96
L	h	1,5	Chemical Engineer	30,00	45,00
L	h	1,5	Physicist	30,00	45,00
		0,02	Complementary direct costs		2,24
				Total	**92,24**

Code	Unit	Quantity	Description	Unit Price (€)	Total (€)
5.2	u		**Set the samples at different**		

Code	Unit	Quantity	Description	Unit Price (€)	Total (€)
			relative humidities		
R	g	0,50	Sodium azide	0,36	0,18
R	g	0,60	Phosphorus oxide III (P_2O_5)	0,12	0,07
R	mg	600,00	Cobalt chloride ($CoCl_2$)	0,09	56,88
R	g	0,80	Potassium sulphate (K_2SO_4)	10,20	8,16
MT	u	1,00	Relative humidity jar	72,52	72,52
L	h	0,20	Chemical Engineer	30,00	6,00
L	h	0,20	Physicist	30,00	6,00
		0,02	Complementary direct costs		3,00
				Total	**152,81**

Chapter 6. Hydrogels characterization

Code	Unit	Quantity	Description	Unit Price (€)	Total (€)
6.1	u		**Determination of molecular weights**		
EM	h	15,00	Gel Permeation Chromatograph	0,61	9,15
L	h	1,00	Chemical Engineer	30,00	30,00
L	h	1,00	Laboratory assistant	15,00	15,00
		0,02	Complementary direct costs		1,08
				Total	**46,08**

Code	Unit	Quantity	Description	Unit Price (€)	Total (€)
6.2	u		**Determination of tyramine grafting**		
R	L	0,40	MilliQ water	3,00	1,20
R	mg	3,75	Tyramine hydrochloride	0,01	0,04
EM	h	0,20	Spectrophotometer	0,14	0,03
L	h	0,50	Chemical Engineer	30,00	15,00
L	h	0,10	Laboratory assistant	15,00	1,50
		0,02	Complementary direct costs		0,36
				Total	**16,92**

Code	Unit	Quantity	Description	Unit Price (€)	Total (€)
6.3	u		**Equilibrium water content**		
R	L	0,40	MilliQ water	3,00	1,20
EM	h	2,00	Precision balance	0,01	0,02
EM	h	24,00	Lyophilizer	0,12	8,16

L	h	2,00	Chemical Engineer	30,00	22,50
		0,02	Complementary direct costs		0,64
				Total	**31,32**

Code	Unit	Quantity	Description	Unit Price (€)	Total (€)
6.4	u		**Morphology**		
MT	u	1,00	Cutting blade	0,04	0,04
EM	h	3,00	Field Emission Scanning Electron Microscopy	25,00	75,00
L	h	3,00	Chemical Engineer	30,00	90,00
L	h	0,50	Laboratory assistant	15,00	7,50
		0,02	Complementary direct costs		3,45
				Total	**175,95**

Code	Unit	Quantity	Description	Unit Price (€)	Total (€)
6.5	u		**Differential Scanning Calorimeter**		
MT	u	5	Tzero low mass hermetic pan	1,90	9,50
MT	u	5	Tzero low mass hermetic lid	1,20	6,00
EM	h	8,00	Differential Scanning Calorimeter	0,17	1,36
L	h	8,00	Chemical Engineer	30,00	240,00
L	h	8,00	Physicist	30,00	240,00
L	h	0,50	Laboratory assistant	15,00	7,50
		0,02	Complementary direct costs		10,09
				Total	**514,45**

Chapter 7. Material in common use.

Code	Unit	Quantity	Description	Unit Price (€)	Total (€)
7.1		u	**Commonly used materials used in various stages of the process or continuously**		
MT	u	3	Glass bottle with screw cap 1 L	11,83	35,49
MT	u	4	Beaker 50 mL	3,49	13,96
MT	u	2	Beaker 100 mL	3,59	7,18
MT	u	3	Beaker 250 mL	4,01	12,03
MT	u	3	Tweezer	1,80	5,40
MT	u	2	Spatula	2,25	4,50
MT	u	1	Cutting blade	0,04	0,04
MT	u	2	Scissors	2,22	4,44
MT	u	3	Magnetic stirrer	2,50	7,50

MT	u	2	Volumetric pipette 1 mL	4,50	9,00
MT	u	1	Volumetric pipette 2 mL	4,50	4,50
MT	u	2	Volumetric pipette 10 mL	5,73	11,46
MT	u	1	Volumetric pipette 25 mL	7,65	7,65
MT	u	4	Pasteur Pipet	0,05	0,20
MT	u	8	Petri dish	0,22	1,76
EPP	u	1	Lab coat	15,00	15,00
EPP	u	250	Disposable latex gloves	0,05	12,50
EPP	u	30	Disposable nitrile gloves	0,27	8,10
EPP	u	1	Gas mask	29,50	29,50
EPP	u	1	Dust Mask	8,32	8,32
EPP	u	1	Safety glasses	2,40	2,40
EM	h	50	Precision balance	0,01	0,50
		0,02	Complementary direct costs		4,03
				Total	**205,46**

Chapter 8. Meetings for the monitoring of work					
Code	**Unit**	**Quantity**	**Description**	**Unit Price (€)**	**Total (€)**
8.1	u		**Follow-up meetings and project schedule**		
L	h	20,00	Project director	50,00	1000,00
L	h	20,00	Project co-director	50,00	1000,00
L	h	45,00	Investigator	30,00	1350,00
L	h	70,00	Chemical Engineer	30,00	2100,00
L	h	70,00	Physicist	30,00	2100,00
		0,02	Complementary direct costs		151,00
				Total	**7701,00**

2.5. Material execution budget

The material execution budget grouped by chapters is shown below.

Chapter 1. Synthesis of low molecular weight hyaluronic acid (LMW)					
Code	**Unit**	**Quantity**	**Description**	**Unit Price (€)**	**Total (€)**
1.1	u	2	Acid degradation process of hyaluronic acid	262,73	525,46
1.2	u	2	Dialysis and lyophilization of hyaluronic acid	107,61	215,22
				Total	**740,68**

Chapter 2. Synthesis of tyramine hyaluronic acid grafting (HA-Tyr)					
Code	**Unit**	**Quantity**	**Description**	**Unit Price (€)**	**Total (€)**
2.1	u	4	Preparation of hyaluronic acid solution for subsequent grafting of tyramine groups	47,54	190,16
2.2	u	4	Grafting tyramine groups into hyaluronic acid	81,09	324,36
2.3	u	4	Dialysis and lyophilization of hyaluronic acid modified	56,07	224,28
				Total	**738,80**

Chapter 3. Synthesis of tyramine gelatin grafting (Gel-Tyr)					
Code	**Unit**	**Quantity**	**Description**	**Unit Price (€)**	**Total (€)**
3.1	u	2	Preparation of gelatin solution for subsequent grafting of tyramine groups	37,67	75,34
3.2	u	2	Grafting tyramine groups into gelatin	48,65	97,30
3.3	u	2	Dialysis and lyophilization of gelatin modified	56,59	113,18
				Total	**285,82**

Chapter 4. Synthesis of hyaluronic acid gelatin hydrogels					
Code	**Unit**	**Quantity**	**Description**	**Unit Price (€)**	**Total (€)**
4.1	u	5	Solutions preparation	429,76	2148,8
4.2	u	5	Formation of hydrogels	185,2	926
				Total	**3074,8**

Chapter 5. Preparation of the hydrogels for the characterization					
Code	**Unit**	**Quantity**	**Description**	**Unit Price (€)**	**Total (€)**
5.1	u	5	Drying of samples and freeze	92,24	461,2
5.2	u	5	Set the samples at different	152,81	764,05
				Total	**1225,25**

Chapter 6. Hydrogels characterization					
Code	**Unit**	**Quantity**	**Description**	**Unit Price (€)**	**Total (€)**
6.1	u	2	Determination of molecular weights	46,08	92,16
6.2	u	6	Determination of tyramine grafting	16,92	101,52
6.3	u	5	Equilibrium water content	31,32	156,6
6.4	u	1	Morphology	175,95	175,95
6.5	u	8	Differential Scanning Calorimeter	514,45	4115,6
				Total	**4641,83**

Chapter 7. Material in common use.					
Code	**Unit**	**Quantity**	**Description**	**Unit Price (€)**	**Total (€)**
7.1	u	1	Commonly used materials used in various	205,46	205,46
				Total	**205,46**

Chapter 8. Meetings for the monitoring of work					
Code	**Unit**	**Quantity**	**Description**	**Unit Price (€)**	**Total (€)**
8.1	u	1	Commonly used materials used in various	2251,00	7701,00
				Total	**7701,00**

2.6. General Budget

For the calculation of the general budget of the project 10% of general expenses and 21% of VAT has been considered.

Code	Description	Amount
Chapter 1	Synthesis of low molecular weight hyaluronic acid (LMW)	740,68
Chapter 2	Synthesis of tyramine hyaluronic acid grafting (HA-Tyr)	738,80
Chapter 3	Synthesis of tyramine gelatin grafting (Gel-Tyr)	285,82
Chapter 4	Synthesis of hyaluronic acid gelatin hydrogels	3074,80
Chapter 5	Preparation of the hydrogels for the characterization	1225,25
Chapter 6	Hydrogels characterization	4641,83
Chapter 7	Material in common use	205,46
Chapter 8	Meetings for the monitoring of work	7701,00
	Material Execution Budget	**18613,64**
	10% General expenses	1861,36
	8% Know-how	1489,09
	Contracted Operation Budget	**21964,10**
	21% VAT	4612,456
	Investment Budget	**26576,56**

The project's investment budget is TWENTY-SIX THOUSAND FIVE HUNDRED SEVENTY-SIX EUROS AND FIFTY-FIVE CENTS.